P-07-93

Forsmark site investigation

Boreholes KFM01A and KFM02B

Micro crack volume measurements and triaxial compression tests on intact rock

Lars Jacobsson, SP Technical Research Institute of Sweden

December 2007

Svensk Kärnbränslehantering AB
Swedish Nuclear Fuel
and Waste Management Co
Box 250, SE-101 24 Stockholm
Tel +46 8 459 84 00

ISSN 1651-4416
SKB P-07-93

Forsmark site investigation

Boreholes KFM01A and KFM02B

Micro crack volume measurements and triaxial compression tests on intact rock

Lars Jacobsson, SP Technical Research Institute of Sweden

December 2007

Keywords: Rock mechanics, Micro crack volume, Hydrostatic compression test, Triaxial compression test, Elasticity parameters, Stress-strain curve, AP PF 400-06-049.

Abstract

Hydrostatic compression tests and subsequent triaxial compression tests have been carried out on 8 specimens of intact rock from borehole KFM01A and 7 specimens from KFM02B in Forsmark. Moreover, the density and porosity of further 8 specimens from KFM02B was determined. The volume of micro cracks, originating from stress relaxation and mechanical effects from the core drilling, was estimated by analysing the volumetric response during the hydrostatic compression tests. The specimens from borehole KFM01A were water saturated prior to the testing and the density was determined at this condition. The specimens from borehole KFM02B were packed into water tight bags right after the field sampling in order to preserve the natural water content. The porosity measurements and the mechanical tests were carried out at this moisture condition. The density was first determined at natural moisture condition and later at water saturation and finally after drying.

The cylindrical specimens were taken from drill cores at depth levels ranging between 232–691 m borehole length (KFM01A) and 197–570 m borehole length (KFM02B). The sampled rock type of all specimens was medium-grained granite, rock code 101057. All specimens have a diagonally oriented foliated material structure. The micro crack volume, elastic properties, represented by the Young's modulus and the Poisson ratio, and the compressive strength were deduced from the mechanical tests. The specimens were photographed before and after the mechanical testing.

The measured density for the water saturated specimens from borehole KFM01A was 2,660 kg/m^3. The density of the specimens from borehole KFM02B had a mean value of 2,652 kg/m^3 at natural moisture content, 2,653 kg/m^3 after 7 days water saturation and 2,649 kg/m^3 after drying, respectively. The mean value of the measured porosity was 0.41%. The estimated micro crack volume was in the range 0.035–0.119% (KFM01A) and 0.021–0.041% (KFM02B) recpectively.

Two confining pressure levels were used, 10 and 50 MPa, and the peak values of the axial compressive stress were in the range 319.5–722.3 MPa (KFM01A) and 342.8–649.6 MPa (KFM02B). The elastic parameters were determined at a load corresponding to 50% of the failure load and it was found that Young's modulus was in the range 73.9–78.2 GPa with a mean value of 76.1 GPa (KFM01A) and 70.2–80.1 GPa with a mean value of 73.6 GPa (KFM02B). The Poisson ratio was in the range of 0.29–0.34 with a mean value of 0.31 (KFM01A and KFM02B). It was seen from the mechanical tests that the material in the specimens responded in a brittle way and that the shear failures have occurred along the diagonally oriented foliations in the majority of the specimens.

Sammanfattning

Hydrostatiska kompressionsprov och efterföljande triaxiella kompressionsprov har utförts på 8 stycken provobjekt av intakt berg från borrhål KFM01A samt 7 stycken från borrhål KFM02B Forsmark. Vidare bestämdes densiteten och porositeten hos ytterligare 8 prover från KFM02B. Mikrosprickvolymen, härrörande från spänningsavlastning och mekaniska effekter från kärnborrningen, uppskattades genom att analysera den volymetriska responsen under de hydrostatiska kompressionsproven. Proverna från borrhål KFM01A vattenmättades före provningen och densiteten bestämdes vid detta tillstånd. Provobjekten från borrhål KFM02B packades in i vattentäta påsar direkt efter provtagningen för att bevara det naturliga fukttillståndet. Porositetsmätningarna samt de mekaniska provningarna utfördes med detta fukttillstånd. Densiteten bestämdes hos proverna först med naturligt fukttillstånd sedan vid full vattenmättnad och slutligen efter torkning.

De cylindriska proven har tagits från borrkärnor vid djupnivåer mellan 232–691 m borrhålslängd (KFM01A) samt mellan 197–570 m borrhålslängd (KFM02B). Bergarten hos alla prover var medelkornig granit, bergartskod 101057. Proverna har en materialstruktur med en diagonalt orienterad foliation. Från de mekaniska provningarna bestämdes mikrosprickvolymen och de elastiska egenskaperna, representerade av elasticitetsmodulen och Poissons tal. Provobjekten fotograferades såväl före som efter de mekaniska proven.

Den uppmätta densiteten hos de vattenmättade proven från borrhål KFM01A var 2 660 kg/m^3. Densiteten hos proverna från borrhål KFM02B hade ett medelvärde på 2 652 kg/m^3 med naturlig fukthalt, 2 653 kg/m^3 efter 7 dagars vattenmättnad samt 2 649 kg/m^3 efter torkning. Medelvärdet hos den uppmätta porositeten var 0,41%. Den uppskattade mikrosprickvolymen varierade mellan 0,035–0,119 % (KFM01A) samt mellan 0,021–0,041 % (KFM02B).

Två olika celltryck användes vid triaxialproven, 10 och 50 MPa, och toppvärdena för den axiella kompressiva spänningen låg mellan 319,5–722,3 MPa (KFM01A) och mellan 342,8–649,6 MPa (KFM02B). De elastiska parametrarna bestämdes vid en last motsvarande 50 % av topplasten vilket gav en elasticitetsmodul mellan 73,9–78,2 GPa med ett medelvärde på 76,1 GPa (KFM01A) respektive 70,2–80,1 GPa med ett medelvärde på 73,6 GPa (KFM02B). Poissons tal varierade inom intervallet 0,29–0,34 med ett medelvärde på 0,31 (KFM01A och KFM02B). Vid belastningsförsöken kunde man se att materialen i provobjekten hade ett sprött beteende samt att skjuvbrotten i de flesta fallen har inträffat längs med de diagonalt orienterade foliationerna.

Contents

1 Introduction

Density and porosity determination, micro crack volume measurements and triaxial compression tests have been carried out on drill core specimens sampled from the boreholes KFM01A and KFM02B in Forsmark, Sweden, see map in Figure 1-1. These tests belong to one of the activities performed as part of the site investigation in the Forsmark area managed by the Swedish Nuclear Fuel and Waste Management Co (SKB) /1/. The tests were carried out in the material and rock mechanics laboratories at the department of Building Technology and Mechanics at Technical Research Institute of Sweden (SP), former Swedish National Testing and Research Institute (before January 2007).

Borehole KFM01A is a drilled telescopic borehole with a total length of c 1,000 m. Moreover, borehole KFM02B is a special rock stress investigation borehole with a total length of c 600 m. The rock has a foliated material structure with a diagonal orientation with respect to the core axis in the sections from both boreholes where the specimens are sampled.

The controlling documents for the activity are listed in Table 1-1. Both Activity Plan and Method Description are SKB's internal controlling documents, whereas the Quality Plan referred to in the table is an SP (The Swedish National Testing and Research Institute) internal controlling document.

The method description SKB MD 160.002, which is based on the ISRM suggested method /2/, was followed for the porosity and density determinations. The method description SKB MD 190.003, which is based on the ISRM suggested methods /3, 4/, was partly followed for sampling and for the triaxial compression tests. As to the measurements of micro crack volume

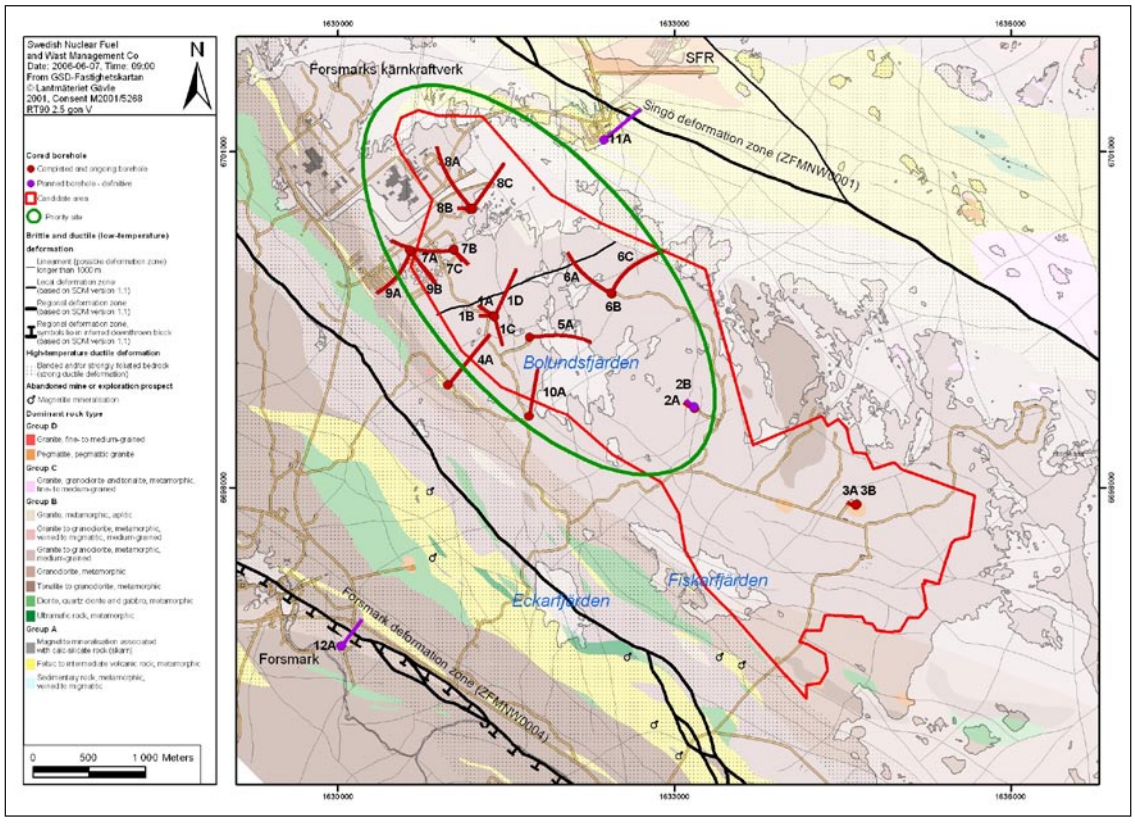

Figure 1-1. *Geologic map over the Forsmark candidate area. The locations of both telescopic boreholes and boreholes of SKB standard type until June 2006 are shown. Boreholes started to drill and finished are marked red, planned are marked with purple.*

Table 1-1. Controlling documents for performance of the activity.

Activity Plan	Number	Version
Mätning av mikrosprickors töjningsvolym vid treaxliga tryckförsök – KFM01A och KFM02B	AP PF 400-06-049	1.0
Method Description	**Number**	**Version**
Determining density and porosity of intact rock	SKB MD 160.002	2.0
Triaxial compression test for intact rock	SKB MD 190.003	2.0
Quality Plan		
SP-QD 13.1		

there is no known standardized test method. Moreover, SKB has no method description for measurements of this parameter. A method was therefore developed to determine the micro crack volume in laboratory on intact rock core specimens that can be carried out prior to triaxial tests. The method is further described below in this chapter and in Section 4.6.

SKB supplied SP with rock cores which arrived at SP in August 2006 (KFM01A) and February 2007 (KFM02B) and were tested during October and November 2006, October and November 2007 (KFM01A) and March, April and November 2007 (KFM02B). Cylindrical specimens were cut from the cores and selected based on the preliminary core logging with the strategy to primarily investigate the properties of metamorphic granite to granodiorite (101057) in the two boreholes.

The specimens from borehole KFM01A were water-saturated prior to the mechanical tests. The wet density was determined on these specimens. Data on density and porosity from previous tests on specimens from the same borehole can be found in /5/. The specimens from borehole KFM02A were packed into sealed plastic bags directly after sampling in order to preserve their natural water content and opened right before the specimen preparation. Each of the specimens packed into plastic bags were split into one specimen for the density and porosity determination and one specimen for the mechanical tests. The porosity was determined based on the natural water content. The dry density and the density at both natural water content and at full saturation was determined. One specimen, KFM02B-80-6B, was dried by storage in air in the laboratory for c 6 months and then water saturated before the porosity was determined.

The specimens from KFM01A were kept and stored in water, with a minimum of 7 days, up to the mechanical testing, whereas the natural water content was kept during the mechanical testing on the specimens from KFM02A. Moreover, the specimens were photographed before and after the mechanical testing. One additional specimen, KFM02B-115-6B, was dried by storage in air in the laboratory for c 6 months and then water saturated and tested in the same manner as the specimens from borehole KFM01A.

The measurement of micro crack volume was conducted by analysing the volumetric response of the specimens during hydrostatic compression. The test procedure was earlier used by e.g. Brace /6/ and Walsh /7/. Tests on aluminium reference specimens were conducted in order to verify the method prior to the tests on the drill core specimens.

The compression tests with axial deformation control were carried out after the hydrostatic compression tests. The axial ε_a and circumferential strain ε_φ together with the axial stress σ_a were recorded during the test. The strains were recorded by means of strain gauges. The peak value of the axial compressive stress σ_c was determined at each test. Furthermore, two elasticity parameters, Young's modulus E and Poisson ratio ν, were deduced from the tangent properties at 50% of the peak load. Diagrams with the volumetric and crack volumetric strain versus axial stress are reported. These diagrams can be used to determine crack initiation stress σ_i and the crack damage stress σ_d, cf /8, 9/.

Mechanical testing on intact rock specimens sampled from borehole KFM01A have previously been reported by /10, 11, 12/.

2 Objective

One purpose of the testing was to determine the volume of micro cracks and the porosity on specimens in laboratory.

The in situ porosity is used when radionuclide transport properties in the rock mass are modeled. There is no established method to determine the in situ porosity in field. Porosity determined on drill core specimens in laboratory has been used instead in the computations. The specimens in laboratory have experienced a stress relaxation and mechanical stressing during the drilling operation. This results in a development of micro cracks which causes an increase of the apparent porosity. Results from the radionuclide transport simulations display a discrepancy to values that have been predicted based on results from in situ experiments. A hypothesis is that the discrepancy in the simulation is caused by using apparent porosity from laboratory measurements instead of the in situ porosity. An estimate of the in situ porosity can be obtained by subtracting the volume of micro cracks in the porosity values from laboratory measurements.

The second part of the testing is carried out in order to determine the elastic properties, represented by Young's modulus and the Poisson ratio, and the compressive strength of cylindrical intact rock cores at different constant confining pressures.

The results from the tests are going to be used in the site descriptive model, which will be established for the candidate area selected for site investigations at Forsmark.

3 Equipment

3.1 Specimen preparation

A circular saw with a diamond blade was used to cut the specimens to their final lengths. The surfaces on the specimens aimed for the mechanical tests were grinded after cutting in a grinding machine in order to achieve a high-quality surface for the axial loading that complies with the required tolerances. The measurements of the specimen dimensions were made with a sliding calliper. Furthermore, the tolerances were checked by means of a dial indicator and a stone face plate. The specimen preparation is carried out in accordance with ASTM 4543-01 /13/.

3.2 Density and porosity measurements

The specimens and the water were weighed using a scale for weight measurements. A thermometer was used for the water temperature measurements. A heating chamber was used for drying the specimens. Further information of the equipment can be found in e.g. /5/. The expanded uncertainty for respective method with covering factor 2 (95% confidence interval) is ± 4 kg/m^3 for determination of wet density and ± 0.09 % for determination of the porosity.

3.3 Deformation measurements and data acquisition

Metal foil strain gauges were used for the deformation measurements. It is found in the literature /14/ that a number of factors have to be considered when resistive metal foil strain gauges are used to determine material deformation during hydrostatic compression tests. The most important factor is the quality of the adhesive layer. Ideally the adhesive layer must be thin with an even thickness and with good bonding characteristics. Moreover, the adhesive layer must be free from air inclusions. The results can be more or less distorted if all these things are not fulfilled. Lateral pressure acting on the strain gauge will produce a small error on the strain readings which is approximately proportional to the acting pressure, see e.g. /14, 15/.

The gauge length must be many times larger than the grain size in the rock material in order to capture a homogenised response. In the present case strain gauges with a gauge length of 20 mm were used. The selection of a proper adhesive is important as it must have good bonding characteristics on rock and must not be negatively affected by the presence of moisture. Lau and Chandler /16/ found that acrylic adhesive was the best working adhesive among various tested adhesives in conjunction with strain gauge measurements on wet rock during tests in a triaxial compression test device. We have therefore chosen a two-part metha-acrylate adhesive in the tests.

Tests on aluminium reference specimens were carried out in order to develop a method to properly mount the strain gauges with an adhesive layer that is thin and with an even thickness and to investigate the pressure sensitivity. This investigation is described in Appendix A.

The data acquisition was made with a HBM MGCplus unit equipped with amplifier modules ML38-AP03 and ML10B-AP03 for the strain gauge channels. Each of the strain gauges was connected to a Wheatstone bridge with a sense connection for temperature compensation. Moreover, the load and pressure signals were also sampled with the HBM MGCplus unit.

3.4 Mechanical testing

The mechanical tests were carried out in a servo controlled testing machine specially designed for rock tests, see Figure 3-1. The system consists of a load frame, a hydraulic pump unit, a controller unit and various sensors. The communication with the controller unit is accomplished by special testing software run on a PC connected to the controller. The load frame is characterized by a high stiffness and is supplied with a fast responding actuator, cf the ISRM suggested method /3/. Furthermore, the sensors, the controller and the servo valves are rapidly responding components. The machine is equipped with a pressure vessel in which the specimens are tested under a confinement pressure. A thin rubber membrane is mounted on the specimen in order to seal the specimen from the oil that is used as the confinement medium, cf Figure 3-1.

The hydrostatic compression tests were carried out by letting pressurized oil act around the specimen where a pressure transducer registered the pressure. In the triaxial tests, the axial load is determined using a load cell, which is located inside the pressure vessel and has a maximum capacity of 1.5 MN. The uncertainty of the load measurement is less than 1%. The strain gauges measured both the axial and circumferential deformations in the tests.

The specimens were photographed with a 4.0 Mega pixel digital camera at highest resolution and the photographs were stored in a jpeg-format.

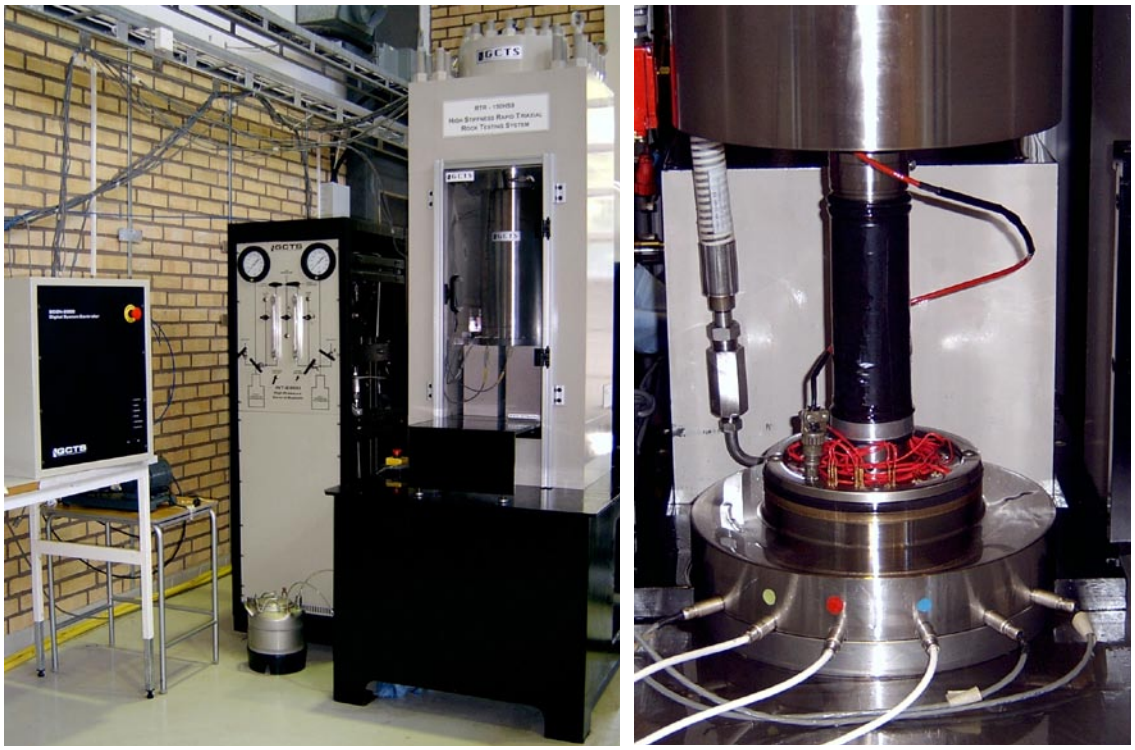

Figure 3-1. *Left: Digital controller unit, pressure cabinet with cell pressure intensifier and oil reservoir inside, and the load frame with closed cell (pressure vessel). Right: Bottom of the cell is lowered. The specimen is instrumented and ready for inserting in the cell.*

4 Execution

The water saturation and determination of the density of the wet specimens were mainly made in accordance with the method description SKB MD 160.002 (SKB internal controlling document, see Table 1-1). This includes determination of density in compliance with ISRM /2/ and water saturation for the specimens from borehole KFM01A by SS-EN 13755 /17/. The micro crack volume measurements were carried out according to the method used by Brace /6/. The method description SKB MD 190.003 (SKB internal controlling document, see Table 1-1) was followed in large, but with a modified procedure regarding the triaxial compression test. For these tests the ISRM suggested method /3/ was followed in which strain gauges were used instead of displacement transducers for the deformation measurements.

A check-list was filled in successively during the work in order to confirm that the different specified steps had been carried out. Moreover, comments were made upon observations made during the mechanical testing that are relevant for the interpretation of the results. The check-list form is an SP internal quality document.

4.1 Description of the specimens

The rock type characterisation was made according to Stråhle /18/ using the SKB mapping system (Boremap). The identification marks, upper and lower sampling depth (Secup and Seclow) and the rock types are shown in Tables 4-1 to 4-3.

Table 4-1. Specimen identification, sampling level (borehole length) and rock type (based on the Boremap overview mapping) for specimens from borehole KFM01A.

Identification	Adj Secup (m)	Adj Seclow (m)	Rock type/occurrence
KFM01A-115-21	232.83	232.83	Granite to granodiorite, metamorphic (101057)
KFM01A-115-22	235.54	235.54	Granite to granodiorite, metamorphic (101057)
KFM01A-115-23	236.28	236.28	Granite to granodiorite, metamorphic (101057)
KFM01A-115-24	491.31	491.31	Granite to granodiorite, metamorphic (101057)
KFM01A-115-25	491.67	491.67	Granite to granodiorite, metamorphic (101057)
KFM01A-115-26	491.91	491.91	Granite to granodiorite, metamorphic (101057)
KFM01A-115-28	689.07	689.07	Granite to granodiorite, metamorphic (101057)
KFM01A-115-29	691.08	691.08	Granite to granodiorite, metamorphic (101057)

Note: No distinction was made between secup and seclow at the time for the depth determination (year 2003).

Table 4-2. Specimen identification, sampling level (borehole length) and rock type (based on the Boremap mapping) for specimens from borehole KFM02B aimed for density and porosity determinations.

Identification	Adj Secup (m)	Adj Seclow (m)	Rock type/occurrence
KFM02B-80-1	197.40	197.81	Granite to granodiorite, metamorphic (101057)
KFM02B-80-2	210.18	210.43	Granite to granodiorite, metamorphic (101057)
KFM02B-80-3	504.31	504.50	Granite to granodiorite, metamorphic (101057)
KFM02B-80-4	504.50	504.93	Granite to granodiorite, metamorphic (101057)

Identification	Adj Secup (m)	Adj Seclow (m)	Rock type/occurrence
KFM02B-80-5	555.45	555.82	Granite to granodiorite, metamorphic (101057)
KFM02B-80-6(*)	556.49	556.88	Granite to granodiorite, metamorphic (101057)
KFM02B-80-6B(*)	556.49	556.88	Granite to granodiorite, metamorphic (101057)
KFM02B-80-012606	570.55	570.83	Granite to granodiorite, metamorphic (101057)

(*) Two specimens were taken from the same piece of core.

Table 4-3. Specimen identification, sampling level (borehole length) and rock type (based on the Boremap mapping) for specimens from borehole KFM02B aimed for mechanical tests.

Identification	Adj Secup (m)	Adj Seclow (m)	Rock type/occurrence
KFM02B-115-1	197.40	197.81	Granite to granodiorite, metamorphic (101057)
KFM02B-115-2	210.18	210.43	Granite to granodiorite, metamorphic (101057)
KFM02B-115-4	504.50	504.93	Granite to granodiorite, metamorphic (101057)
KFM02B-115-5	555.45	555.82	Granite to granodiorite, metamorphic (101057)
KFM02B-115-6(*)	556.49	556.88	Granite to granodiorite, metamorphic (101057)
KFM02B-115-6B(*)	556.49	556.88	Granite to granodiorite, metamorphic (101057)
KFM02B-115-012606	570.55	570.83	Granite to granodiorite, metamorphic (101057)

(*) Two specimens were taken from the same piece of core.

4.2 Density and porosity measurements

The density of the specimens from KFM02B was determined at natural water content, at water saturation and after drying. Moreover, the porosity was determined on measurements at the natural water content and at dry condition. An overview of the activities for the density and porosity determination is shown in the step-by step description in Table 4-4.

Results from previously performed density and porosity measurements on drill cores from borehole KFM01A are found in /5, 10, 11, 12/.

Table 4-4. Activities during the density and porosity determination on the specimens from borehole KFM02B. The specimen KFM02B-80-6B was tested using the steps 1 and 5–11, with 14 days in tap water during step 5.

Step	Activity
1	The specimens were cut according to the marks on the rock cores to a thickness of about 25 mm.
2	The specimens were weighed in tapwater with their natural water content. The temperature of the water was 19.7°C and the density 998.3 kg/m^3.
3	The specimens were surface dried with a towel and weighed.
4	The density of the specimen having natural water content was determined.
5	The specimens were put in tap water for 7 days for water saturation.
6	The specimens were weighed in tap water. The temperature of the water was 19.7°C and the density 998.3 kg/m^3.
7	The specimens were surface dried with a towel and weighed.
8	The density at water saturation was determined.
9	The specimens were dried in a heating chamber for six days at 105°C.
10	The specimens were transported to a desiccator for cooling.
11	The dry density and porosity based on the natural water content were determined.

4.3 Preparation of specimens for mechanical tests

The specimens were cut to a prescribed length and the end surfaces of the specimens aimed for the mechanical testing were in addition grinded in order to comply with the required shape tolerances. The specimens from KFM01A were put in water for minimum 7 days in order to obtain complete water saturation and the specimens from KFM02A were put in plastic bags after the cutting and grinding in order to preserve the natural moisture content. One additional specimen, KFM02B-115-6B, was prepared as the specimens from KFM01A.

The micro crack volume measurements are based on measuring and interpreting the volumetric response during hydrostatic compression tests. The deformations are measured by means of strain gauges. Six strain gauges, three in the axial direction and three in the circumferential direction, were mounted at mid height of the specimens. A coating was applied on the strain gauges as a mechanical protection. The specimens were tested right after the coating had been set.

Care has been taken to preserve the moisture up to testing. However, it has to be taken in account that some moisture may have evaporated despite of this.

An overview of the activities during the specimen preparation is shown in the step-by step description in Table 4-5.

Table 4-5. Activities during the preparation of specimens for the mechanical tests.

Step	Activity
1	The drill cores were marked where the specimens are to be taken.
2	The specimens were cut to the specified length according to markings and the cutting surfaces were grinded.
3	The tolerances were checked: parallel and perpendicular end surfaces, smooth and straight circumferential surface.
4	The diameter and height were measured three times each. The respective mean value determines the dimensions that are reported.
5	The specimens from KFM01A and specimen KFM02B-115-6B were water saturated according to the method described in SKB MD 160.002 and were stored for minimum 7 days in water. The specimens from KFM02B were repacked into plastic bags.

4.4 Mechanical tests

The specimen was placed inside the pressure cell between platens and sealed using a thin rubber membrane. Oil surrounded the specimen except under the lower platen as the platen was fixed to the cell bottom. This set-up yields an isotropic loading. Tests with two different load sequences were conducted on the specimens from borehole KFM01A. Type 1: Loading from 0.1–50 MPa, hold at 50 MPa for 15 minutes and unload 50–0.1 MPa and hold for 15 minutes. Type 2: Loading from 0.1–50 MPa, hold at 50 MPa for 5 minutes, loading from 50–100 MPa, hold for 5 minutes, unload 100–50 MPa, short hold time, and unload 50–0.1 MPa and hold for 5 minutes. The pressure rate was 10 MPa/min during both loading and unloading.

Some creep deformation at peak load was noted during the tests on the specimens from borehole KFM01A. The loading rate was decreased to 5 MPa/min for the subsequent tests on the specimens from KFM02A in order to decrease the rate effects during loading and unloading. The hold times during loading and at peak were shortened to 5 minutes instead of 15 min as the loading rate was lower. Moreover, the specimens were unloaded to atmospheric pressure instead of 0.1 MPa and the hold time at full unloading was 10 minutes instead of 5 minutes.

The triaxial compression tests were carried out after the micro crack volume measurements using axial displacement control. The specimens from borehole KFM01A had been stored approximately 76–93 days in water when the hydrostatic and the hydrostatic and triaxial compression tests were carried out. However, the specimens were taken out from the water a few days prior to the mechanical tests in order to mount the strain gauges.

An overview of the activities during the mechanical testing is shown in the step-by step description in Table 4-6.

Table 4-6. Activities during the mechanical tests. The steps 1–9 concern the micro crack volume measurements whereas the steps 10–14 concern the triaxial compression tests.

Step	Activity
1	Digital photos were taken on each specimen prior to the testing.
2	The specimen was put in testing position and centred between the loading platens.
3	A rubber membrane was mounted on the specimen and strain gauges were connected to the Wheat stone bridges.
4	The triaxial cell was closed and filled with oil whereby a cell pressure of 0.1 MPa is applied. The frame piston is positioned such that it will have a gap in the spherical joint to the upper loading platen.
5	The strain gauge channels were calibrated by means of a shunt resistance.
6	The sampling started and the cell pressure was ramped up to a pressure level of 50 MPa with a given constant rate. The pressure was held constant at 50 MPa at a given time.
7	Step 7 is only for the tests with a maximum pressure of 100 MPa (type 2). The pressure was ramped from 50 MPa to 100 MPa with a given constant rate. The pressure was held constant at 100 MPa at a given time.
8	Step 8 is only for the tests with a maximum pressure of 100 MPa (type 2). The pressure was ramped from 100 MPa to 50 MPa with a given constant rate. The pressure was held constant at 50 MPa for a short time (approximately 2–3 min).
9	The pressure was ramped from 50 MPa to 0.1 (0) MPa with a given constant rate. The pressure was held constant at the unloaded state for a given time.
10	The frame piston was brought down into contact with the specimen with a force corresponding to a deviatoric stress of 1 MPa. The cell pressure was then raised to the specified level and at the same time keeping the deviatoric stress constant.
11	The loading was started with an axial displacement rate of the piston of 0.41 mm/min.
12	The test was stopped immediately after the axial peak load was rached.
13	The oil pressure was brought down to zero and the oil was poured out of the cell. The cell was opened and the specimen removed.
14	Digital photos were taken on each specimen after the mechanical testing.

4.5 Data handling

The test results were exported as text files from the test software and stored in a file server on the SP computer network after each completed test. The main data processing, in which the micro crack volume and elastic modulii were computed and the peak stress was determined, has been carried out in the program MATLAB /19/. Moreover, MATLAB was used to produce the diagrams shown in Sections 5.2 and 5.3. The summary of results in Sections 5.1 and 5.4 with tables containing mean value and standard deviation of the different parameters and diagrams was provided using MS Excel. MS Excel was also used for reporting data to the sicada database.

4.6 Analyses and interpretation

As to the definition of the different result parameters we begin with the axial stress σ_a, which is defined as

$$\sigma_a = \frac{F}{A}$$

where F is the axial force acting on the specimen, and A is the specimen cross section area. The pressure vessel (triaxial cell) filled with oil is pressurized with a cell (confining) pressure p. This implies that the specimen, located inside the pressure vessel, becomes confined and attains a radial stress σ_r equal to the confining pressure p. The (effective) deviatoric stress is defined as

$$\sigma_{dev} = \sigma_a - \sigma_r$$

The stress during hydrostatic compression is $\sigma_a = \sigma_r = p$ (i.e. $\sigma_{dev} = 0$). The peak value of the axial stress during a test is representing the triaxial compressive strength σ_c, for the actual confining pressure used in the test, see the results presentation.

The strain measurements were carried out using strain gauges. The strain gauges are sensitive to lateral pressure. The lateral pressure sensitivity was investigated and quantified in Appendix A. The measurement error made during a lateral pressure has two contributions which have to be accounted for. First, the lateral pressure acting on a strain gauge mounted on a plane surface was found to yield an underestimation of the strain results in the range of 22–34 microstrains at a lateral pressure of 50 MPa with the current set-up. A second superposed effect was observed on strain gauges mounted on a convex single-curved surface with the curvature in the direction of the measuring grid. This effect was estimated to increase the measured strain value about 17.5 microstrains at lateral pressure of 50 MPa. The results by of the lateral pressure sensitivity are summarized in Table A-2. Moreover, it was found that the amount of deviation was linearly proportional to the acting lateral pressure, see Figure A-4.

The strain data have been adjusted by using the findings above. Three strain gauges denoted AV, BV and CV, respectively, are measuring the axial strain at a 120 degrees division at mid height of the specimen. The correction of the vertical strain gauges (AV, BV and CV) are made according to

$$\varepsilon_{AV,corr} = \varepsilon_{AV} + C_{lat} \cdot p_{lat}$$

for AV and similar for BV and CV, where ε_{AV} is the strain value of strain gauge AV obtained from measurements, p_{lat} is the lateral pressure and the constant $C_{lat} = 28/50 =$ 0.56 microstrain/MPa was computed based on the results in Table A-2. The median value, 28 microstrains, was chosen to be used in the computation of C_{lat}. Moreover, the lateral pressure p_{lat} is equal to the cell (confining) pressure in both the hydrostatic and in the triaxial compression tests. Similarly, three strain gauges denoted AH, BH and CH, respectively, are measuring the circumferential strain at mid height of the specimen, with a division of 120 degrees. A correction of both the lateral pressure as stated above and due to the effect of curvature has to be made in this case. The correction in this case becomes

$$\varepsilon_{AH,corr} = \varepsilon_{AH} + C_{lat} \cdot p_{lat} - C_{curvature} \cdot p_{lat}$$

for AH and similar for BH and CH, where ε_{AH} is the strain value of strain gauge AH obtained from measurements and the constant $C_{curvature} = 17.5/50 = 0.35$ microstrain/MPa was computed using the value given in Table A-2.

The axial and radial strains are represented by the mean values of respectively set of strain gauges as

$$\varepsilon_a = (\varepsilon_{AV,corr} + \varepsilon_{BV,corr} + \varepsilon_{CV,corr}) / 3 \quad (1)$$

and

$$\varepsilon_r = \varepsilon_\varphi = (\varepsilon_{AH,corr} + \varepsilon_{BH,corr} + \varepsilon_{CH,corr}) / 3 \quad (2)$$

The volumetric strain ε_{vol} is given as

$$\varepsilon_{vol} = \varepsilon_a + 2\varepsilon_r \quad (3)$$

Furthermore, the tangent bulk compliance β is defined as

$$\beta = d\varepsilon_{vol} / dp$$

The initial response during hydrostatic compression tests yields a non-linear response. For low porosity rock, the non-linearity is related to mainly closing of micro cracks, cf /7/. The deformation becomes approximately linear when the micro cracks are closed and the deformations at this stage are associated with closing of natural pores and compression of the bulk material. With this view in mind, the micro crack volume strain ε_{MC} is computed as, cf /7/,

$$\varepsilon_{MC} = \varepsilon_{vol,max} - \beta_{max}\, p_{max}, \quad (4)$$

where $\varepsilon_{vol,max}$ and p_{max} refer to values at 50 MPa in this investigation. The bulk compliance β_{max} was evaluated at $p = p_{max}$ (in the interval 48.0–49.6 MPa) at the unloading curve after further compression due to the creep deformations representing a compressed material as in situ. The principal stages of deformation during the hydrostatic compression test and the definition of the micro crack volume is visualised in Figure 4-1. In addition, the volumetric strain at 20 MPa pressure, denoted $\varepsilon_{vol,20}$, was determined as the mean value of the volumetric strain obtained at loading and at unloading. The level 20 MPa was chosen as it is in the same order as the in situ rock stresses in the two boreholes. The value of $\varepsilon_{vol,20}$ can be used to relate to the magnitude of volumetric deformations as they are in situ, with consideration of the micro crack volume strain ε_{MC}.

The stresses and the strains are defined as positive in compressive loading and deformation, respectively. The elasticity parameters are defined by the tangent Young's modulus E and tangent Poisson ratio v as

$$E = \frac{\sigma_a(0.60\sigma_c) - \sigma_a(0.40\sigma_c)}{\varepsilon_a(0.60\sigma_c) - \varepsilon_a(0.40\sigma_c)}$$

$$v = -\frac{\varepsilon_r(0.60\sigma_c) - \varepsilon_r(0.40\sigma_c)}{\varepsilon_a(0.60\sigma_c) - \varepsilon_a(0.40\sigma_c)}$$

The tangents were evaluated with values corresponding to an axial load between 40% and 60% of the axial peak stress σ_c.

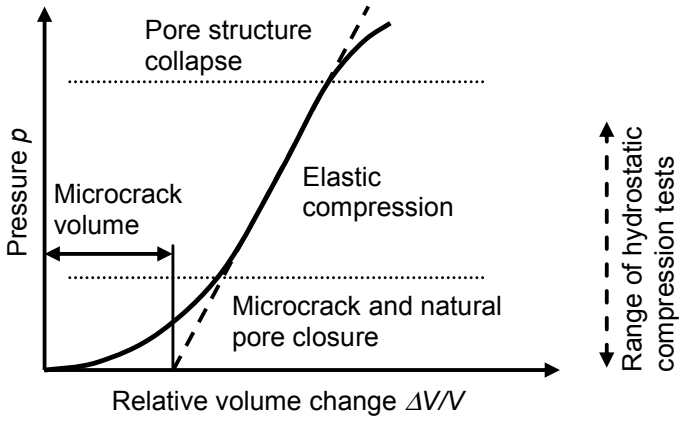

Figure 4-1. *Deformation phases during the hydrostatic compression test. The pore structure collapse will occur at very high pressures for a low porosity rock. The definition of the micro crack volume is shown.*

A closure of present micro cracks will take place initially during confinement and axial loading. Development of new micro cracks will start when the axial load is further increased and axial stress reaches the crack initiation stress σ_i. The crack growth at this stage is as stable as increased loading is required for further cracking. A transition from a development of micro cracks to macro cracks will take place when the axial load is further increased. At a certain stress level the crack growth becomes unstable. The stress level when this happens is denoted the crack damage stress σ_d, cf /8, 9/. In order to determine the stress levels we look at the volumetric strain.

By subtracting the elastic volumetric strain ε_{vol}^{e} from the total volumetric strain, a volumetric strain ε_{vol}^{cr} corresponding to the crack volume is obtained. This has been denoted calculated crack volumetric strain in the literature, cf /8, 9/. We thus have

$$\varepsilon_{vol}^{cr} = \varepsilon_{vol} - \varepsilon_{vol}^{e}$$

Assuming axisymmetric loading, as in the triaxial compression test, and linear elasticity leads to

$$\varepsilon_{vol}^{cr} = \varepsilon_{vol} - \frac{1-2\nu}{E}(\sigma_a + 2\sigma_r)$$

Experimental investigations have shown that the crack initiation stress σ_i coincides with the onset of increase of the calculated crack volume, cf /8, 9/. The same investigations also indicate that the crack damage stress σ_d can be defined as the axial stress at which the total volume starts to increase, i.e. when a dilatant behaviour is observed.

4.7 Nonconformities

The specimens from borehole KFM02B aimed for the density and porosity measurements were first weighed with their natural water content and later water saturated and tested according to the method description SKB MD 160.002. The remaining part of the core from KFM02B-80-6 was kept in air and naturally dried for 6 months. Two additional specimens KFM02B-80-6B and KFM02B-115-6B were sampled from the remaining core piece. The new specimens were water saturated before determining the porosity, wet density and carrying out the mechanical tests.

The specimens aimed for the mechanical tests were first subjected to hydrostatic loading and unloading and after that a triaxial compression test with constant confining pressure and axial deformation control. The initial hydrostatic compression load cycle and using axial deformation control at the triaxial compression tests are deviations from the method description SKB MD 190.003.

The specimens KFM01A-115-21 to -26 were subjected to mechanical testing as given in the activity plan. However, the sampling depth intervals suggested in the activity plan for some of the specimens were not correct. The correct sampling depths are given in this report. Specimen KFM02B-115-3 had a sealed joint and was replaced by specimen KFM02B-115-012606, which is not specified in the activity plan. As to the porosity and the density determination, one additional specimen KFM02B-80-012606 was tested.

5 Results

The results of the density and porosity measurements are presented in Section 5.1. The results from the mechanical tests of the individual specimens from boreholes KFM01A and KFM02B are presented in Sections 5.2 and 5.3, respectively, and a summary of the results is given in Section 5.4. The reported parameters are based on unprocessed raw data obtained from the testing. One exception is the strain results that were adjusted due to a distortion caused by lateral pressure acting on the gauges. The results were reported to the sicada database, where they are traceable by the activity plan number. Only data in SKB's database are accepted for further interpretation and modelling. Data presented in this report are regarded or copies of the original data. Data in the database may be revised if needed. However, such revision will not necessarily result in a revision of this report, although major revisions are the normal procedure for a P-report. Minor revisions are normally presented as supplements, available at www.skb.se. Main results from the mechanical tests based on uncorrected strain measurement results are shown in Appendix B.

The data together with the digital photographs of the individual specimens were stored on a CD and handed over to SKB. The handling of the results follows SDP-508 (SKB internal controlling document) in general.

5.1 Density and porosity measurements

The results from the porosity and density determinations are shown in Tables 5-1 and 5-2. Diagrams showing the porosity and the density values versus sampling level are shown in Figures 5-1 and 5-2.

Table 5-1. Summary of results for porosity, dry density and wet density.

Identification	Porosity(*) (%)	Dry density (kg/m³)	Density at natural moisture condition (kg/m³)	Density at water saturation (kg/m³)
KFM02B-80-1	0.42	2,644	2,648	2,648
KFM02B-80-2	0.37	2,649	2,653	2,652
KFM02B-80-3	0.43	2,649	2,653	2,656
KFM02B-80-4	0.43	2.645	2,650	2,650
KFM02B-80-5	0.37	2,652	2,655	2,656
KFM02B-80-6	0.41	2,653	2,657	2,657
KFM02B-80-6B	0.38	2,652	(**)	2,656
KFM02B-80-012606	0.47	2,647	2,651	2,652

(*) Note: The results are given with two significant digits. This has to be put in view of the calculated expanded uncertainty of ± 0.09 % evaluated with a covering factor of two, cf Section 3.2.

(**) The specimen had no natural water moisture condition at the time for the testing.

Table 5-2. Mean values and standard deviation of the results for porosity and density measurements.

	Porosity (%)	Dry density (kg/m³)	Density at natural moisture condition (kg/m³)	Density at water saturation (kg/m³)
Mean value	0.41	2,649	2,652	2,653
Std dev	0.03	3.3	3.2	3.6

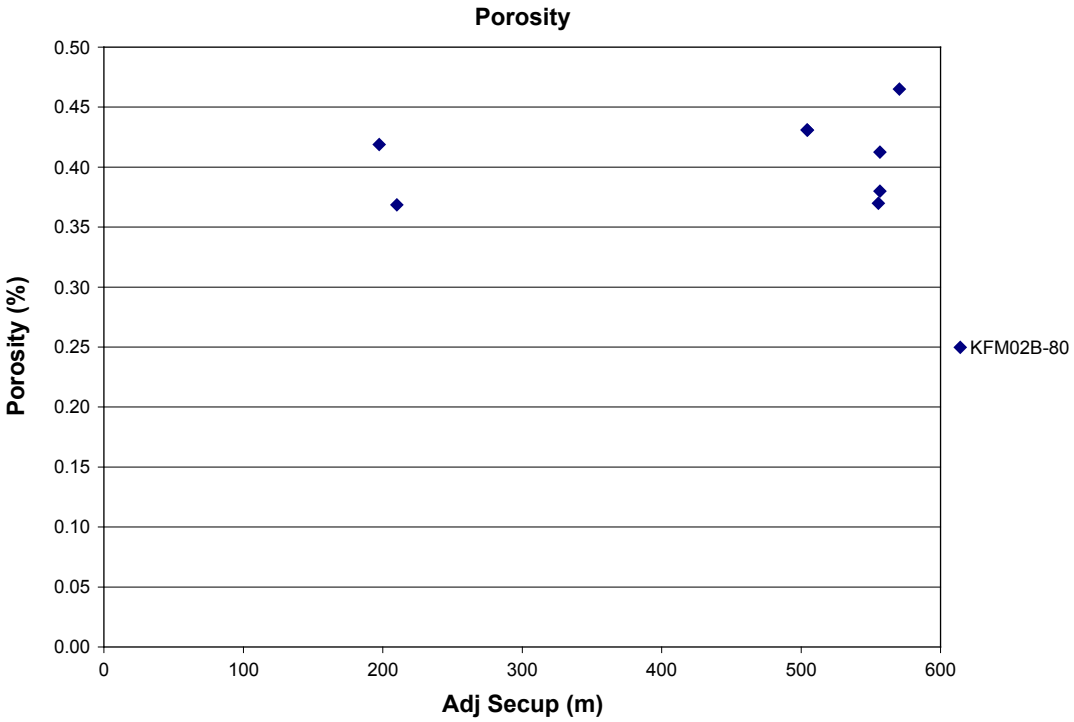

Figure 5-1. *Porosity versus sampling level (borehole length).*

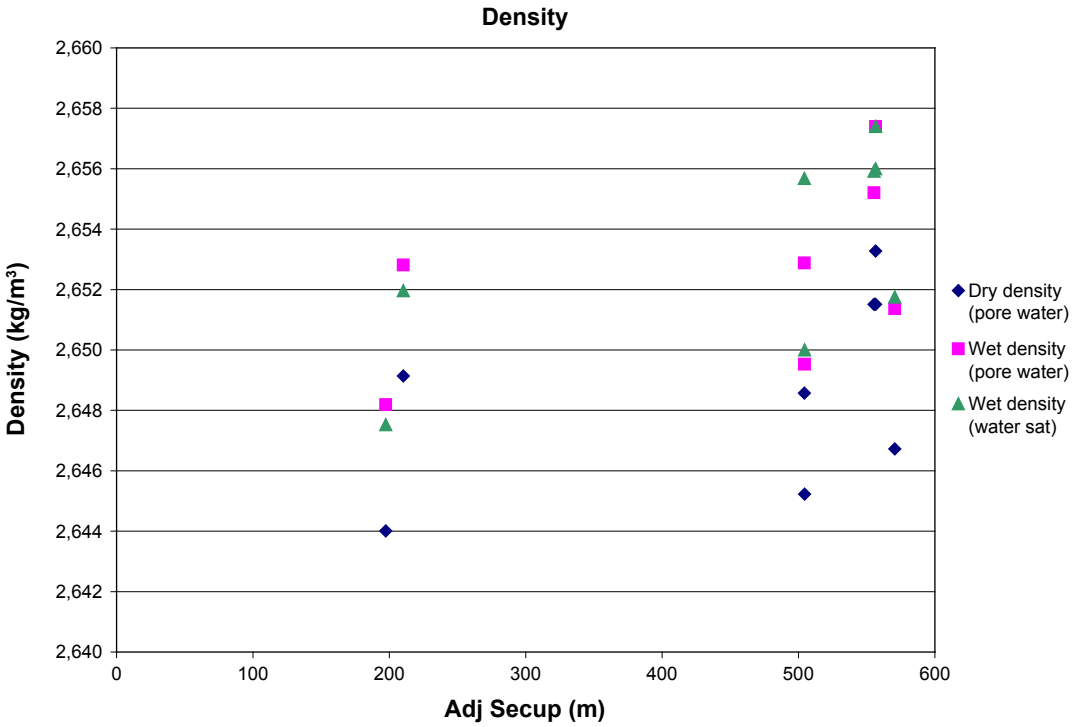

Figure 5-2. *Density versus sampling level (borehole length).*

5.2 Results from mechanical tests for each individual specimen – KFM01A

Pictures taken on the specimens before and after the mechanical test are presented below together with comments on observations made during testing. Results graphs from both the hydrostatic and triaxial compression tests are shown. The text “Based on all SGs” in the legend for the hydrostatic compression tests means that the results are computed using values from all strain gauges and evaluated according to (1)–(3). Moreover, the labels for strain gauges that have failed during the hydrostatic compression test are put in brackets in the legends in the results diagrams. The strain results are adjusted with respect to the active lateral pressure according to Section 4.6. The results for the individual specimens are as follows.

Specimen ID: KFM01A-115-21

Before mechanical test

After mechanical test

AV, AH

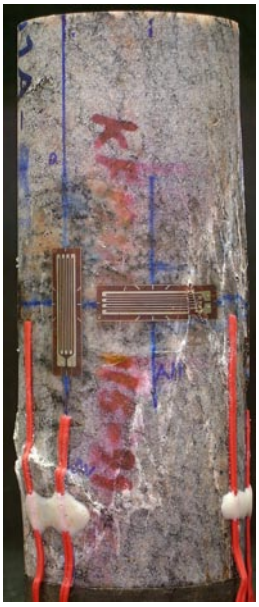

BV, BH

CV, CH

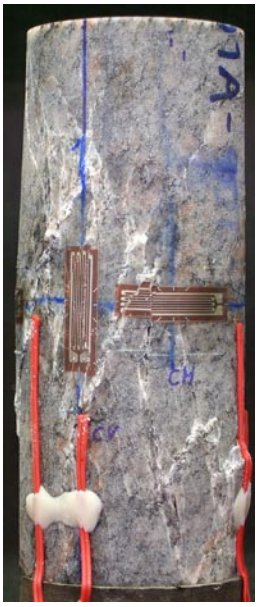

Diameter (mm)	Height (mm)	Density (kg/m³)
50.8	127.3	2,660

Comments: A v-shaped shear failure is observed which is partly following the diagonally oriented material foliations.

Specimen ID: KFM01A-115-21

Bulk compliance (β_{max}): 0.0204 [GPa^{-1}]

Microcrack volume (ε_{MC}): 0.037 [%]

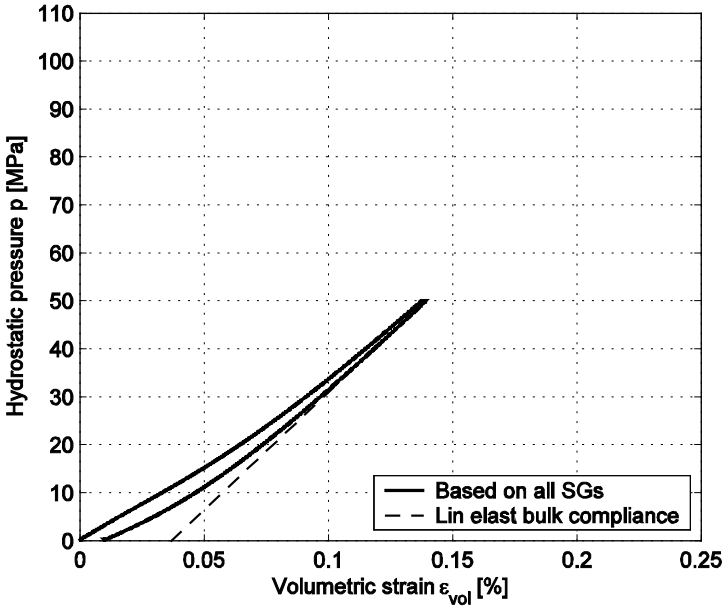

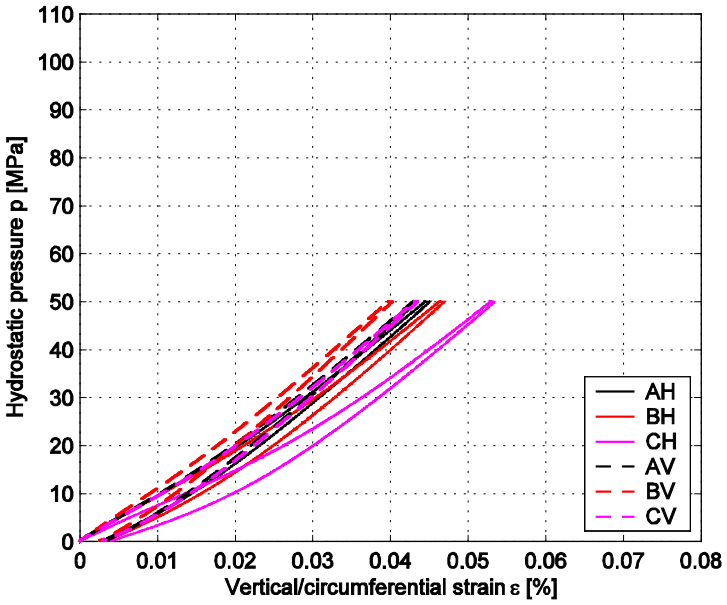

Specimen ID: KFM01A-115-21

Youngs Modulus (E):	75.3	[GPa]	Cell pressure:	10	[MPa]
Poisson Ratio (ν):	0.34	[-]			
Axial peak stress (σ_c):	319.5	[MPa]			

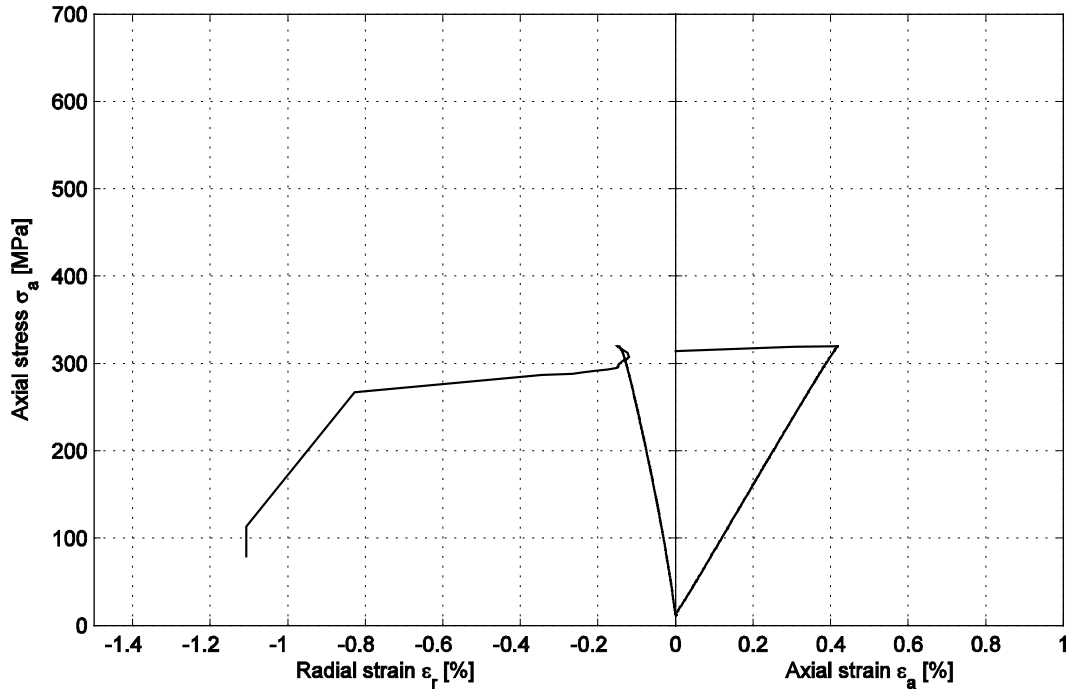

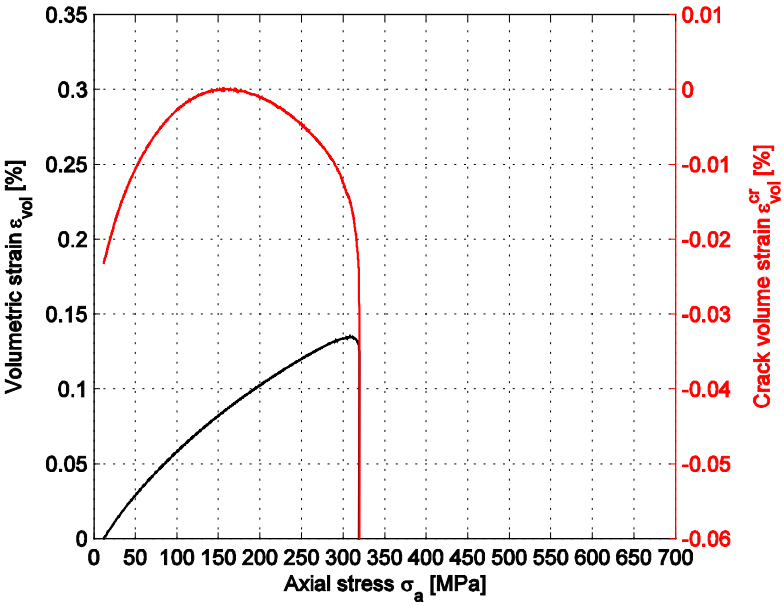

Specimen ID: KFM01A-115-22

Before mechanical test

After mechanical test

AV, AH

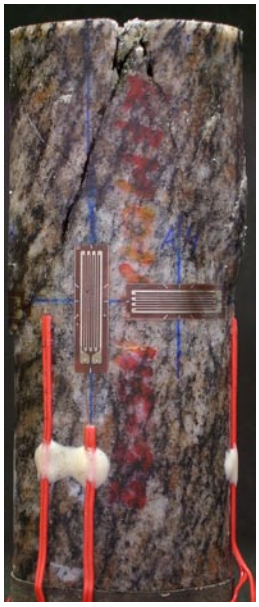

BV, BH

CV, CH

Diameter (mm)	Height (mm)	Density (kg/m^3)
50.8	127.3	2,660

Comments: The specimen has a v-shaped shear failure which is partly following the diagonally oriented material foliations.

Specimen ID: KFM01A-115-22

Bulk compliance (β_{max}): 0.0202 [GPa^{-1}]

Microcrack volume (ε_{MC}): 0.035 [%]

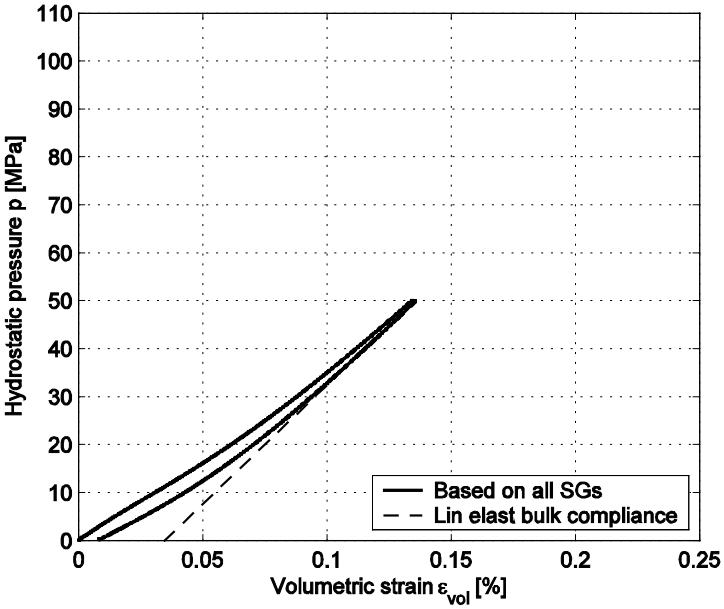

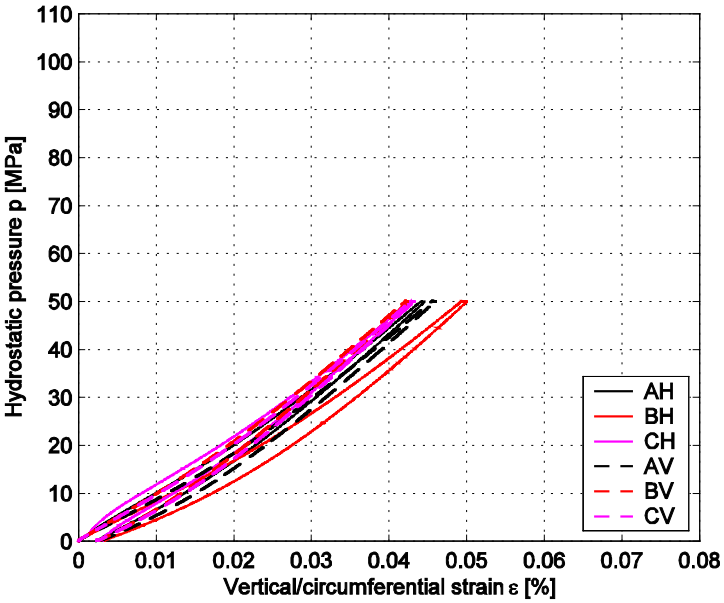

Specimen ID: KFM01A-115-22

Youngs Modulus (E):	78.2	[GPa]	Cell pressure:	50	[MPa]
Poisson Ratio (ν):	0.317	[-]			
Axial peak stress (σ_c):	598.7	[MPa]			

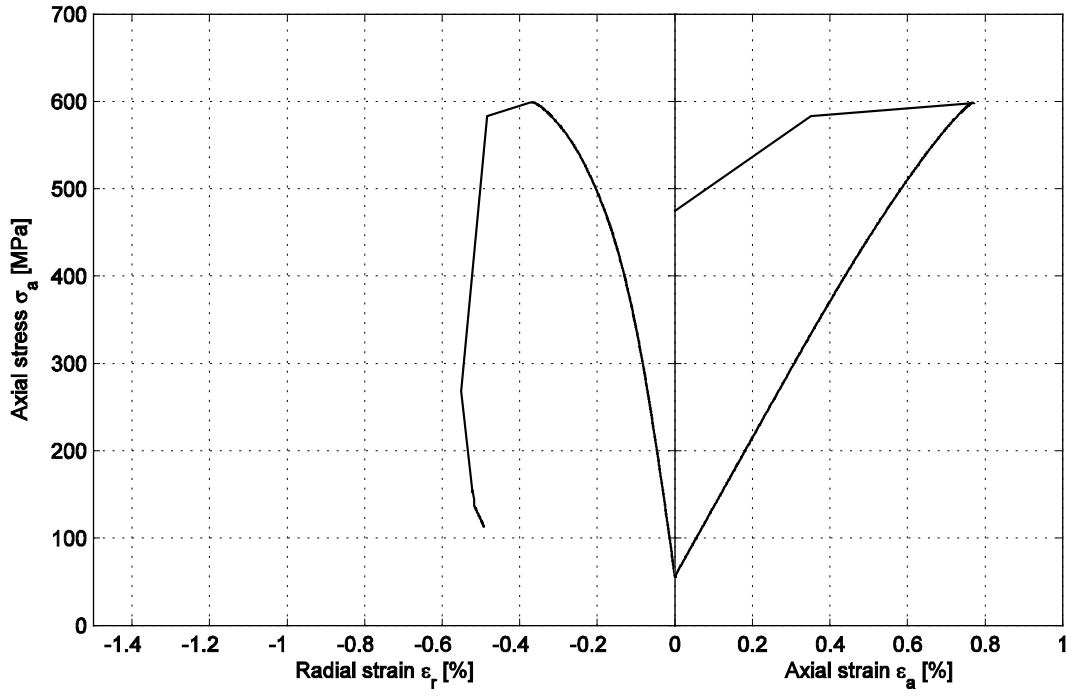

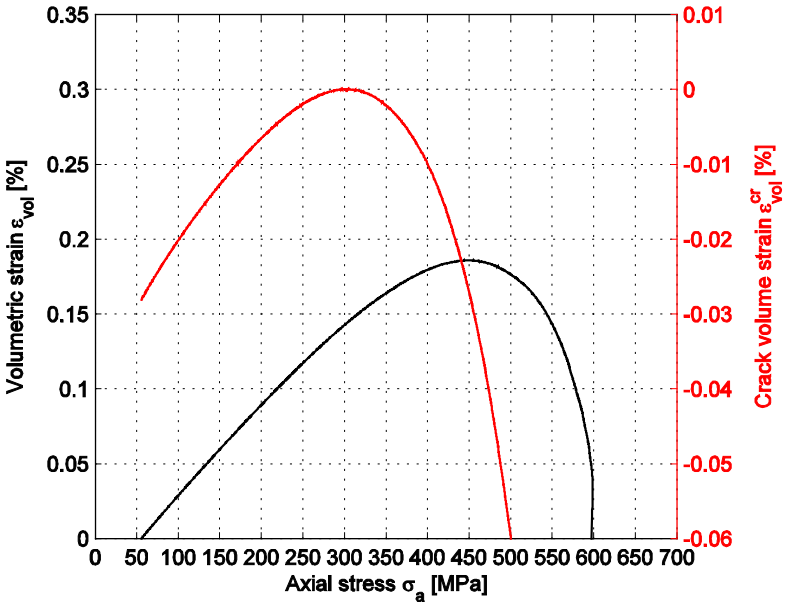

Specimen ID: KFM01A-115-23

Before mechanical test

After mechanical test

AV, AH

BV, BH

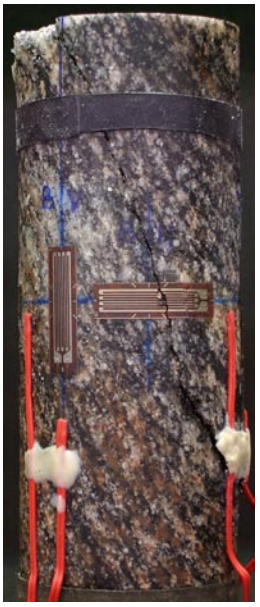

CV, CH

Diameter (mm)	Height (mm)	Density (kg/m³)
50.8	127.2	2,660

Comments: Strain gauge AH has failed during the measurement. The measured strain ε_{AH} has been replaced by the mean value of the strains measured by the strain gauges BH and CH in the volumeteric strain calculation, i.e. $\varepsilon_{AH} = (\varepsilon_{BH} + \varepsilon_{CH}) / 2$. The specimen has a diagonal shear failure which is following the diagonally oriented material foliations.

Specimen ID: KFM01A-115-23

Bulk compliance (β_{max}): 0.021 [GPa^{-1}]

Microcrack volume (ε_{MC}): 0.046 [%]

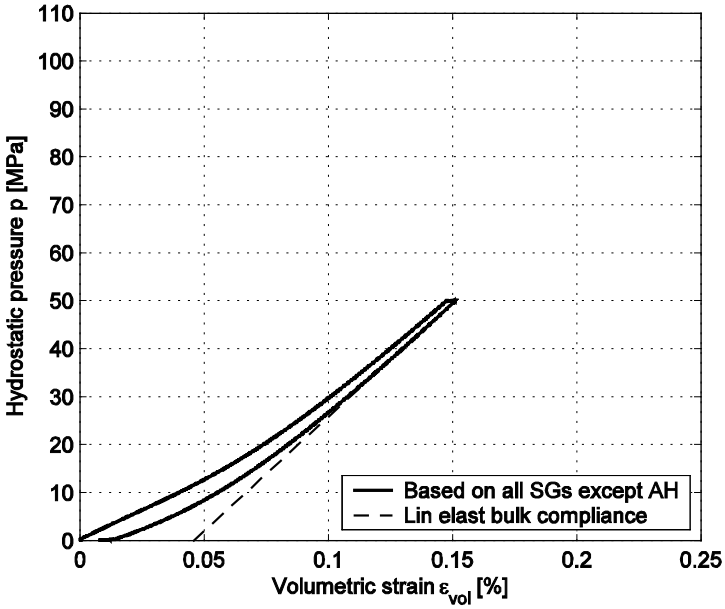

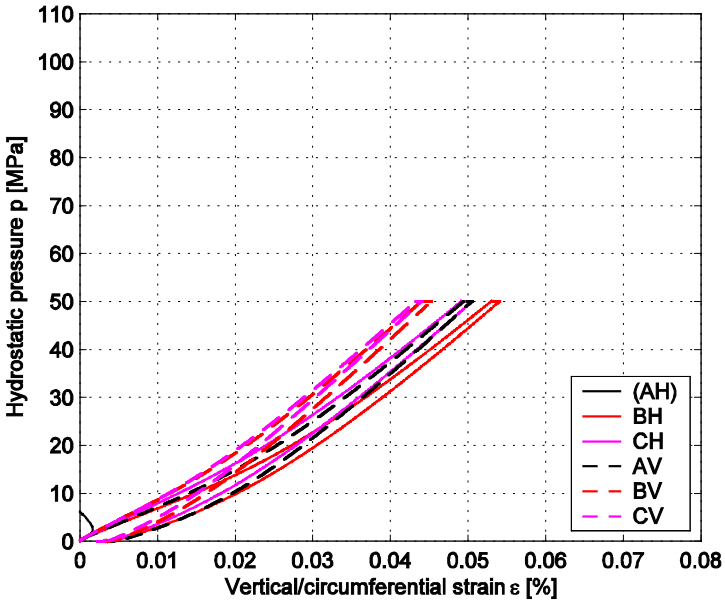

Specimen ID: KFM01A-115-23

Youngs Modulus (E):	74.4	[GPa]	Cell pressure:	10	[MPa]
Poisson Ratio (ν):	0.309	[-]			
Axial peak stress (σ_c):	327.5	[MPa]			

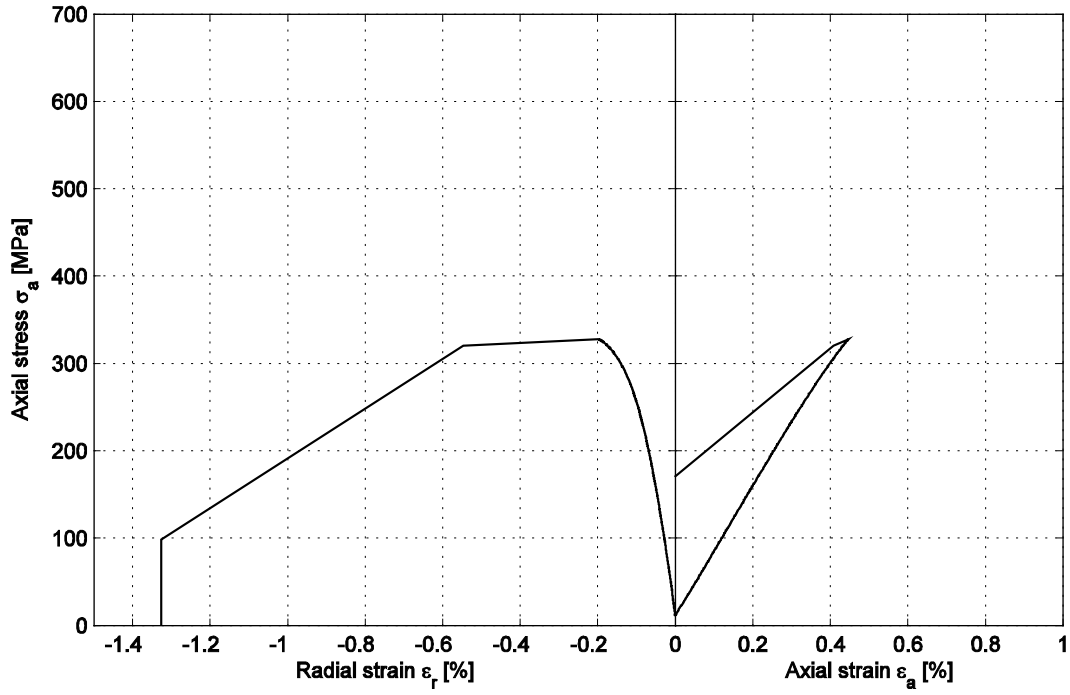

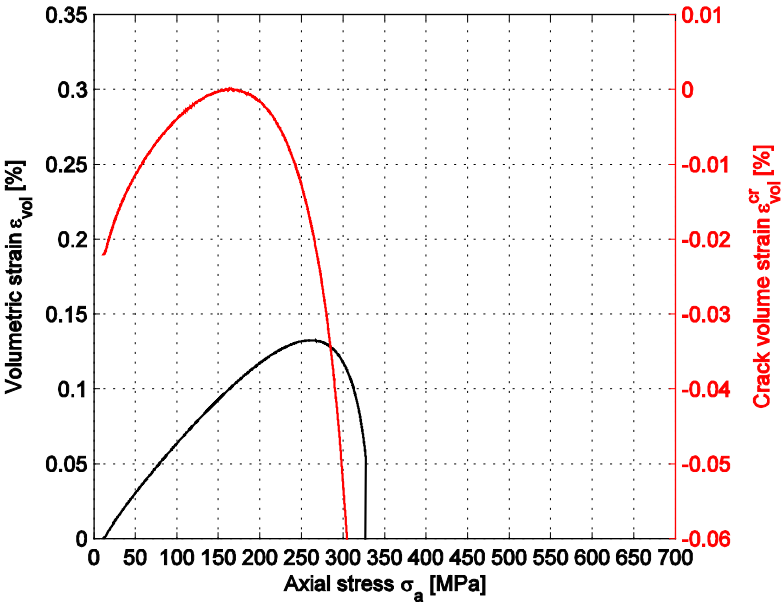

Specimen ID: KFM01A-115-24

Before mechanical test	After mechanical test		
	AV, AH	BV, BH	CV, CH

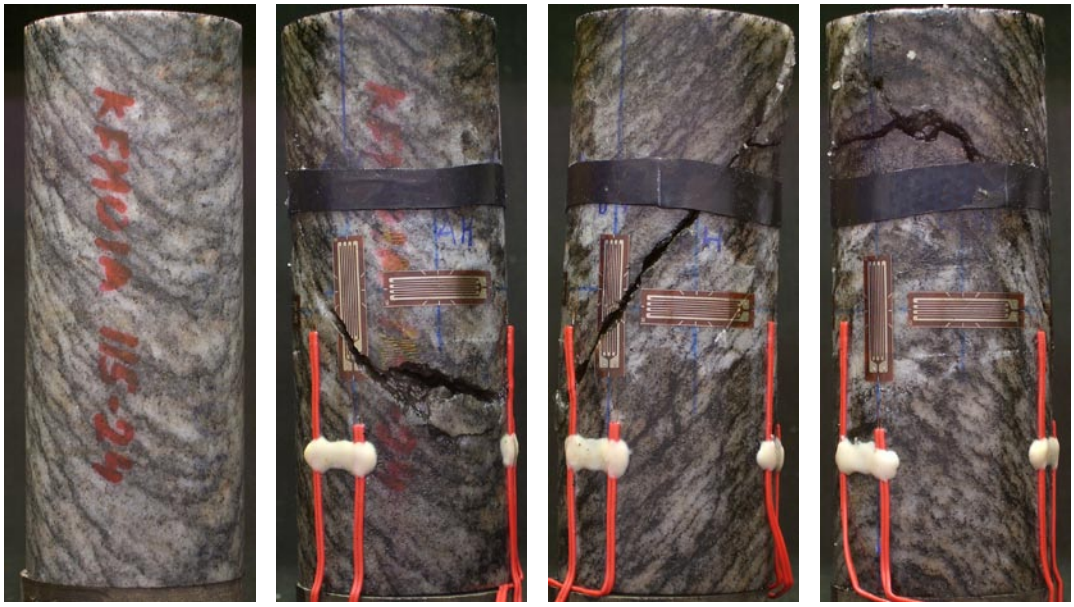

Diameter (mm)	Height (mm)	Density (kg/m^3)
50.8	127.2	2,660

Comments: The specimen has a diagonal shear failure which is following the diagonally oriented material foliations.

Specimen ID: KFM01A-115-24

Bulk compliance (β_{max}): 0.021 [GPa^{-1}]

Microcrack volume (ε_{MC}): 0.078 [%]

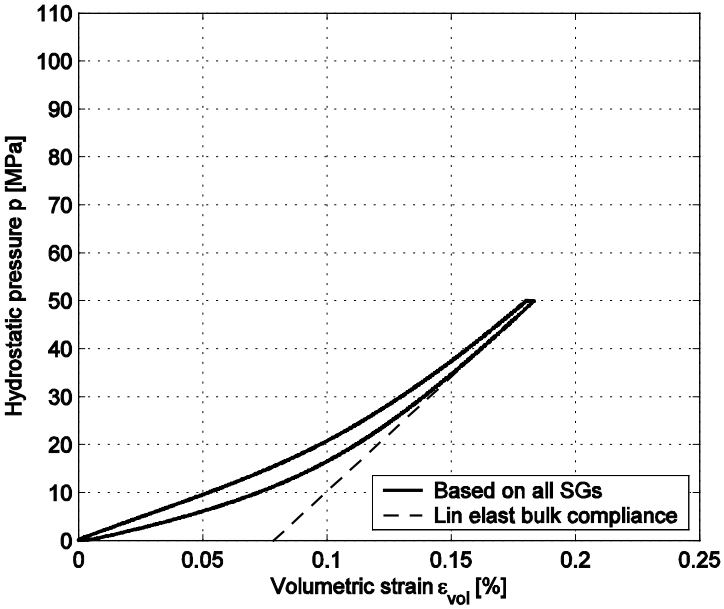

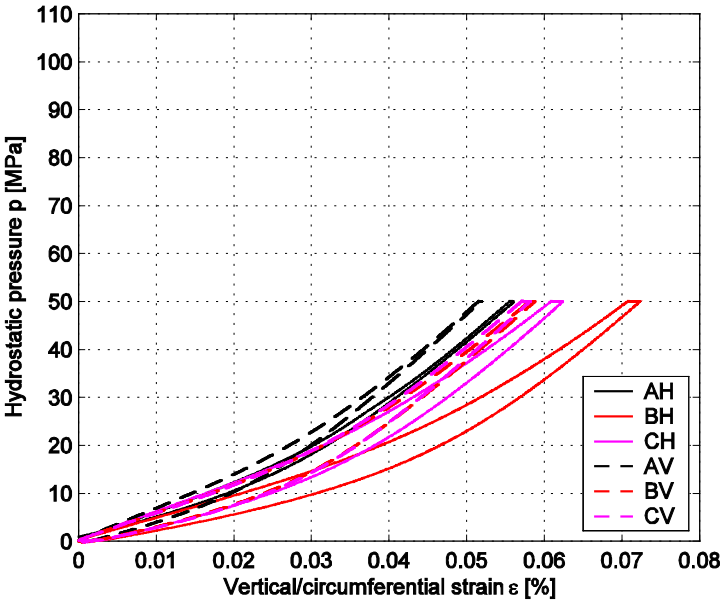

Specimen ID: KFM01A-115-24

Youngs Modulus (E):	77.8	[GPa]	Cell pressure:	50	[MPa]
Poisson Ratio (ν):	0.311	[-]			
Axial peak stress (σ_c):	515.4	[MPa]			

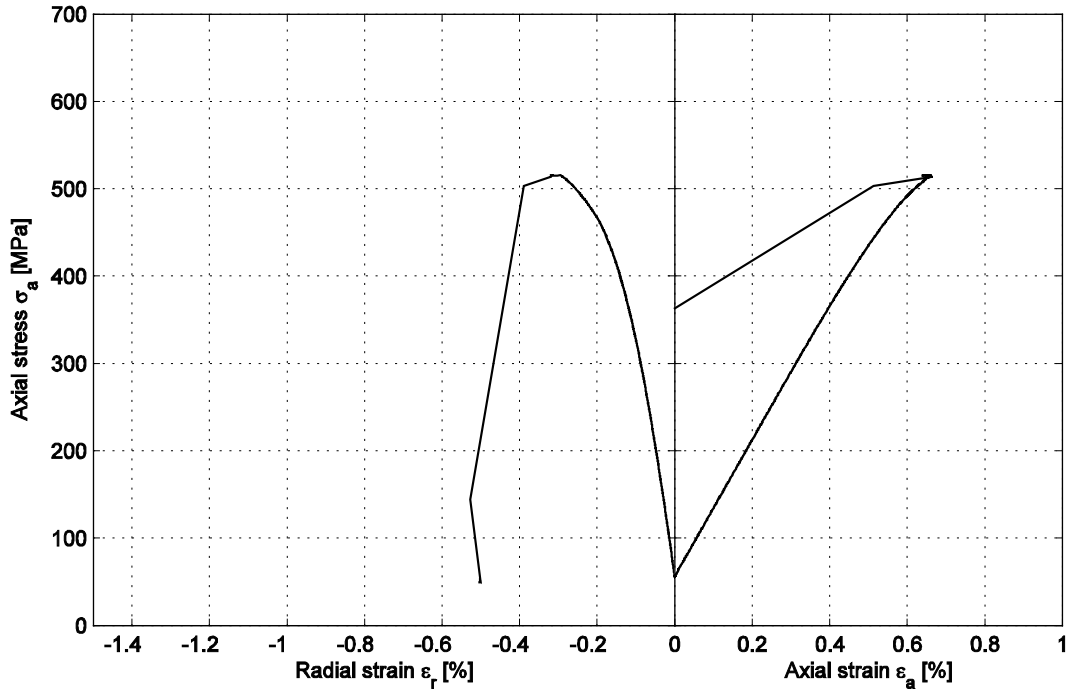

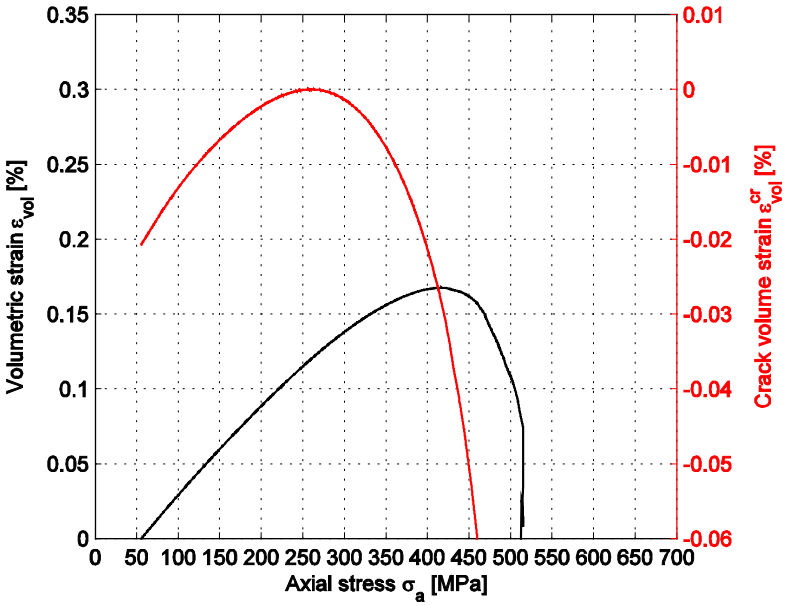

Specimen ID: KFM01A-115-25

Before mechanical test **After mechanical test**

AV, AH BV, BH CV, CH

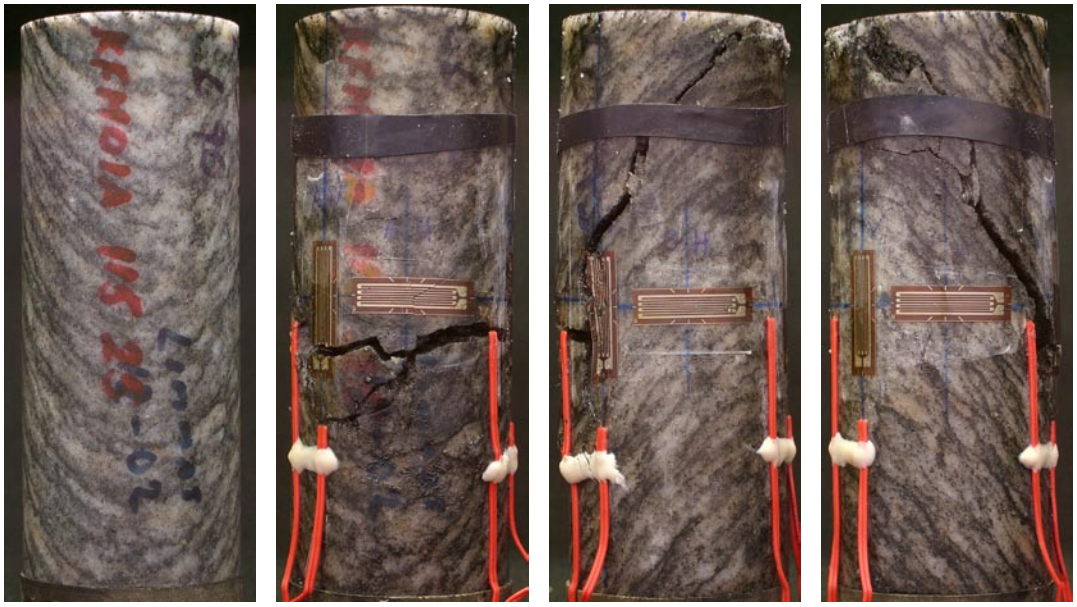

Diameter (mm)	Height (mm)	Density (kg/m³)
50.8	127.4	2,660

Comments: Strain gauge BH seems to have failed during the measurement. The measured strain ε_{BH} has been replaced by the mean value of the strains measured by the strain gauges AH and CH in the volumeteric strain calculation, i.e. $\varepsilon_{BH} = (\varepsilon_{AH} + \varepsilon_{CH}) / 2$. The specimen has a diagonal shear failure which is following the diagonally oriented material foliations.

Specimen ID: KFM01A-115-25

Bulk compliance (β_{max}): 0.0194 [GPa^{-1}]

Microcrack volume (ε_{MC}): 0.054 [%]

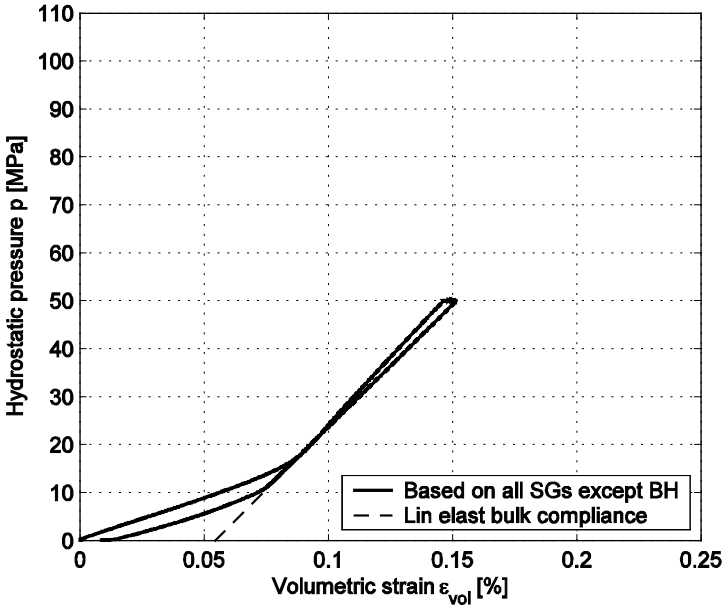

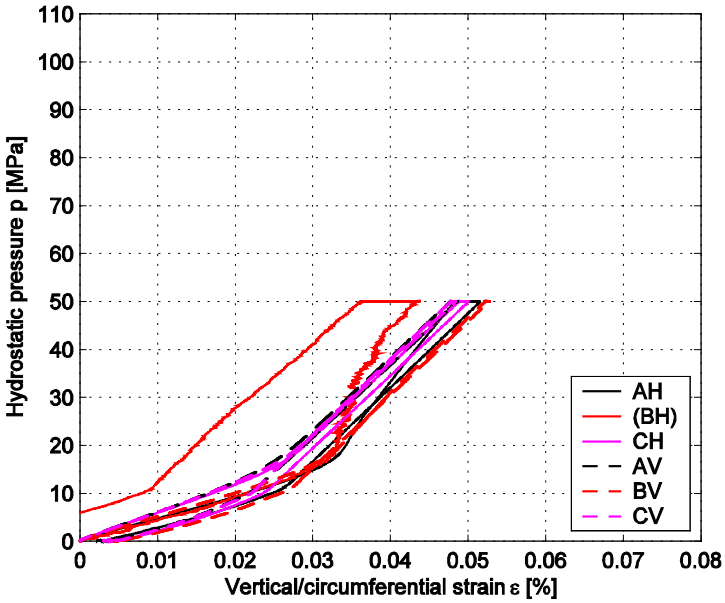

Specimen ID: KFM01A-115-25

Youngs Modulus (E):	74.6	[GPa]	Cell pressure:	10	[MPa]
Poisson Ratio (ν):	0.319	[-]			
Axial peak stress (σ_c):	356.8	[MPa]			

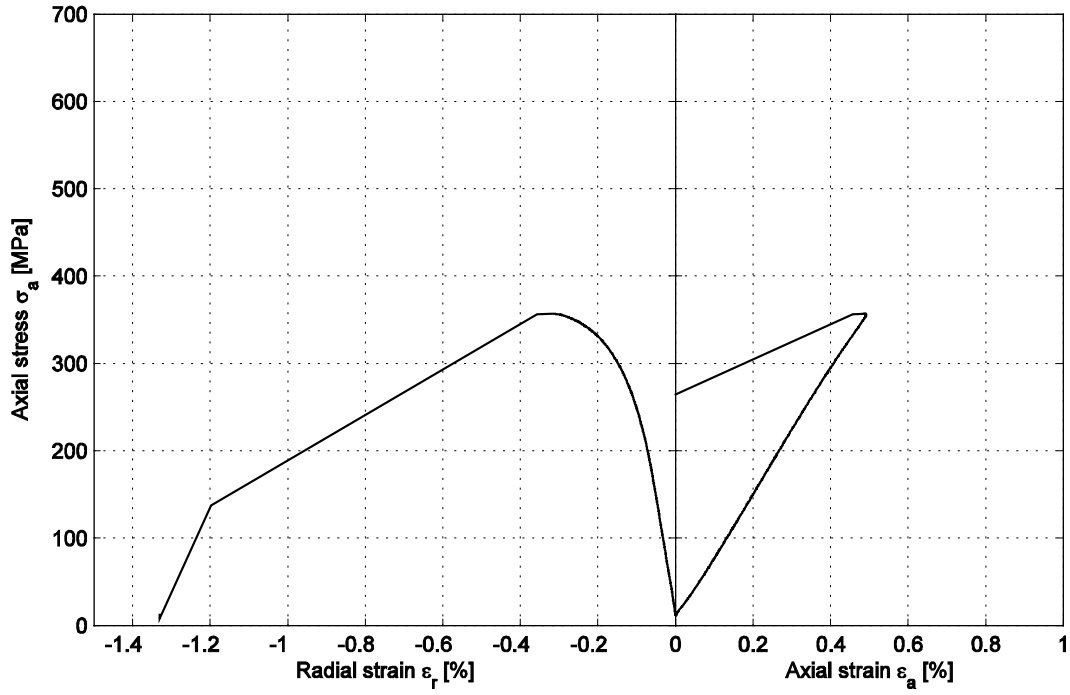

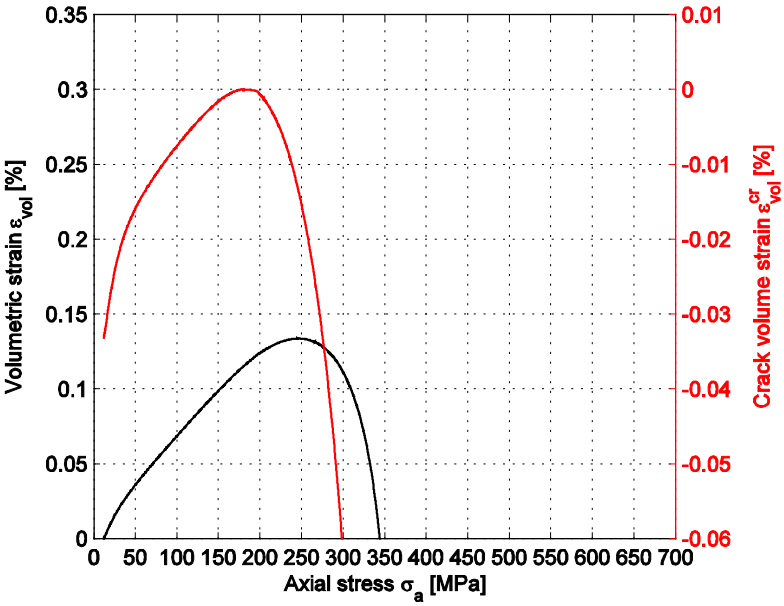

Specimen ID: KFM01A-115-26

Before mechanical test	After mechanical test		
	AV, AH	BV, BH	CV, CH

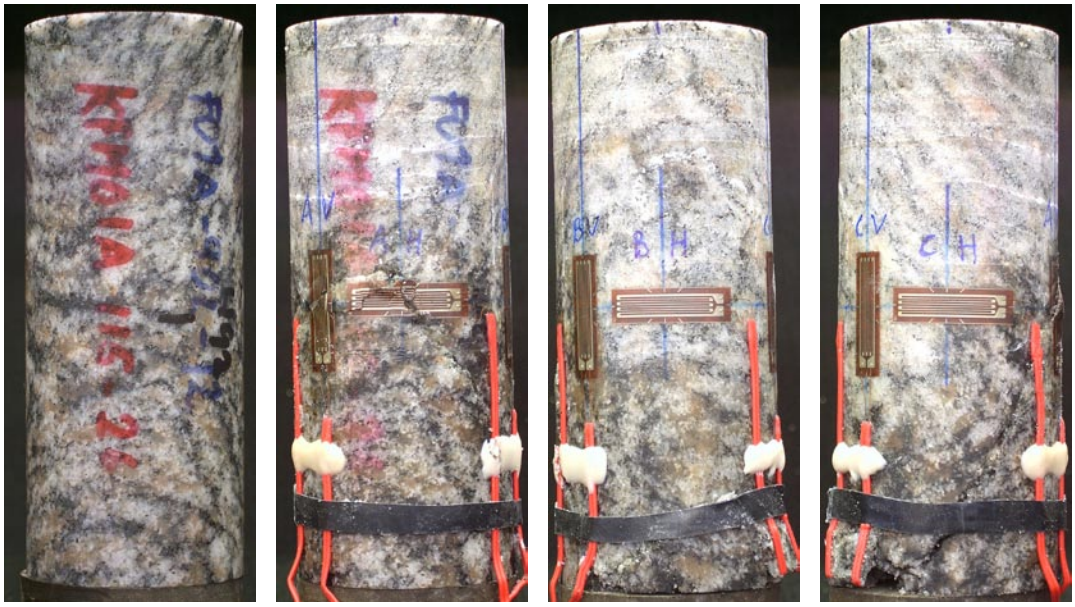

Diameter (mm)	Height (mm)	Density (kg/m^3)
50.8	127.4	2,660

Comments: The specimen has a v-shaped shear failure which is possibly initiated by the diagonally oriented material foliations.

Specimen ID: KFM01A-115-26

Bulk compliance (β_{max}): 0.0207 [GPa^{-1}]

Microcrack volume (ε_{MC}): 0.057 [%]

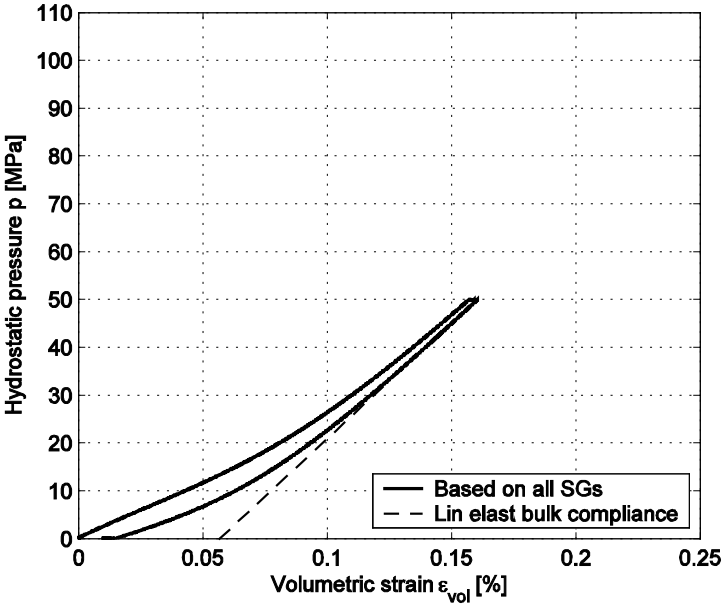

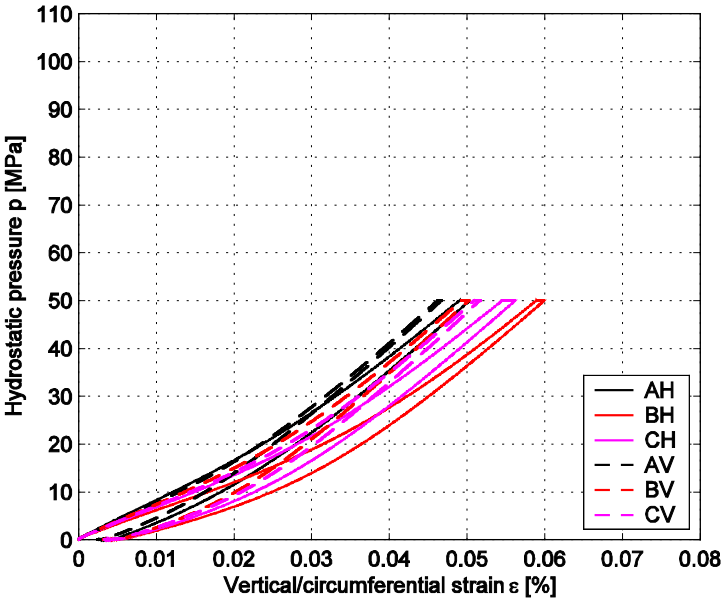

Specimen ID: KFM01A-115-26

Youngs Modulus (E):	77.9	[GPa]	Cell pressure:	50	[MPa]
Poisson Ratio (ν):	0.292	[-]			
Axial peak stress (σ_c):	682.8	[MPa]			

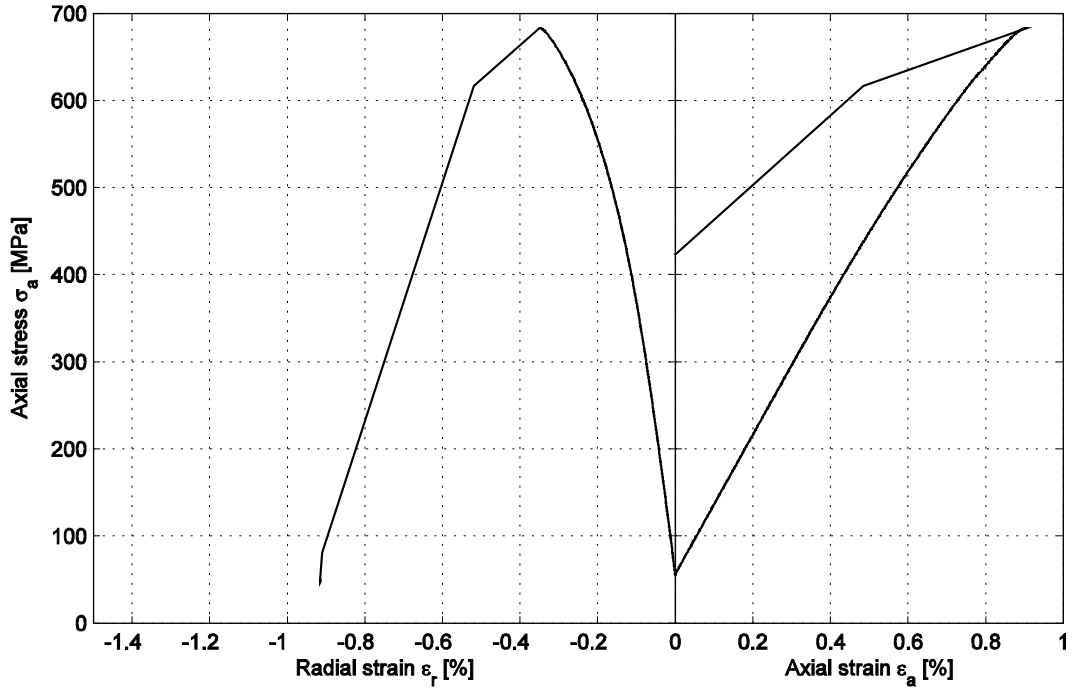

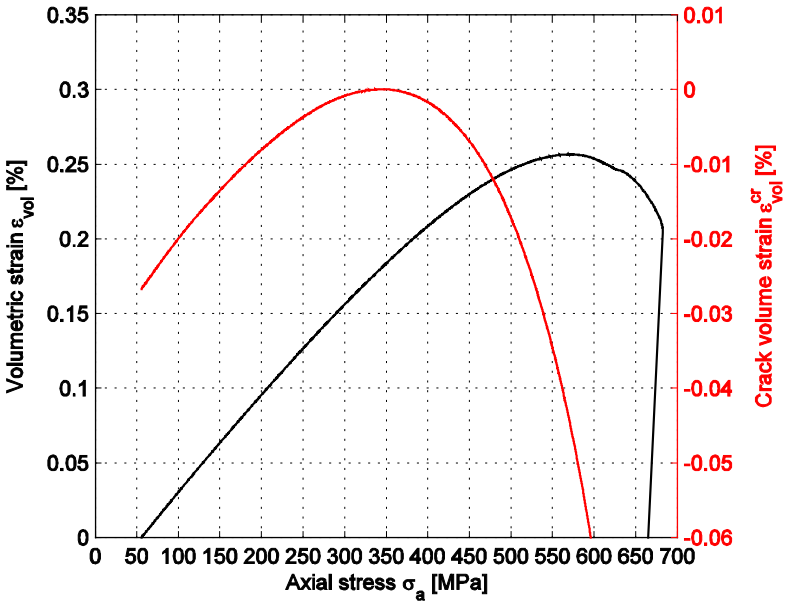

Specimen ID: KFM01A-115-28

Before mechanical test

After mechanical test

AV, AH

BV, BH

CV, CH

Diameter (mm)	Height (mm)	Density (kg/m^3)
51.1	128.8	2,660

Comments: The specimen has a v-shaped shear failure which is possibly initiated by the diagonally oriented material foliations.

Specimen ID: KFM01A-115-28

Bulk compliance (β_{max}): 0.0212 [GPa^{-1}]

Microcrack volume (ε_{MC}): 0.09 [%]

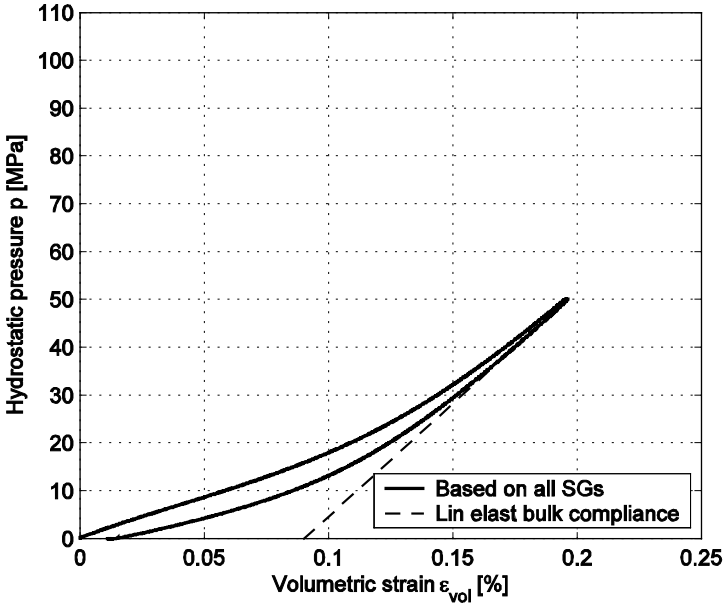

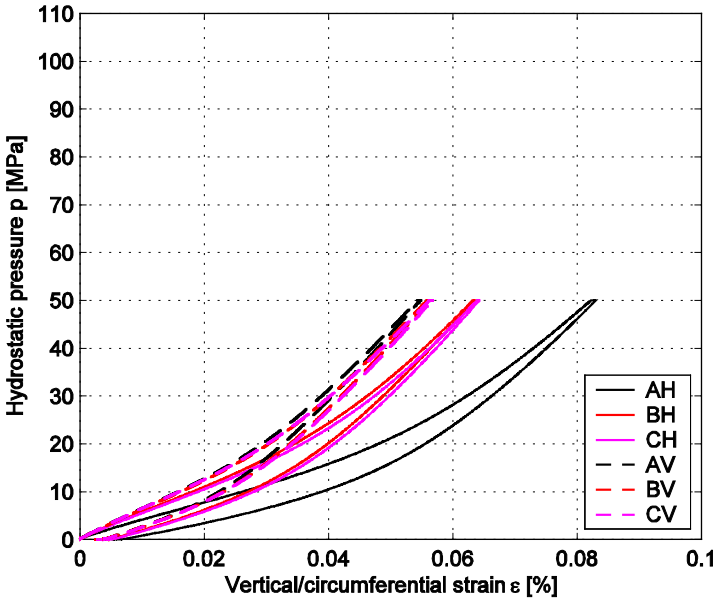

Specimen ID: KFM01A-115-28

Youngs Modulus (E):	73.9	[GPa]	Cell pressure:	10	[MPa]
Poisson Ratio (ν):	0.318	[-]			
Axial peak stress (σ_c):	366	[MPa]			

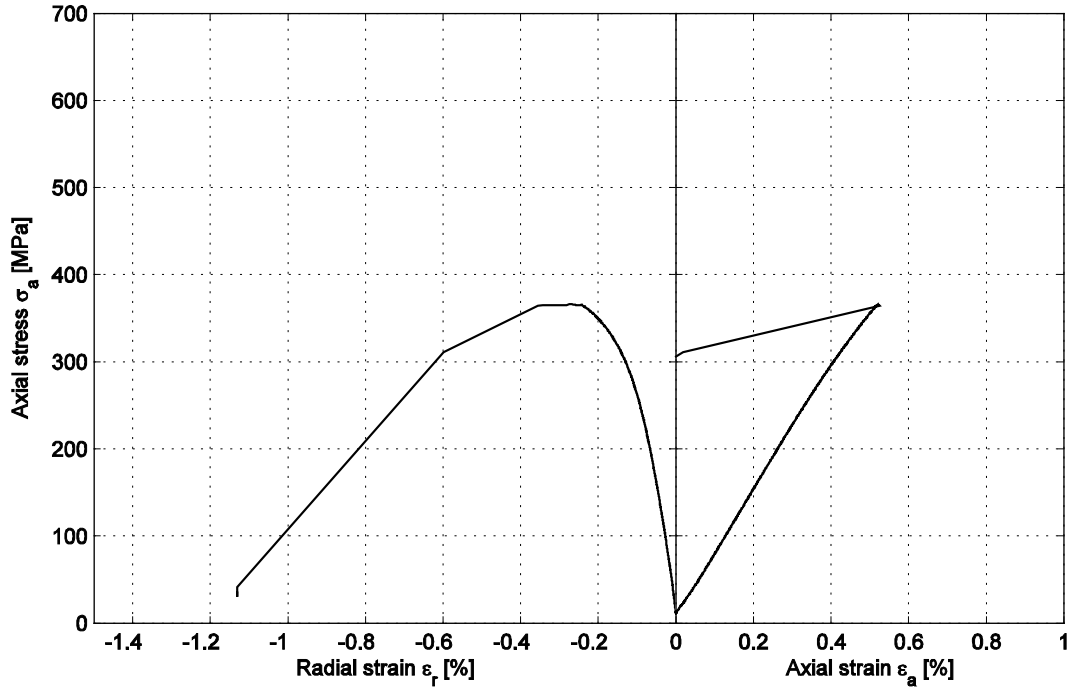

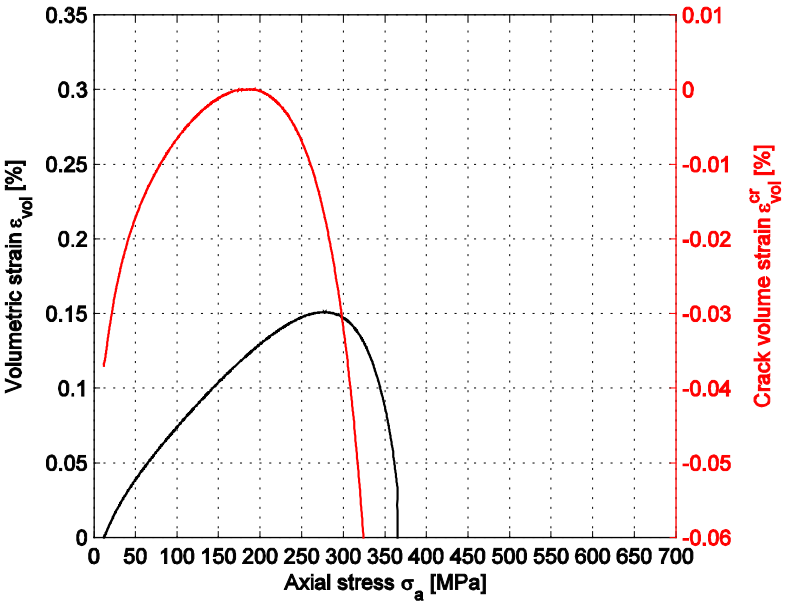

Specimen ID: KFM01A-115-29

Before mechanical test

After mechanical test

AV, AH

BV, BH

CV, CH

Diameter (mm)	Height (mm)	Density (kg/m^3)
51.0	128.6	2,660

Comments: The specimen has a v-shaped shear failure which is possibly initiated by the diagonally oriented material foliations.

Specimen ID: KFM01A-115-29

Bulk compliance (β_{max}): 0.0221 [GPa^{-1}]

Microcrack volume (ε_{MC}): 0.119 [%]

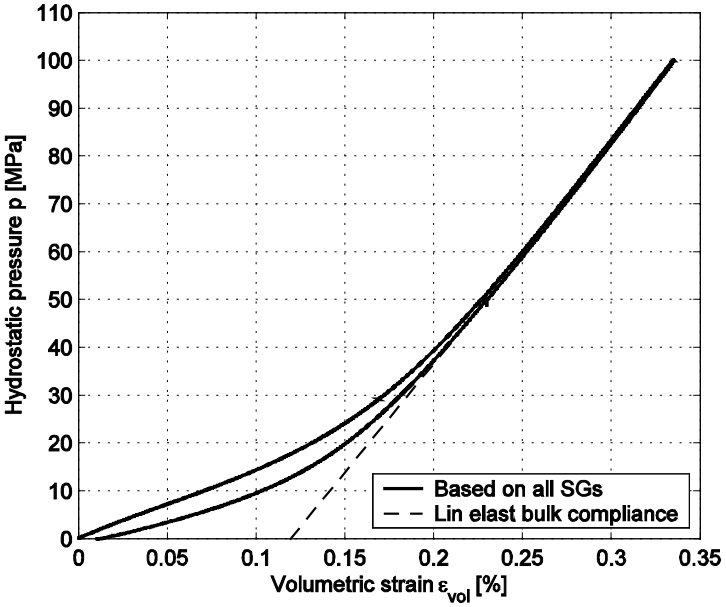

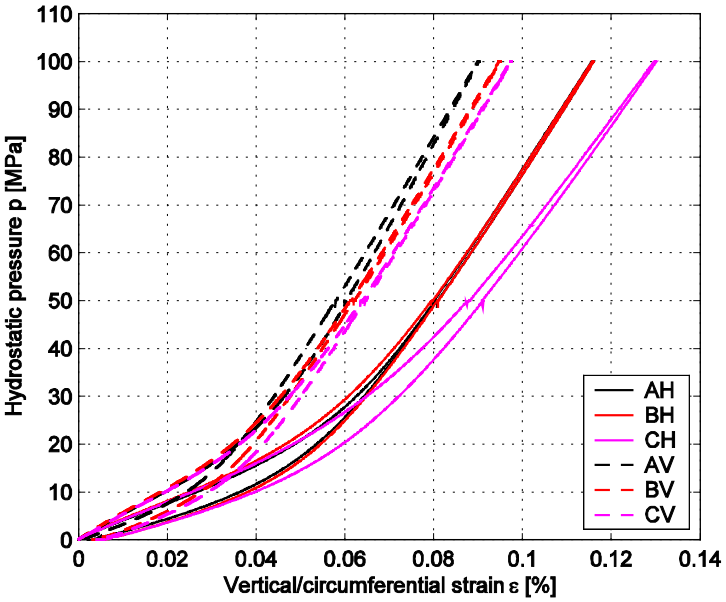

Specimen ID: KFM01A-115-29

Youngs Modulus (E):	76.9	[GPa]	Cell pressure:	50	[MPa]
Poisson Ratio (ν):	0.318	[-]			
Axial peak stress (σ_c):	722.3	[MPa]			

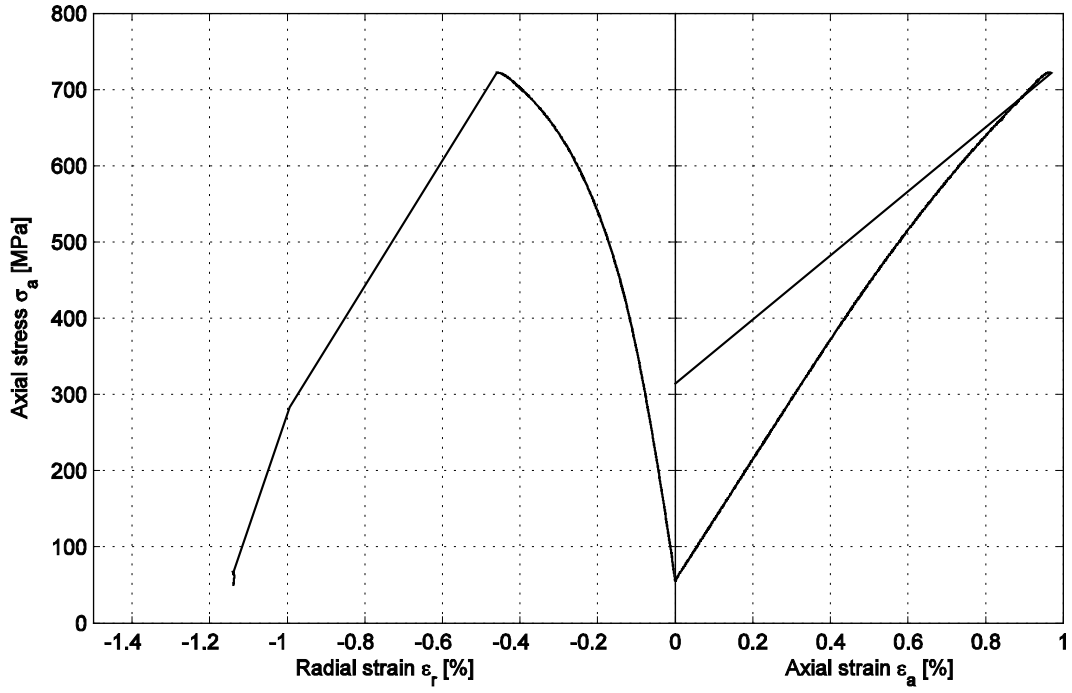

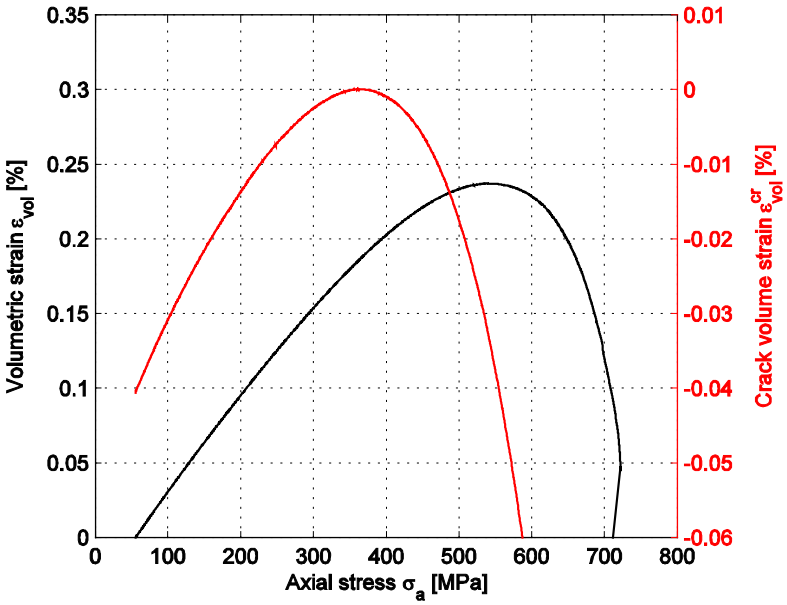

5.3 Results from mechanical tests for each individual specimen – KFM02B

Pictures taken on the specimens before and after the mechanical test are presented below together with comments on observations made during testing. Results graphs from both the hydrostatic and triaxial compression tests are shown. The text “Based on all SGs” in the legend for the hydrostatic compression tests means that the results are computed using values from all strain gauges and evaluated according to (1)–(3). Moreover, the labels for strain gauges that have failed during the hydrostatic compression test are put in brackets in the legends in the results diagrams. The strain results are adjusted with respect to the active lateral pressure according to Section 4.6. The results for the individual specimens are as follows:

Specimen ID: KFM02B-115-1

Before mechanical test **After mechanical test**

AV, AH BV, BH CV, CH

Diameter (mm)	Height (mm)	Density (kg/m³)
50.1	126.5	–

Comments: Strain gauge BH has failed during the measurement. The measured strain ε_{BH} has been replaced by the mean value of the strains measured by the strain gauges AH and CH in the volumeteric strain calculation, i.e. $\varepsilon_{BH} = (\varepsilon_{AH} + \varepsilon_{CH}) / 2$. The specimen has a diagonal shear failure.

Specimen ID: KFM02B-115-1

Bulk compliance (β_{max}): 0.0201 [GPa^{-1}]

Microcrack volume (ε_{MC}): 0.021 [%]

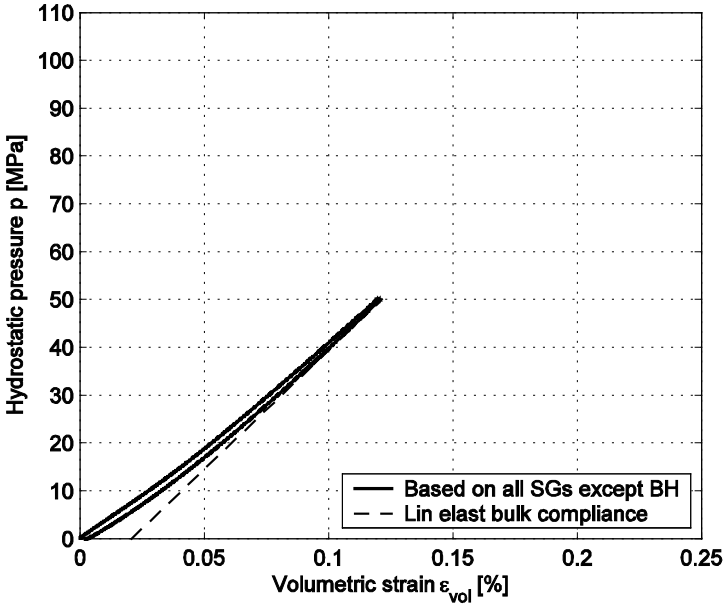

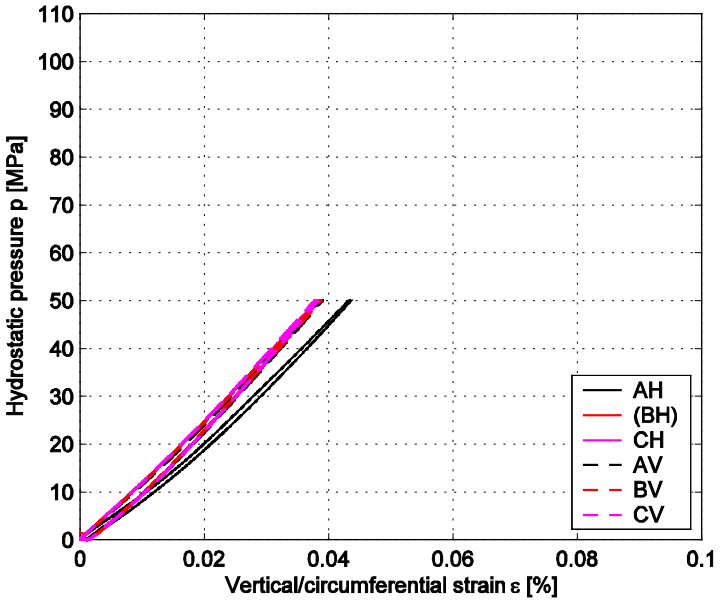

Specimen ID: KFM02B-115-1

Youngs Modulus (E):	71.4	[GPa]	Cell pressure:	10	[MPa]
Poisson Ratio (ν):	0.324	[-]			
Axial peak stress (σ_c):	365.2	[MPa]			

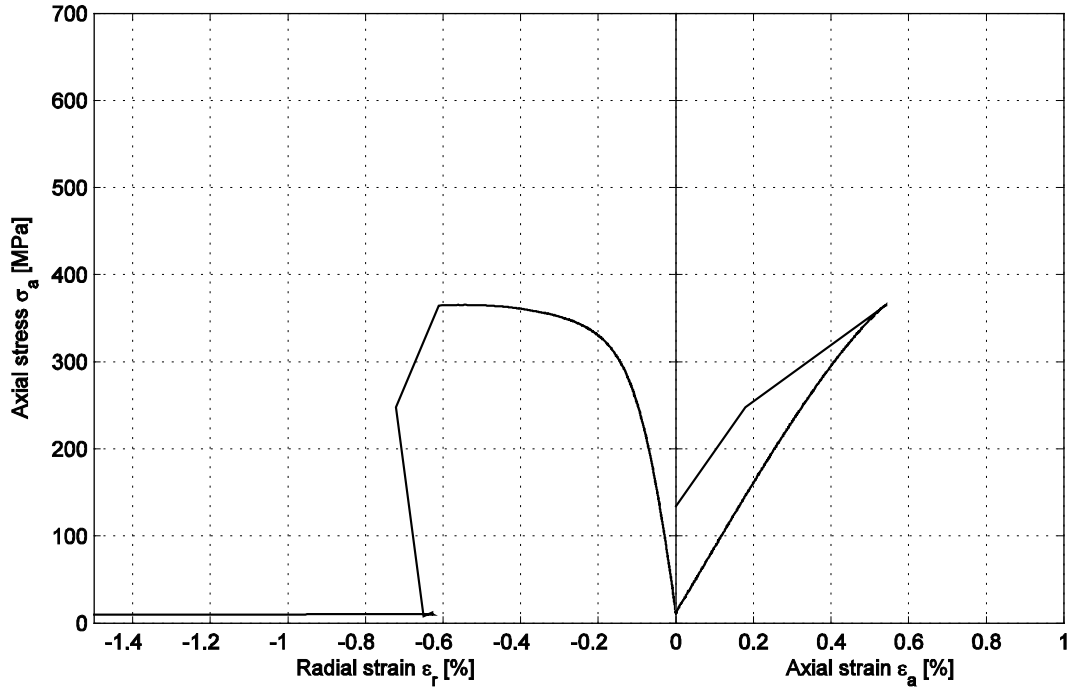

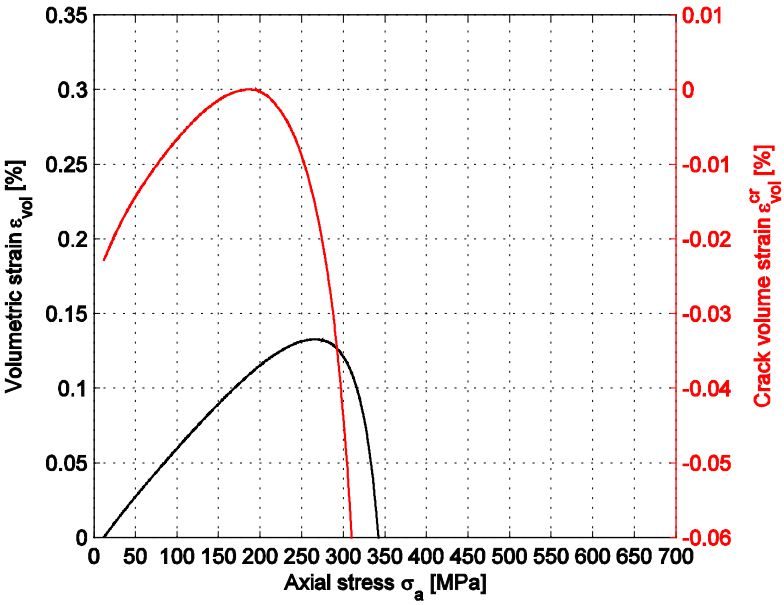

Specimen ID: KFM02B-115-2

Before mechanical test **After mechanical test**

AV, AH BV, BH CV, CH

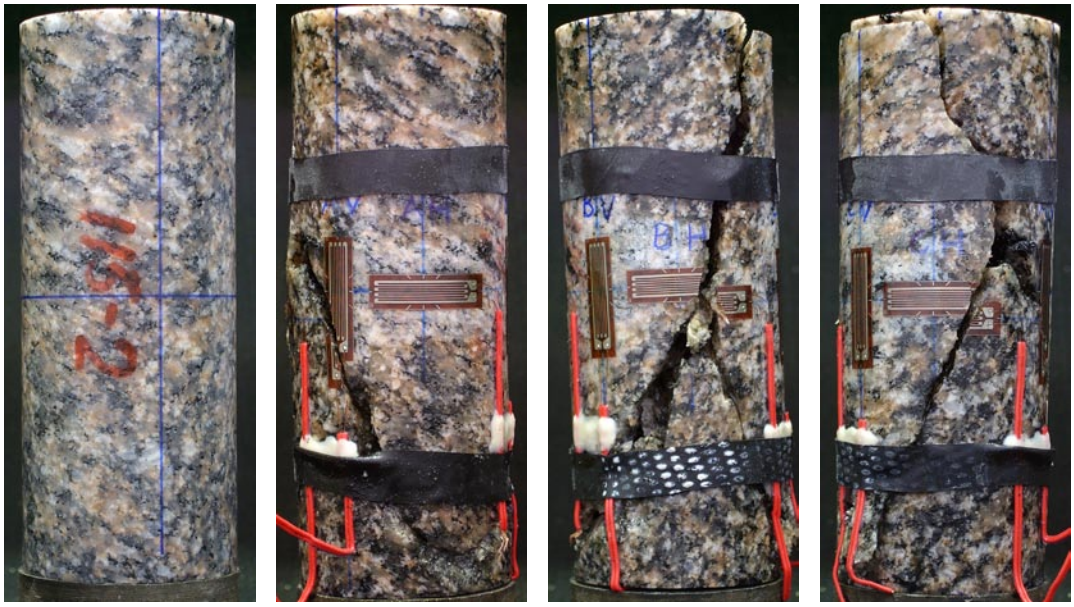

Diameter (mm)	Height (mm)	Density (kg/m³)
50.1	127.1	–

Comments: The specimen has a v-shaped shear failure which is partly following the diagonally oriented material foliations.

Specimen ID: KFM02B-115-2

Bulk compliance (β_{max}): 0.0207 [GPa^{-1}]

Microcrack volume (ε_{MC}): 0.03 [%]

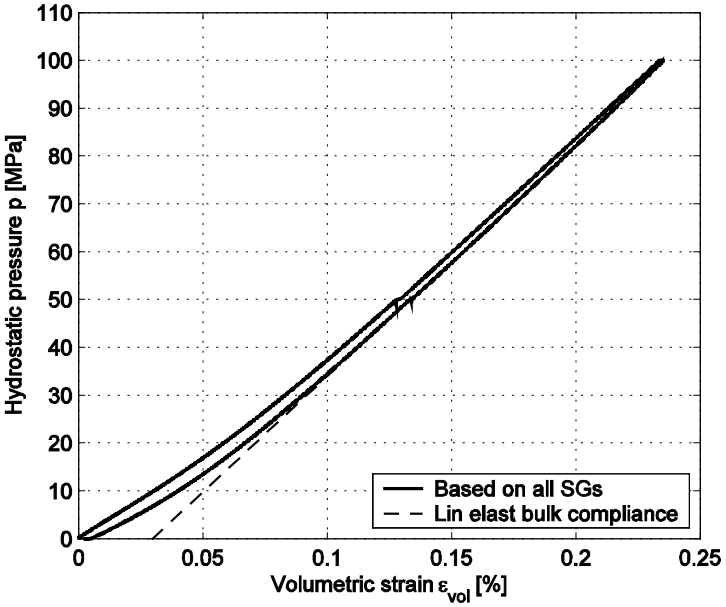

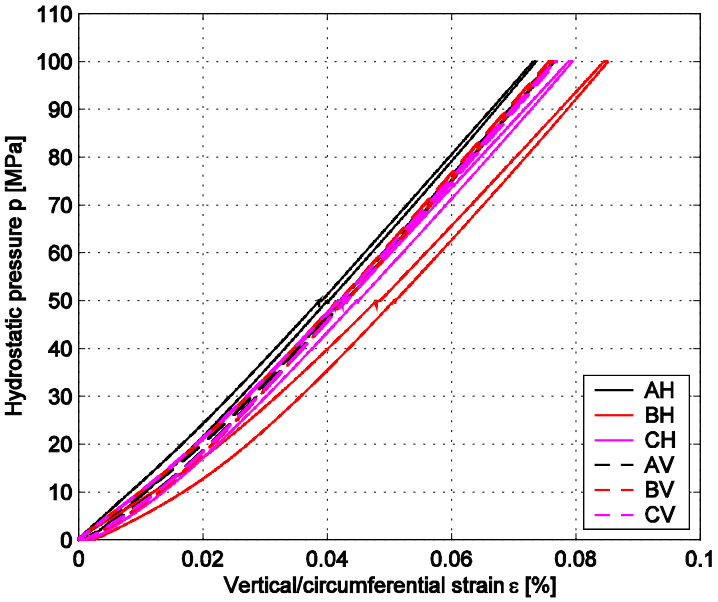

Specimen ID: KFM02B-115-2

Youngs Modulus (E):	73.1	[GPa]	Cell pressure:	50	[MPa]
Poisson Ratio (ν):	0.287	[-]			
Axial peak stress (σ_c):	619	[MPa]			

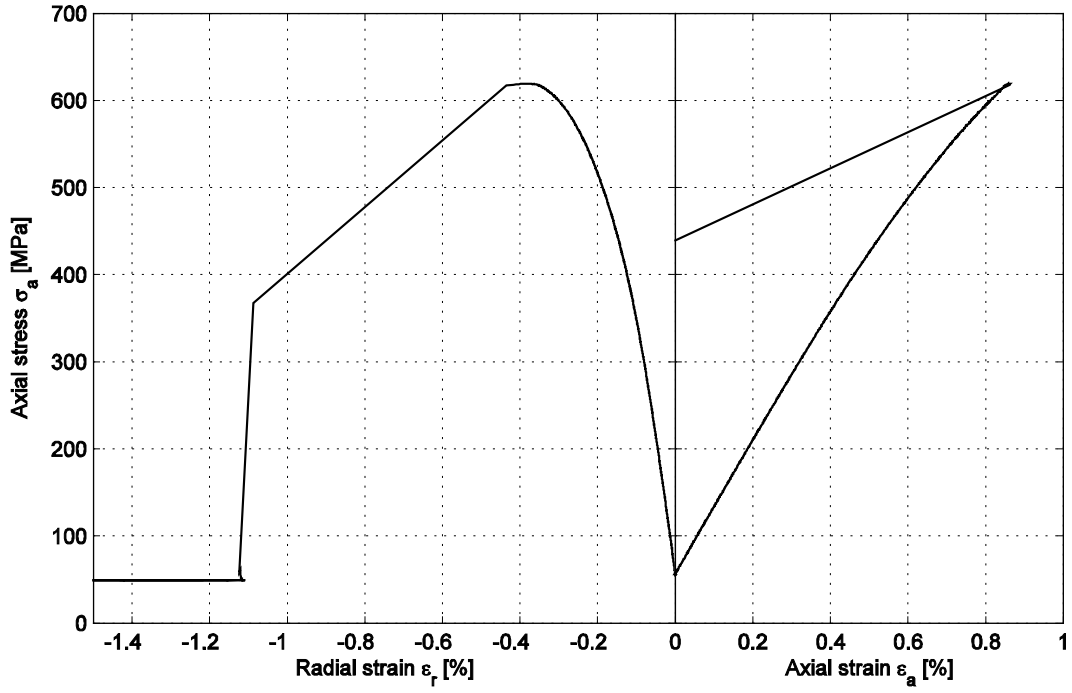

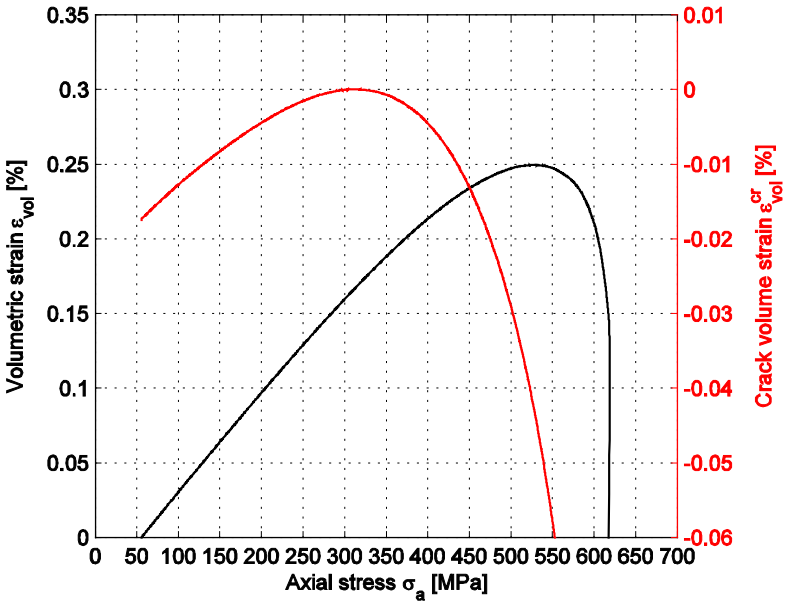

Specimen ID: KFM02B-115-4

Before mechanical test

After mechanical test

AV, AH

BV, BH

CV, CH

Diameter (mm)	Height (mm)	Density (kg/m³)
50.2	125.3	–

Comments: The gauge channel AV displays a noicy signal due to an intermittent contact in the connector for the strain gauge during the hydrostatic compresion test. The measured strain ε_{AV} has therefore been replaced by the mean value of the strains measured by the strain gauges BV and CV in the volumeteric strain calculation, i.e. $\varepsilon_{AV} = (\varepsilon_{BV} + \varepsilon_{CV}) / 2$. A diagonal shear failure is observed after the triaxial compression test.

Specimen ID: KFM02B-115-4

Bulk compliance (β_{max}): 0.0209 [GPa^{-1}]

Microcrack volume (ε_{MC}): 0.024 [%]

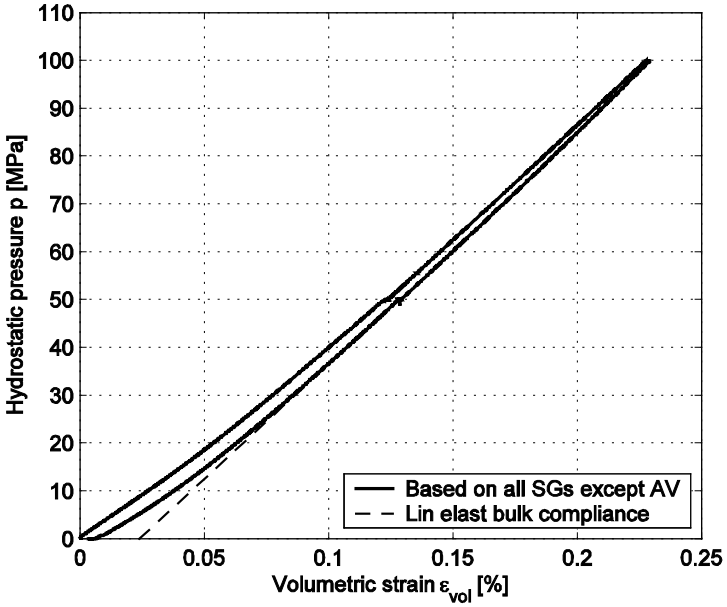

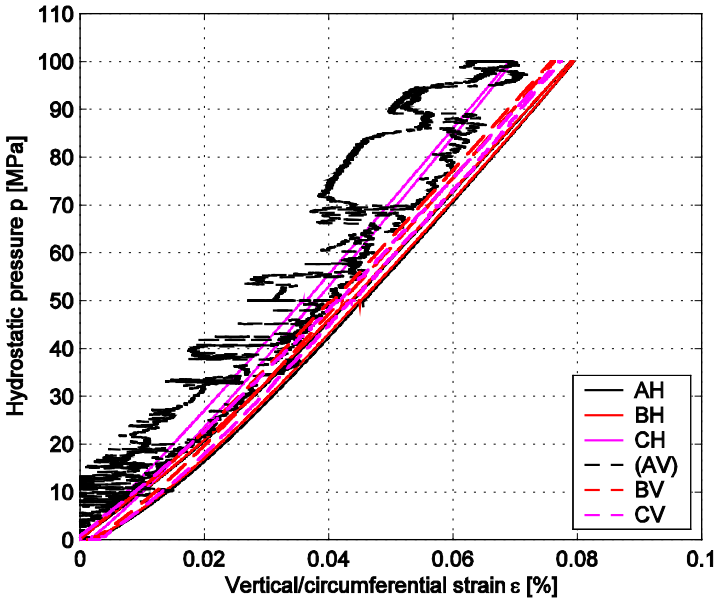

Specimen ID: KFM02B-115-4

Youngs Modulus (E):	80.1	[GPa]	Cell pressure:	50	[MPa]
Poisson Ratio (ν):	0.344	[-]			
Axial peak stress (σ_c):	642.8	[MPa]			

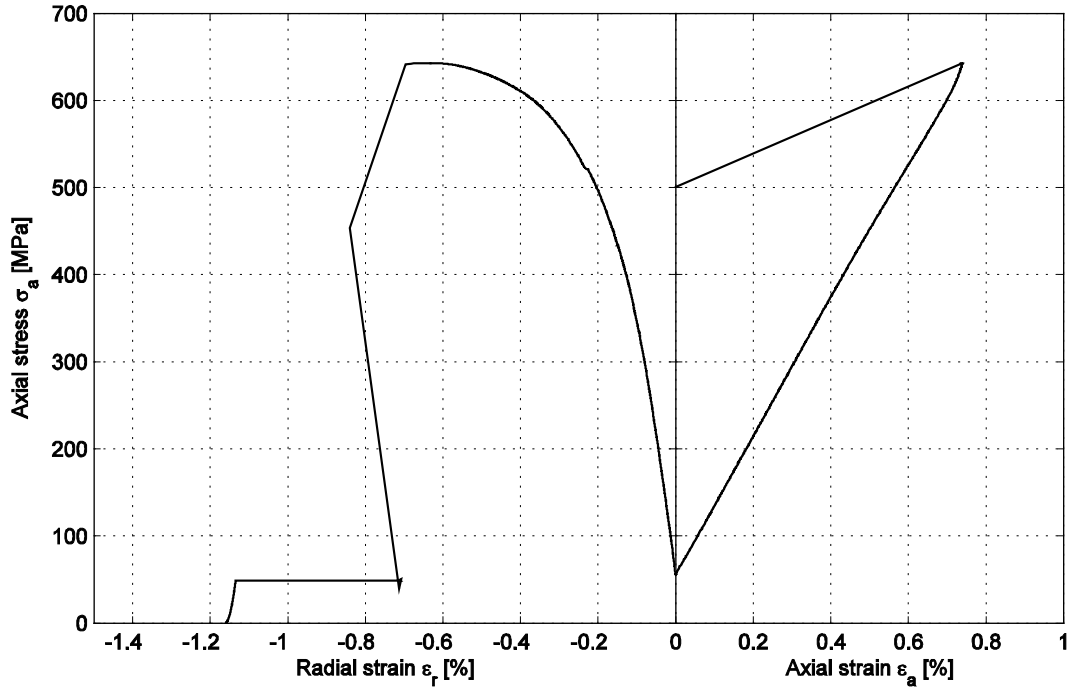

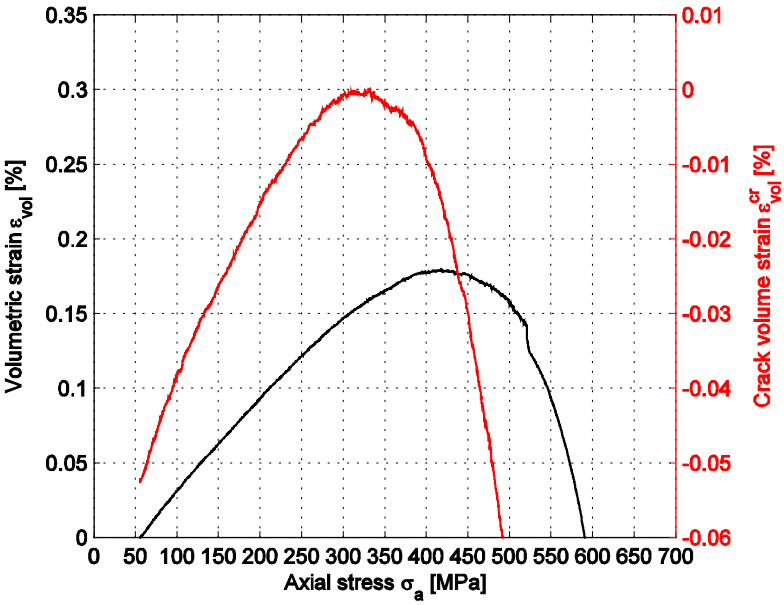

Specimen ID: KFM02B-115-5

Before mechanical test

After mechanical test

AV, AH

BV, BH

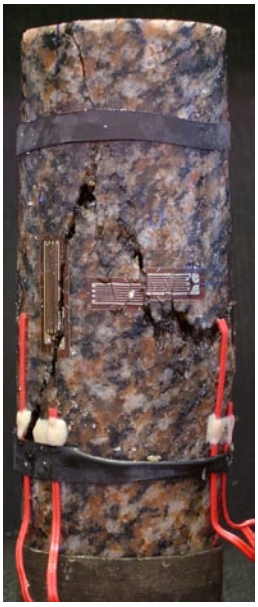

CV, CH

Diameter (mm)	Height (mm)	Density (kg/m^3)
50.2	125.6	–

Comments: The measured strain from strain gauge AV during the very first part of the hydrostatic loading indicates that there may be a slight error with this measurement. The measured strain ε_{AV} has therefore been replaced by the mean value of the strains measured by the strain gauges BV and CV in the volumeteric strain calculation, i.e. $\varepsilon_{AV} = (\varepsilon_{BV} + \varepsilon_{CV}) / 2$. The specimen has a v-shaped shear failure which is partly following the diagonally oriented material foliations.

Specimen ID: KFM02B-115-5

Bulk compliance (β_{max}): 0.0203 [GPa^{-1}]

Microcrack volume (ε_{MC}): 0.038 [%]

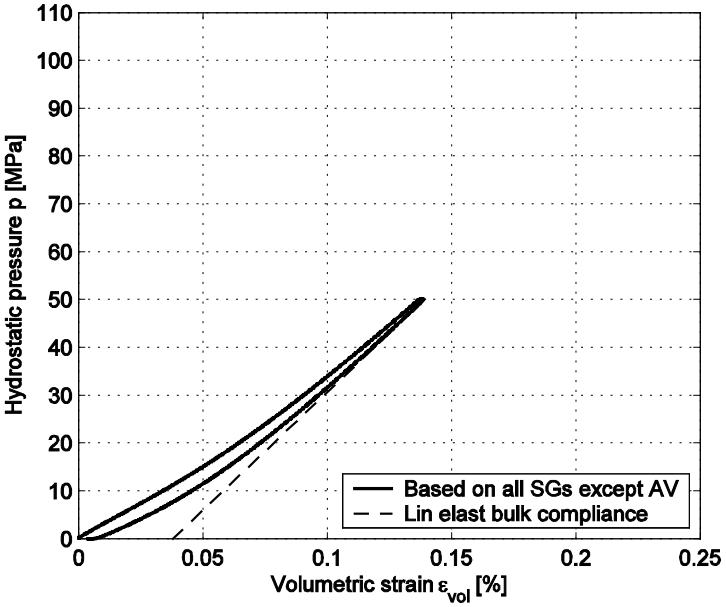

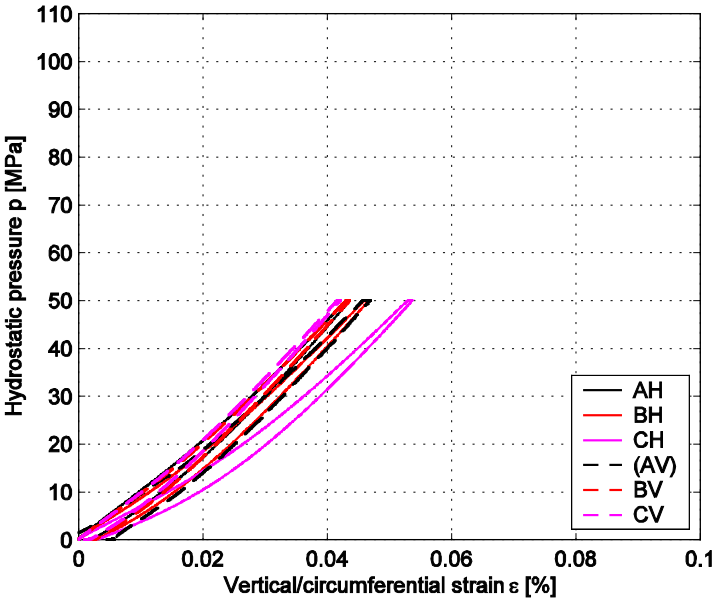

Specimen ID: KFM02B-115-5

Youngs Modulus (E):	72.1	[GPa]	Cell pressure:	10	[MPa]
Poisson Ratio (ν):	0.314	[-]			
Axial peak stress (σ_c):	364.8	[MPa]			

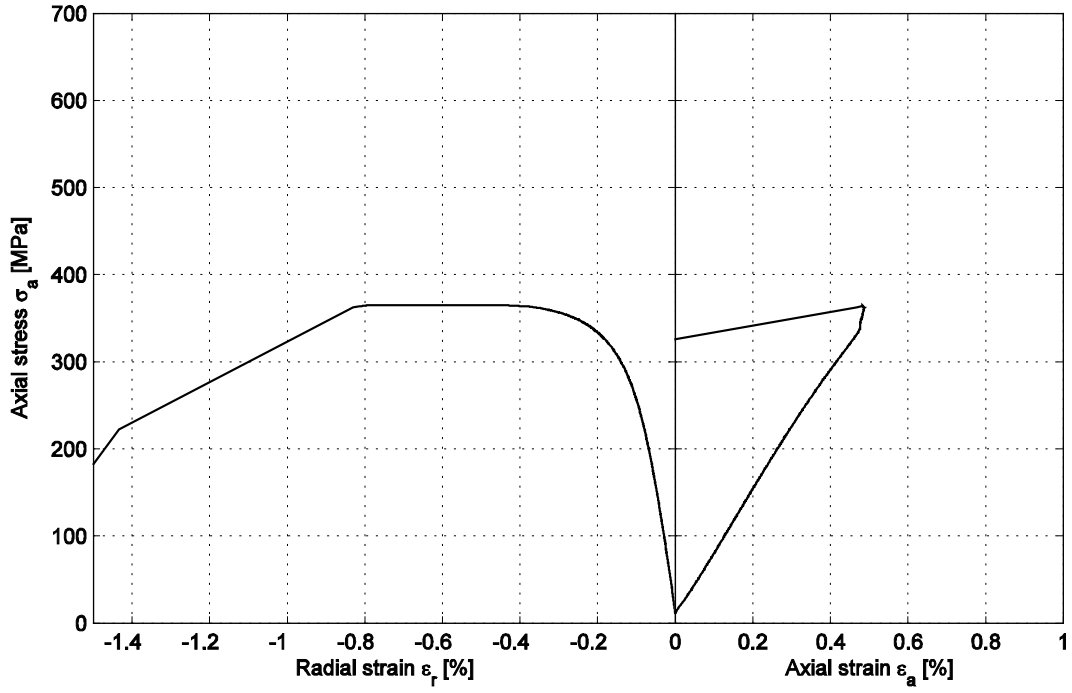

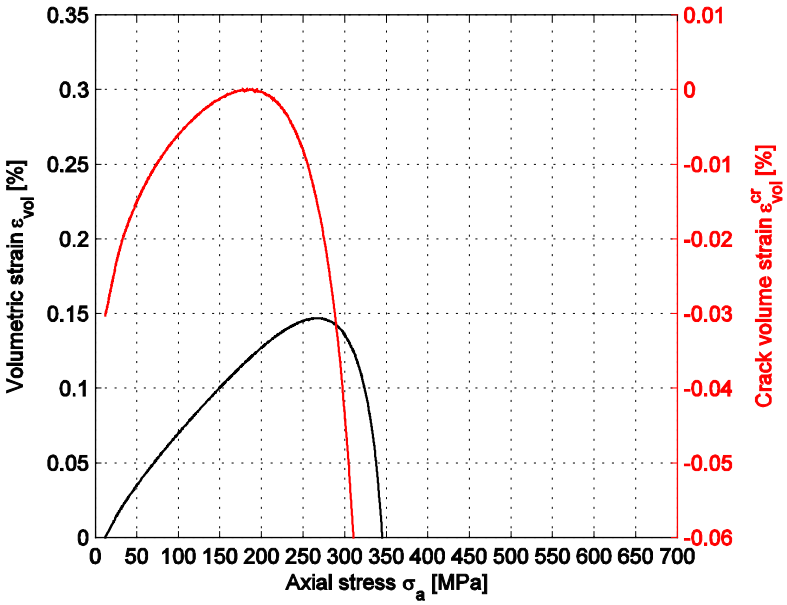

Specimen ID: KFM02B-115-6

Before mechanical test

After mechanical test

AV, AH

BV, BH

CV, CH

Diameter (mm)	Height (mm)	Density (kg/m^3)
50.2	126.2	–

Comments: The specimen has a diagonal shear failure which is following the diagonally oriented material foliations.

Specimen ID: KFM02B-115-6

Bulk compliance (β_{max}): 0.0205 [GPa^{-1}]

Microcrack volume (ε_{MC}): 0.041 [%]

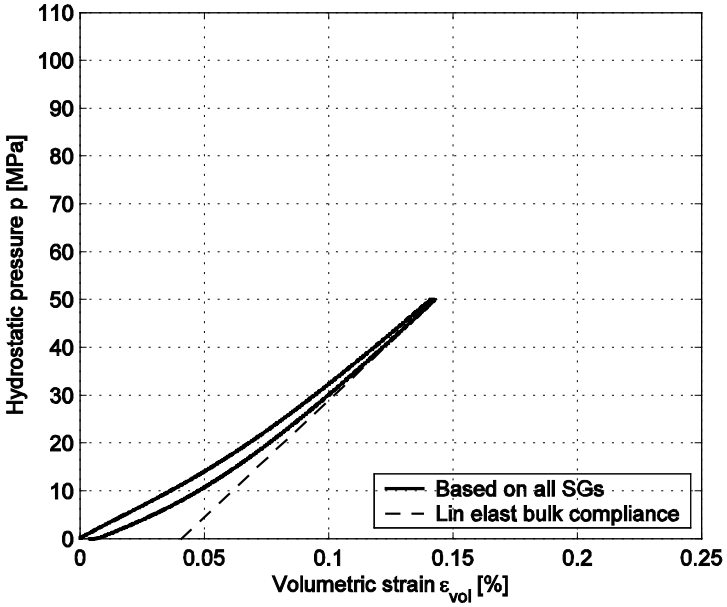

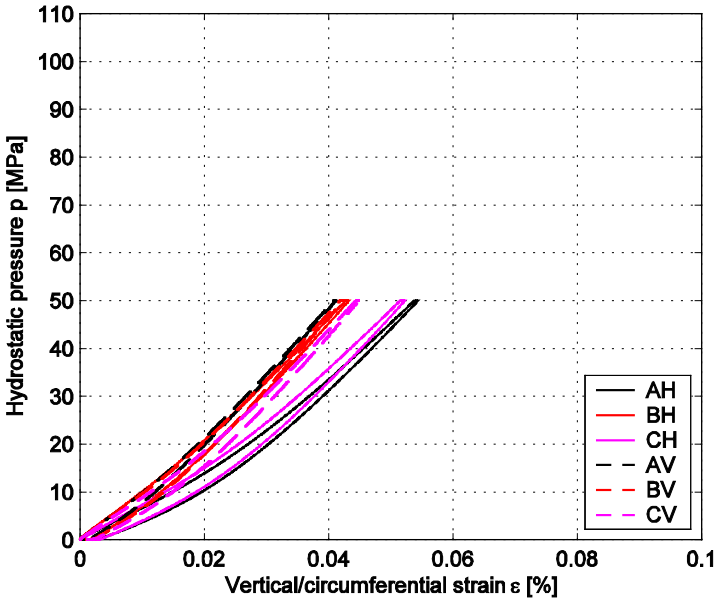

Specimen ID: KFM02B-115-6

Youngs Modulus (E):	70.2	[GPa]	Cell pressure:	10	[MPa]
Poisson Ratio (ν):	0.3	[-]			
Axial peak stress (σ_c):	342.8	[MPa]			

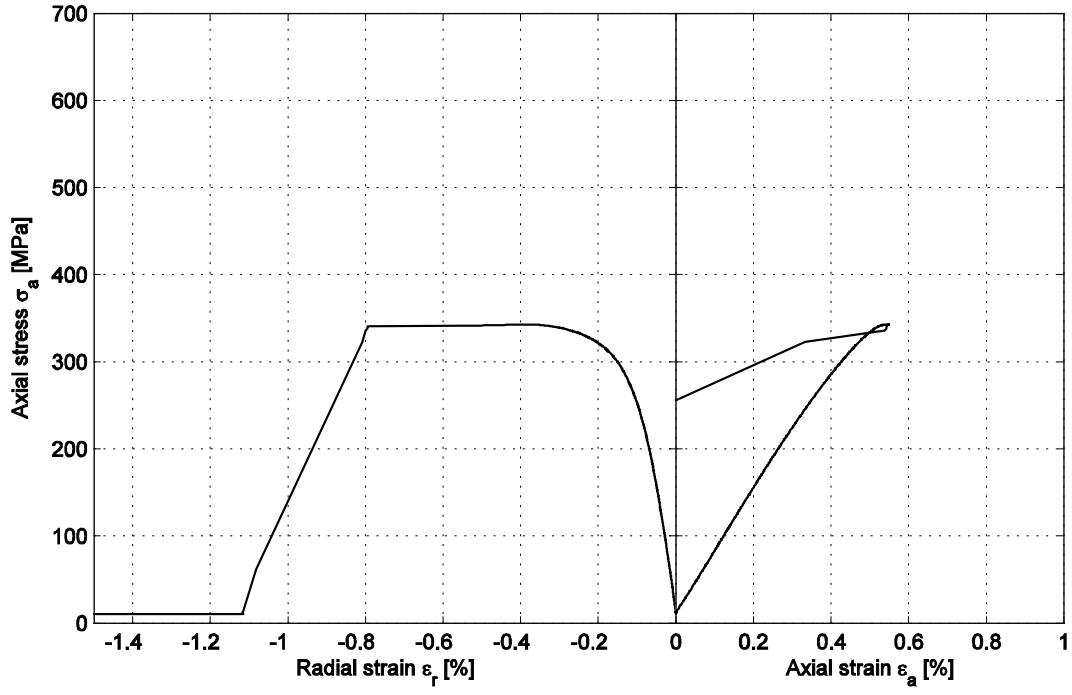

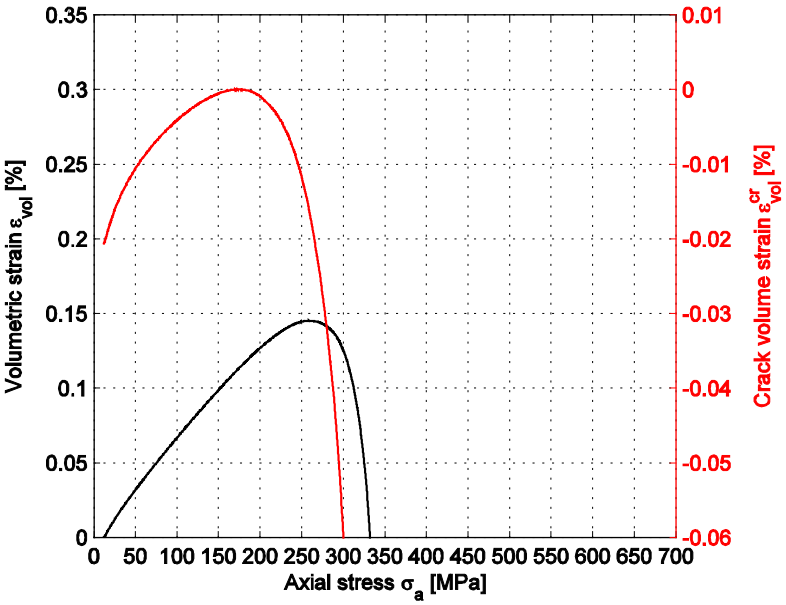

Specimen ID: KFM02B-115-6B

Before mechanical test

After mechanical test

AV, AH

BV, BH

CV, CH

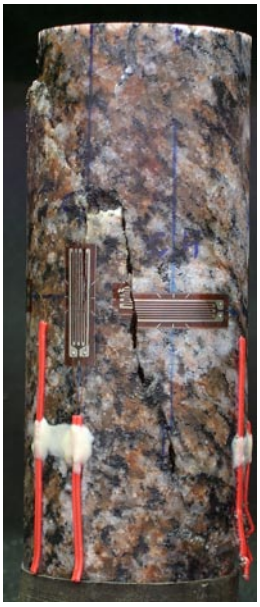

Diameter (mm)	Height (mm)	Density (kg/m^3)
50.2	129.0	2,660

Comments: The specimen has a diagonal shear failure which is following the diagonally oriented material foliations.

Specimen ID: KFM02B-115-6B

Bulk compliance (β_{max}): 0.0205 [GPa^{-1}]

Microcrack volume (ε_{MC}): 0.041 [%]

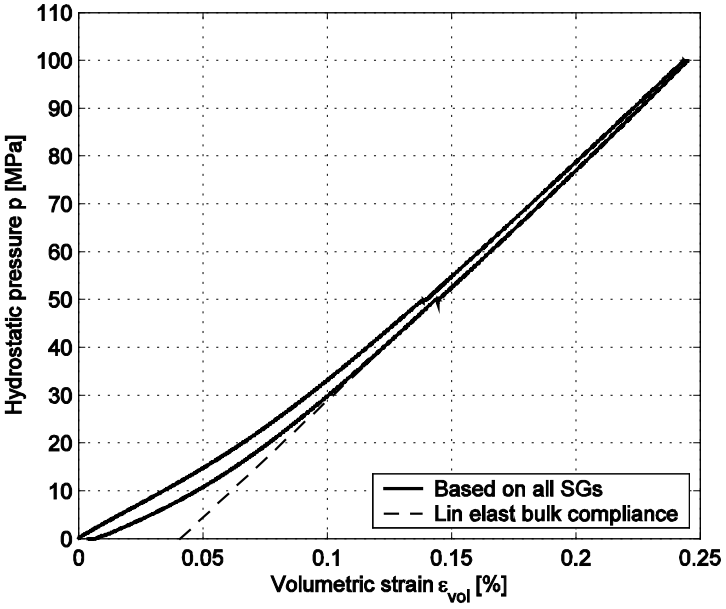

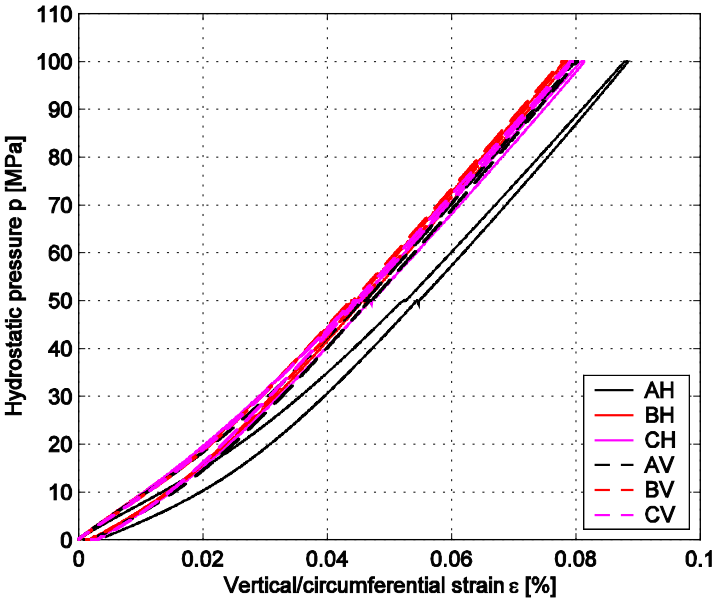

Specimen ID: KFM02B-115-6B

Youngs Modulus (E):	73.8	[GPa]	Cell pressure:	50	[MPa]
Poisson Ratio (ν):	0.297	[-]			
Axial peak stress (σ_c):	649.6	[MPa]			

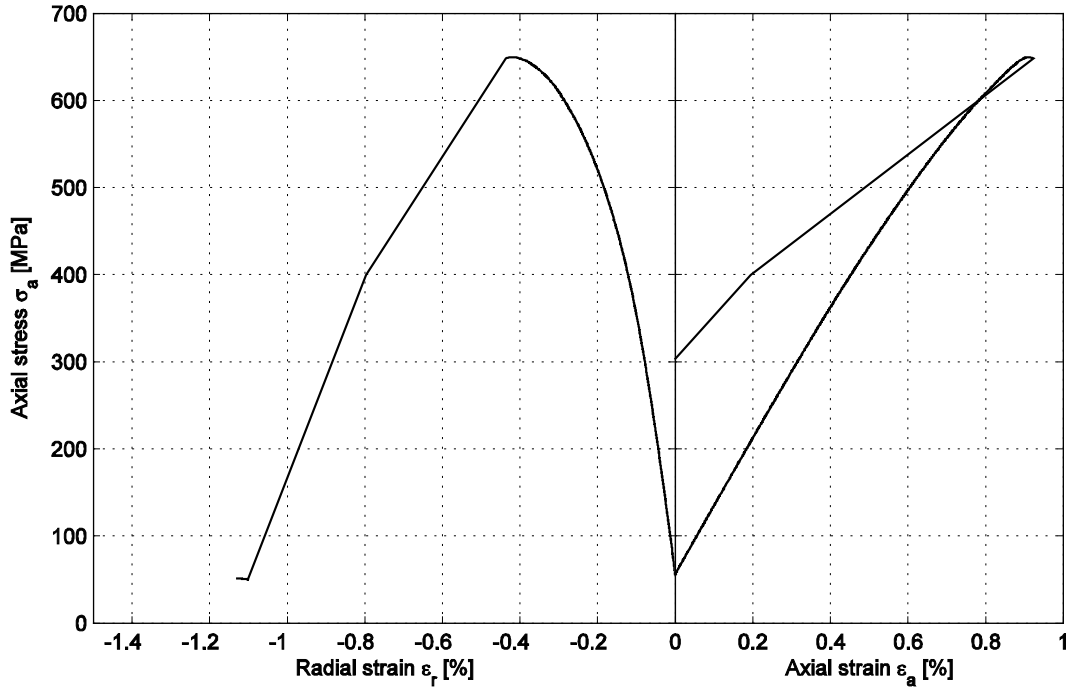

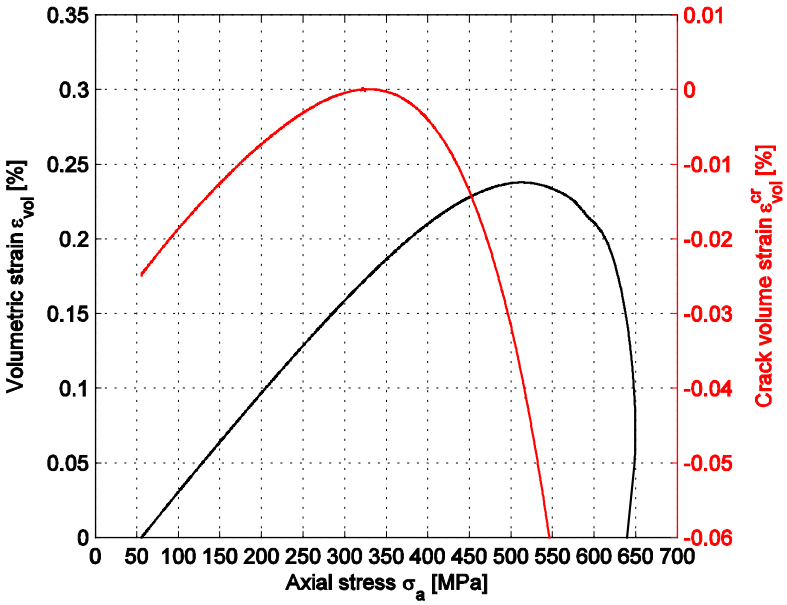

Specimen ID: KFM02B-115-012606

Before mechanical test

After mechanical test

AV, AH

BV, BH

CV, CH

Diameter (mm)	Height (mm)	Density (kg/m^3)
50.1	125.9	–

Comments: The specimen has a diagonal shear failure which is following the diagonally oriented material foliations.

Specimen ID: KFM02B-115-012606

Bulk compliance (β_{max}): 0.0203 [GPa^{-1}]

Microcrack volume (ε_{MC}): 0.024 [%]

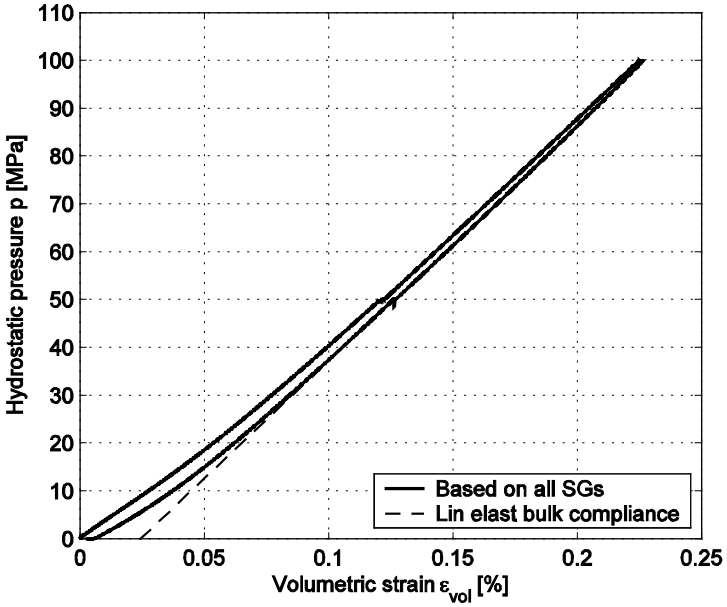

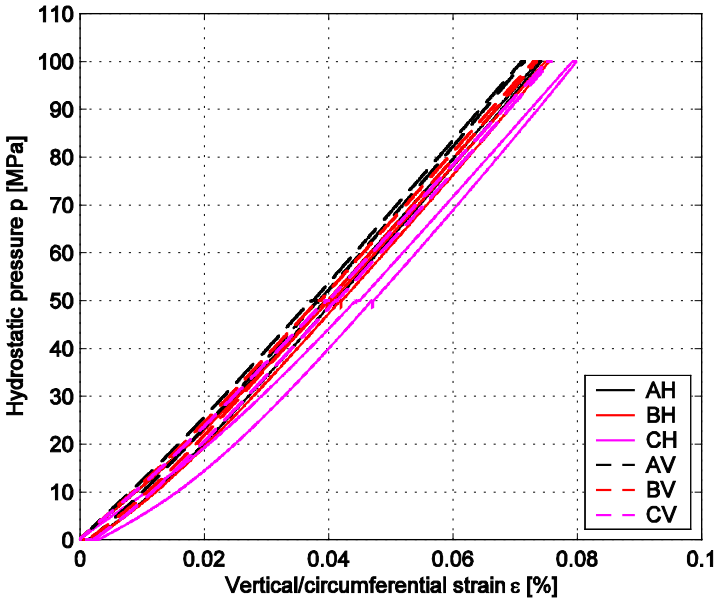

Specimen ID: KFM02B-115-012606

Youngs Modulus (E):	74.7	[GPa]	Cell pressure:	50	[MPa]
Poisson Ratio (ν):	0.294	[-]			
Axial peak stress (σ_c):	639.9	[MPa]			

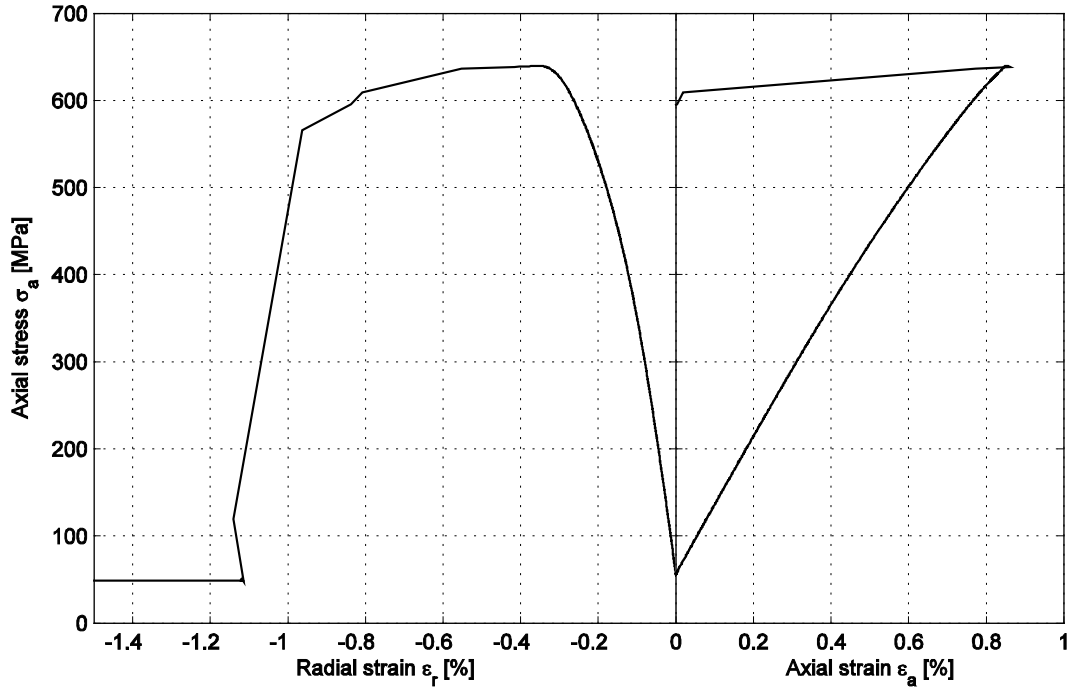

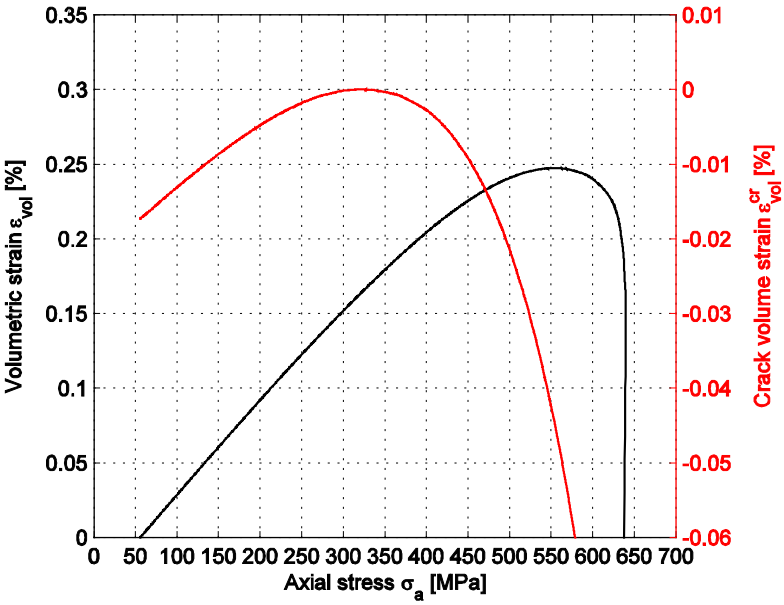

5.4 Summary of results from the mechanical tests

A summary of results from the mechanical tests is shown in Tables 5-3 to 5-6. The micro crack volume, densities, triaxial compressive strength, the tangent Young's modulus and the tangent Poisson ratio versus sampling level (borehole length), are presented in Figures 5-3 to 5-7. The results are based on adjusted data from the strain measurements. Results based on strain data without the lateral pressure correction are shown in Appendix B.

Table 5-3. Summary of results – KFM01A.

Identification	Hydrostatic compr tests			Triaxial compression tests				
	β_{max} (GPa^{-1})	ε_{MC} (%)	$\varepsilon_{vol,20}$ (%)	Conf press (MPa)	Density (kg/m^3)	Compressive strength (MPa)	Young's modulus (GPa)	Poisson ratio (–)
KFM01A-115-21	0.0204	0.037	0.073	10	2,660	319.5	75.3	0.34
KFM01A-115-22	0.0202	0.035	0.070	50	2,660	598.7	78.2	0.32
KFM01A-115-23	0.0210	0.046	0.084	10	2,660	327.5	74.4	0.31
KFM01A-115-24	0.0210	0.078	0.112	50	2,660	515.4	77.8	0.31
KFM01A-115-25	0.0194	0.054	0.093	10	2,660	356.8	74.6	0.32
KFM01A-115-26	0.0207	0.057	0.093	50	2,660	682.8	77.9	0.29
KFM01A-115-28	0.0212	0.090	0.124	10	2,660	366.0	73.9	0.32
KFM01A-115-29	0.0221	0.119	0.151	50	2,660	722.3	76.9	0.32

Table 5-4. Calculated mean values and standard deviation – KFM01A.

	Density (kg/m^3)	Young's modulus (GPa)	Poisson ratio (–)
Mean value	2,660	76.1	0.31
Std dev	0	1.8	0.02

Table 5-5. Summary of results – KFM02B.

Identification	Hydrostatic compr tests			Triaxial compression tests				
	β_{max} (GPa^{-1})	ε_{MC} (%)	$\varepsilon_{vol,20}$ (%)	Conf press (MPa)	Density (kg/m^3)	Compressive strength (MPa)	Young's modulus (GPa)	Poisson ratio (–)
KFM02B-115-1	0.0201	0.021	0.057	10	(*)	365.2	71.4	0.32
KFM02B-115-2	0.0207	0.030	0.067	50	(*)	619.0	73.1	0.29
KFM02B-115-4	0.0209	0.024	0.063	50	(*)	642.8	80.1	0.34
KFM02B-115-5	0.0203	0.038	0.073	10	(*)	364.8	72.1	0.31
KFM02B-115-6	0.0205	0.041	0.076	10	(*)	342.8	70.2	0.30
KFM02B-115-6B	0.0205	0.041	0.076	50	2,660	649.6	73.8	0.30
KFM02B-115-012606	0.0203	0.024	0.062	50	(*)	639.9	74.7	0.29

(*) Not measured for these specimens. See results in Section 5.1 for density results on neighbouring specimens.

Table 5-6. Calculated mean values and standard deviation – KFM02B.

	Density (kg/m^3)	Young's modulus (GPa)	Poisson ratio (–)
Mean value	–	73.6	0.31
Std dev	–	3.2	0.02

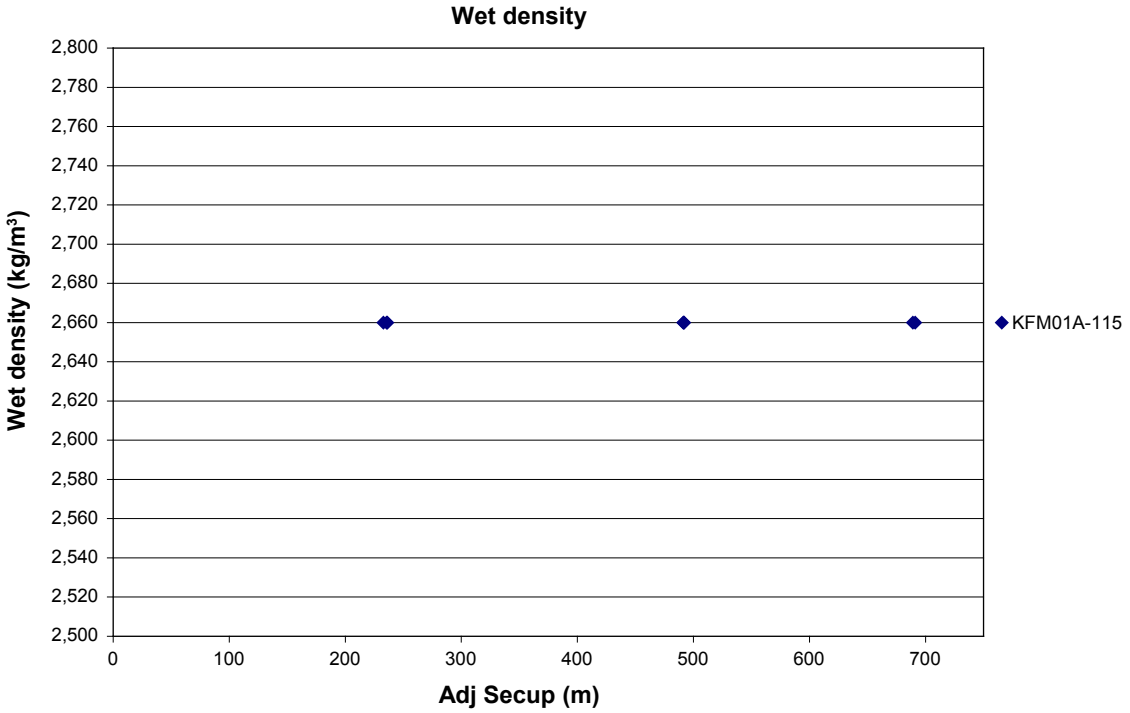

Figure 5-3. *Density versus sampling level (borehole length).*

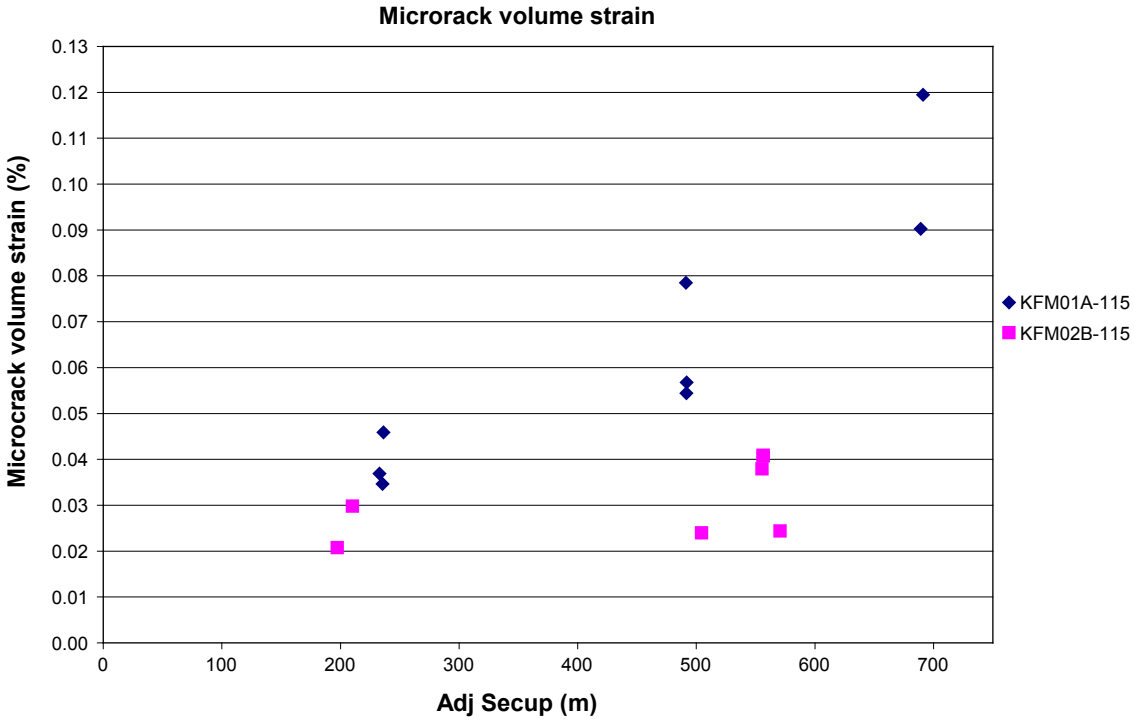

Figure 5-4. *Micro crack volume versus sampling level (borehole length).*

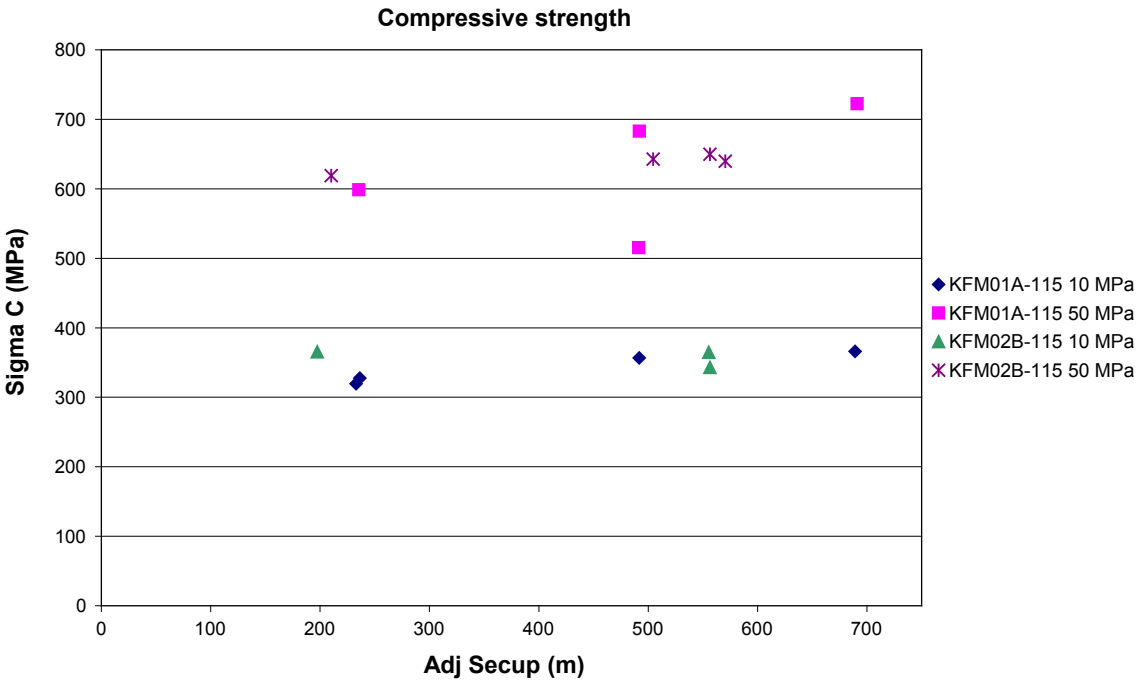

Figure 5-5. *Compressive strength versus sampling level (borehole length).*

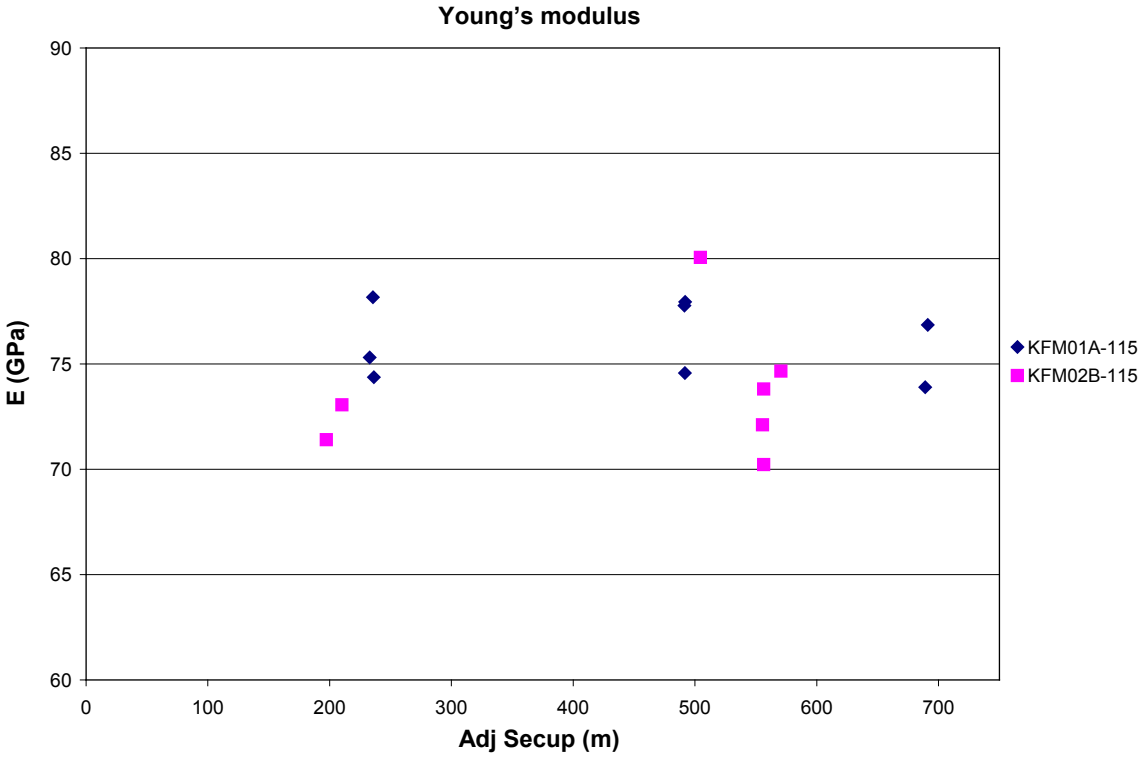

Figure 5-6. *Tangent Young's modulus versus sampling level (borehole length).*

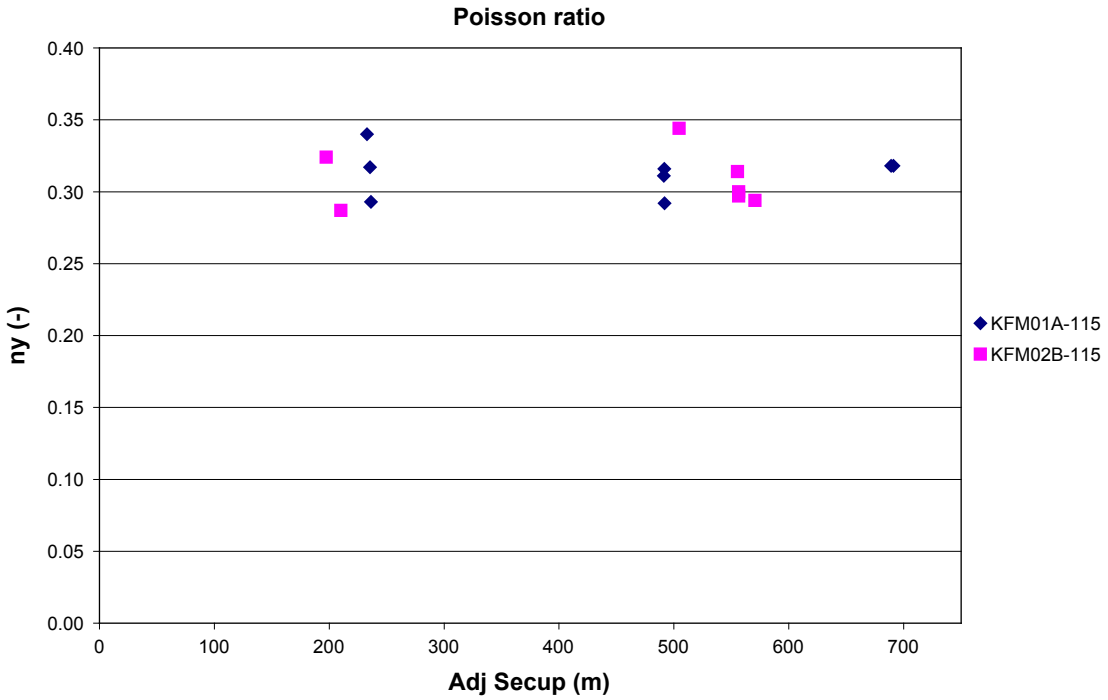

Figure 5-7. *Tangent Poisson ratio versus sampling level (borehole length).*

5.6 Discussion of results

The results of the porosity measurement of the specimens from KFM02B display no variation with depth. As to the density measurements, a slight tendency of increasing density with increasing depth can be seen. It is seen in Table 5-3 and in Figure 5-4 that the micro crack volume is increasing with depth in the specimens from borehole KFM01A. In situ rock stress measurements have shown increasing lateral rock stresses with depth in the Forsmark investigation area. A hypothesis can be that the observed micro cracks are induced due to stress relaxation and due to stressing in conjunction with the core drilling process. The trend of increasing micro crack volume with depth is not possible to confirm in the specimens from borehole KFM02B. Moreover, the micro crack volume is smaller in the specimens from KFM02B (0.021–0.041% for KFM02B as compared to 0.035–0.119% for KFM01A). There are differences in the conditions between the sites, the sampling, and the initial conditions of the specimens prior to the testing and in the test procedure. The various differences are briefly described below. It is difficult at this stage to determine the impact on the test results of each one of the parameters without further investigations.

A number of factors affect the outcome of the tests for the determination of the micro crack volume and are important to understand for the interpretation of the results. They can be related to the specimens or to the test method. The specimens have different history and are sampled from two boreholes located about 2,500 metres from each other. Some circumstances that make a difference in history between the specimens are listed below without order of significance and without further elaborations:

- The rock types can vary between the two boreholes and with sampling depth.
- The history of in situ rock stresses and the in situ stress state at the time of sampling.

- The time for the sampling is different between the boreholes. Borehole KFM01A was drilled during 2003 and the specimens have been stored in the core archive in a stress relaxed condition since then. The borehole KFM02B was drilled during the second part of 2006 and the beginning of 2007.
- The drill equipment and procedure may be different between the boreholes, which can affect the mechanical forces acting on the cores during the drilling.
- The drill core from borehole KFM01A has lost its natural water content during storage, whereas the core parts from KFM02B used for the testing were packed into watertight packages directly after drilling in order to preserve the natural water content and sent to the laboratory for testing.

The results of the tests are dependent on how the tests were conducted and how the results have been extracted, factors that may contribute to the total measurement error. Some of the contributing parts are listed below:

- The drill core from borehole KFM01A has lost its natural water content during the storage period until the time for the renewed water saturation by immersion into water for minimum 7 days in conjunction with the current tests. This yields a difference in water saturation as compared with the fresh sampled cores in which the natural water content had been preserved.
- The specimens from borehole KFM01A were loaded up to 50 MPa during the hydrostatic compression tests with a rate of 10 MPa/min during loading and unloading with a hold time of 15 minutes at full loading. Two things could be observed from those tests: (1) The loading-unloading curve displayed some hysteresis, (2) Some creep deformation took place during the hold time. However, the creep rate rapidly decreased during the hold time and the state of deformations was approaching a steady-state condition. The loading rate was decreased to 5 MPa/min in the subsequent tests on the specimens from KFM02B in order to decrease the amount of hysteresis. The hold time was also decreased to 5 minutes at full loading. Moreover, every second test was loaded up to 100 MPa in order to have results clearly within the pressure threshold which corresponds to full closure of stress induced micro cracks, cf Figure 4-1.
- The tangent value of the bulk compliance was evaluated at the unloading path at a pressure level of 50 MPa. A linear elastic bulk response was assumed when no stress induced micro cracks were present. The micro crack volume strain was computed according to (4), cf Figure 4-1. This approximation yields a model error, which is dependent on the deviation from linearity of the true elastic bulk response and on the amount of the hysteresis, which affects the evaluation of the tangent bulk compliance (β_{max}). It can be observed that the real response displays a slight non-linearity within the pressure range which is above the limit for the closure of stress induced micro cracks.

Further investigations may concern the effect of various types of sampling procedure. For example the time of storage in a stress relaxed condition or drying of the specimens can be investigated. For example, it is reasonable to believe that recently drilled cores which have not dried should preferable be used in the tests in order to eliminate the questions about effect of the storage. Moreover, other investigations may concern evaluation of the model error of the linearity approximation of the bulk response. Moreover, tests with a further decreased loading rate would probably decrease the hysteresis. A smaller hysteresis will help when the value of β_{max} is computed, in conjunction with the determination of the micro crack volume. Moreover, a smaller hysteresis is also helpful if the linearity approximation of the bulk response is investigated.

References

/1/ **SKB, 2001.** Site investigations. Investigation methods and general execution programme. SKB TR-01-29, Svensk Kärnbränslehantering AB.

/2/ **ISRM, 1979.** Suggested Method for Determining Water Content. Porosity, Density, Absorption and Related Properties and Swelling and Slake-durability Index Properties, Int. J. Rock. Mech. Min. Sci. & Geomech. Abstr. 16(2), pp 141–156.

/3/ **ISRM, 1983.** Suggested method for determining the strength of rock material in triaxial compression: Revised version, Int. J. Rock. Mech. Min. Sci. & Geomech. Abstr. 20(6), pp 283–290.

/4/ **ISRM, 1999.** Draft ISRM suggested method for the complete stress-strain curve for intact rock in uniaxial compression, Int. J. Rock. Mech. Min. Sci. 36(3), pp 279–289.

/5/ **Savukoski M, 2004.** Forsmark site investigation, drill hole KFM01A. Determination of porosity by water saturation and density by buoyancy technique. SKB P-04-166, Svensk Kärnbränslehantering AB.

/6/ **Brace W F, 1965.** Some new measurements of linear compressibility of rocks, J. Geophys. Res. 70(2), pp 391–398.

/7/ **Walsh J B, 1965.** The effect of cracks on the compressibility of rock, J. Geophys. Res. 70(2), pp 381–389.

/8/ **Martin C D, Chandler N A, 1994.** The progressive fracture of Lac du Bonnet granite, Int. J. Rock. Mech. Min. Sci. Geomech. Abstr. 31(6), pp 643–659.

/9/ **Eberhardt E, Stead D, Stimpson B, Read R S, 1998.** Identifying crack initiation and propagation thresholds in brittle rock. Can. Geotech. J. 35, pp 222–233.

/10/ **Jacobsson L, 2004.** Forsmark site investigation. Borehole KFM01A. Uniaxial compression test of intact rock. SKB P-04-223, Svensk Kärnbränslehantering AB.

/11/ **Jacobsson L, 2004.** Forsmark site investigation. Borehole KFM01A. Triaxial compression test of intact rock. SKB P-04-227, Svensk Kärnbränslehantering AB.

/12/ **Jacobsson L, 2004.** Forsmark site investigation. Drill hole KFM01A. Indirect tensile strength test. SKB P-04-170, Svensk Kärnbränslehantering AB.

/13/ **ASTM 4543-01, 2001.** Standard practice for preparing rock core specimens and determining dimensional and shape tolerance.

/14/ **Hoffman K, 1989.** An introduction to measurements using strain gages. Hottinger Baldwin Messtechnik GmbH, Darmstadt.

/15/ **Brace W F, 1964.** Effect of pressure on electrical resistance strain gages, Exp. Mech 4, pp 212–216.

/16/ **Lau J S O, Chandler N A, 2004.** Innovative laboratory testing, Int. J. Rock. Mech Sci. 41(8), pp 1427–1445.

/17/ **SS-EN 13755.** Natural stone test methods – Determination of water absorption at atmospheric pressure.

/18/ **Stråhle A, 2001.** Definition och beskrivning av parametrar för geologisk, geofysisk och bergmekanisk kartering av berg. Report SKB R-01-19, Swedish Nuclear Fuel and Waste Management Co, Stockholm. In Swedish.

/19/ **MATLAB, 2002.** The Language of Technical computing. Version 6.5. MathWorks Inc.

/20/ **Milligan R V, 1965.** The effects of high pressure on foil strain gages on convex and concave surfaces, Exp. Mech 5(2), pp 59–64.

/21/ **Andreae G, 1974.** Über den Einfluβ hydrostatischen Druckes auf Dehnungsmeβstreifen, Materialprüfung 16(4), pp 98–102.

/22/ **Hoffman K, Jost D, Keil St, 1978.** Experimentelle Untersuchung des Einflusses hydrostatischen Drucks auf Dehnungsmeβstreifen – Applikationen und die Ermittlung von Korrekturwerten, VDI-Berichte 313, pp 553–558.

Appendix A

Reference tests

A.1 General

Hydrostatic compression tests of aluminium reference specimens, with deformation measurements by means of strain gauges, were carried out in order to

(1) develop and verify a proper method to mount the strain gauges on cylindrical specimens resembling the drill core specimens,

(2) to determine the lateral pressure sensitivity on the selected type of adhesive and strain gauge and,

(3) to obtain an estimate of the results uncertainty for the actual method.

The lateral pressure sensitivity can be determined by comparing measured response with theoretical response. Aluminium behaves as an isotropic linear elastic material during hydrostatic compression. Hence, the response during hydrostatic compression can be computed by means of elasticity theory, provided that the elasticity constants are known. The elasticity constants, represented by the Young's modulus E and Poisson ratio ν, were determined by uniaxial compression tests, in which no lateral pressure is acting on the strain gauges, conducted prior to the hydrostatic compression tests.

Aluminium was selected as material for the reference specimens as the elastic properties coincide well with the elastic properties of the rock material to be tested.

A.2 Experimental set-up

Cylindrical specimens with a diameter of 52.0 mm and a height of 128.0 mm were used. The material was aluminium 7075-T6. Strain gauges from KYOWA with a gauge length of 20 mm were used for the deformation measurements. A two-part metha-acrylate adhesive was used to mount the strain gauges which were protected by applying a coating after the adhesive was cured. Strain gauge cement was used to fixate the cables.

Six strain gauges were placed along the circumference at mid height of the specimen, see Figure A-1. Three strain gauges measure the axial strain and three other strain gauges measure the circumferential strain.

The equipment normally used for triaxial compression tests was used both for the uniaxial and the hydrostatic compression tests. The specimen was placed within the pressure vessel in both cases. No oil was filled in the pressure vessel and no membrane was mounted on the specimens during the uniaxial compression tests. The specimen was loaded by the piston that is going in the cell and the force was measured by the internal in-vessel load cell.

The cell was opened and a membrane was mounted on the specimen and the strain gauge cables were sealed such that no oil could penetrate in between the membrane and the specimen. The cell was closed and filled with oil. The hydrostatic compression of the specimen was accomplished by pressurizing the oil in the cell.

The data acquisition was made with a HBM MGCplus unit equipped with amplifier modules ML38-AP03 and ML10B-AP03 for the strain gauge channels. Each of the strain gauges was connected to a Wheatstone bridge with a sense connection for temperature compensation. Moreover, the load and pressure signals were sampled with the HBM MGCplus unit.

The strain gauge channels were calibrated using a shunt resistance, whereas the amplifying constants for the force and pressure measurements channels were determined by a two-point calibration using the reference values obtained from the test system.

A.3 Results from uniaxial compression tests

Uniaxial compression tests were carried out within the triaxial cell. A picture of the specimen in place between the loading platens is shown in Figure A-2. The specimens were subjected to two load cycles with an axial stress σ_a varying between 1 MPa and 200 MPa.

Results from a uniaxial compression test are shown in Figure A-3, where it can be seen that the results of the individual strain gauges coincide well in the axial as well as in the circumferential direction. The values of the elastic modulii, found in Table A-1, were determined as the secant values evaluated between σ_a = 50 MPa and σ_a = 150 MPa where

$$E = \frac{\Delta \sigma_a}{\Delta \bar{\varepsilon}_a} \text{ and } \nu = -\frac{\Delta \bar{\varepsilon}_\phi}{\Delta \bar{\varepsilon}_a} \tag{A1a,b}$$

and where

$$\bar{\varepsilon}_a = \frac{\varepsilon_{AV} + \varepsilon_{BV} + \varepsilon_{CV}}{3} \text{ and } \bar{\varepsilon}_\phi = \frac{\varepsilon_{AH} + \varepsilon_{BH} + \varepsilon_{CH}}{3}.$$

It is seen that equal values of Poisson ratio is obtained in the two measurements, whereas a difference of 0.7% is obtained between the values of Young's modulus. The difference could have the following origins. For example, the gauge factor supplied by the strain gauge manufacturer is given with an accuracy of 1%. This gauge factor was used when the strain gauge channels were configured in the standard data acquisition instrument. A two-point calibration procedure using a known shunt resistance yielding a certain strain reading was used when the strain gauge channels were configured in the high precision data acquisition instrument.

The values E = 74.6 MPa and ν = 0.342 will be used subsequently when the theoretical volumetric response during hydrostatic compression is computed.

A.4 Results from hydrostatic compression tests

The hydrostatic compression tests were carried out within the triaxial cell. Hydrostatic loading was accomplished by letting pressurized oil acting on the specimen which is enclosed between the loading platens and a rubber membrane. A gap in the spherical seat at the upper loading platen permits oil pressure to act on top of the loading platen. The specimens were subjected to two load cycles with an oil pressure varying between 0.1 MPa and 50 MPa.

By assuming linear elasticity, the elastic strain during hydrostatic compression can be computed as

$$\varepsilon_a = \varepsilon_\phi = \frac{p}{K} \tag{A2}$$

where K is the bulk stiffness given as

$$K = \frac{E}{1 - 2\nu} \tag{A3}$$

and ε_a is the axial strain, ε_ϕ is the circumferential strain and p is the hydrostatic pressure. For the previously determined values of the elasticity constants, E = 74.6 MPa and ν = 0.342, we find that the theoretical value of the bulk stiffness is K = 236 GPa.

The results of the hydrostatic compression test are shown in Figure A-4. The response of the strain gauges displays a linear behaviour. The mounting of strain gauge CH failed and the results should be omitted in the evaluation. It is seen that the results from the vertical strain gauges (AV, BV and CV) that measure the axial strains yield smaller strain values than the horizontal ones, which measure the circumferential strains. The strain gauges that measure the axial strain experience a plane surface in the direction in which the strains are measured (the active direction of the strain gauge), whereas the strain gauges that measure the circumferential strain (AH, BH and CH) are mounted on a convex surface in the measuring direction.

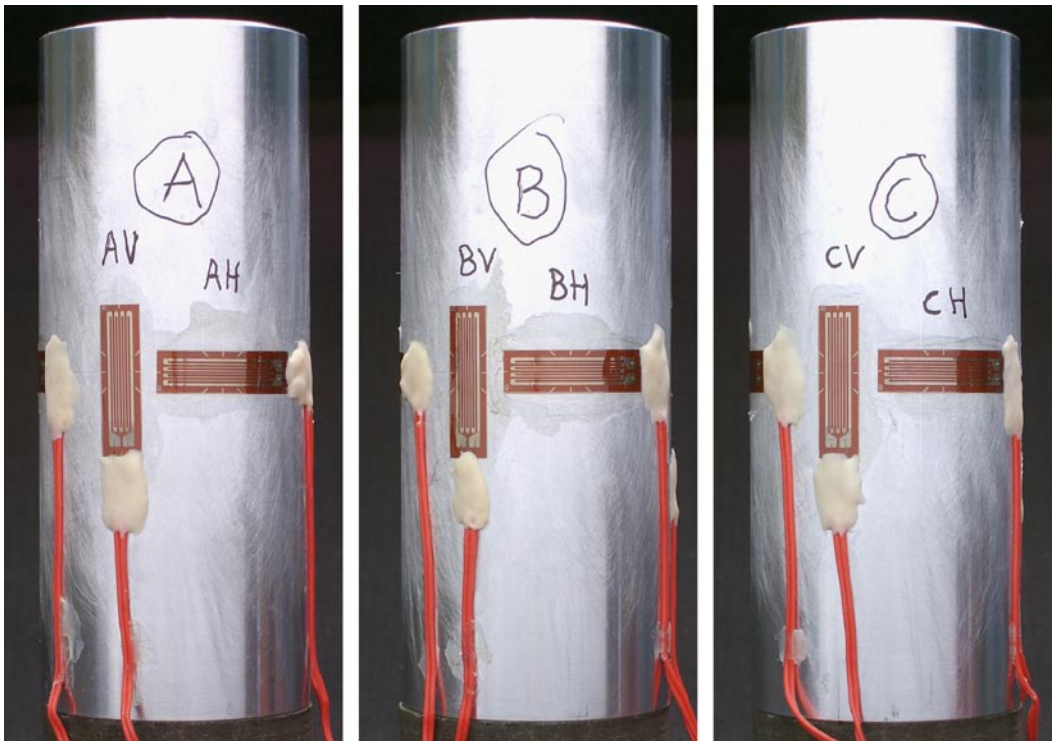

Figure A-1. *Aluminium reference specimen 1 with three strain gauges vertically oriented (AV, BV and CV) and three horizontally oriented (AH, BH and CH).*

Experimental investigations by Milligan /20/ and Andreae /21/ show that results from strain measurements are affected by the curvature of the surface in the measuring direction in conjunction with lateral pressure acting on strain gauges. On a theoretical basis Andreae /21/ derived an expression for the strain deviation due to the curvature at a given lateral pressure p as

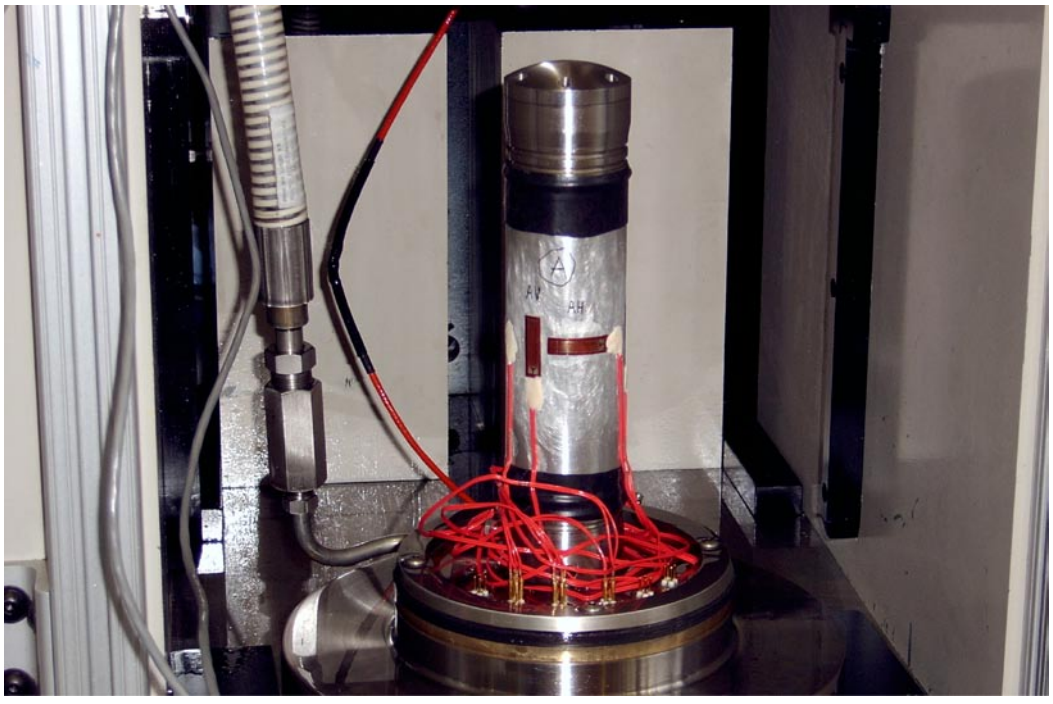

Figure A-2. *Specimen placed between the loading platens.*

$$\Delta\varepsilon \approx \frac{d}{r+d} \cdot \frac{p}{E_{A+C}}(1-\nu_{A+C}^2) \qquad \text{(A4)}$$

where d is the distance (offset) from the strain gauge foil to the material surface, r is the surface radius, E_{A+C} and ν_{A+C} are the compound (effective) Young's modulus and the Poisson ratio of the adhesive layer (A) and the carrier plate (C) or the base plate together on which the foil is attached. The effect of the curvature on a convex surface will lead to an increase of the measured values.

Andreae /21/ estimated that d = 0.1 mm, E_{A+C} = 9.897 GPa (1,000 kp/mm^2) and ν_{A+C} = 0.32. By inserting the values used by /21/ and the surface radius is r = 26 mm, i.e. the specimen diameter divided by two, and p = 50 MPa in (A4) we obtain a strain deviation $\Delta\varepsilon$ = 17.5 microstrains at maximum pressure. This deviation will subsequently be denoted $\varepsilon_{curvature}$.

The effect of curvature can be corrected for by subtracting $\varepsilon_{curvature}$ from the measured values for strain gauges AH, BH and CH. Hence, after doing this, it is possible to compare the experimental values with the theoretical values and estimate the lateral pressure effect on the strain results.

The calculations outlined above have been carried out on the experimental results and are shown in Table A-2. The last row in the table suggests that the lateral pressure acting on a strain gauge mounted on a flat surface will underestimate the strain value with approximately 30 microstrains at 50 MPa lateral pressure. This implies an underestimation of 14% at each pressure level for the current test set-up. This result coincides well to earlier investigations reported by /14, 22/.

Table A-1. Values on the elastic modulii obtained from uniaxial compression tests.

Load sequence	E (GPa)	ν (–)	E_{AV} (GPa)	E_{BV} (GPa)	E_{CV} (GPa)
loading 1	74.60	0.3423	74.50	74.13	75.18
unloading 1	74.59	0.3430	74.55	74.15	75.08
loading 2	74.59	0.3424	74.53	74.06	75.19
unloading 2	74.61	0.3429	74.58	74.12	75.12
Mean value	**74.60**	**0.3427**	**74.54**	**74.12**	**75.14**

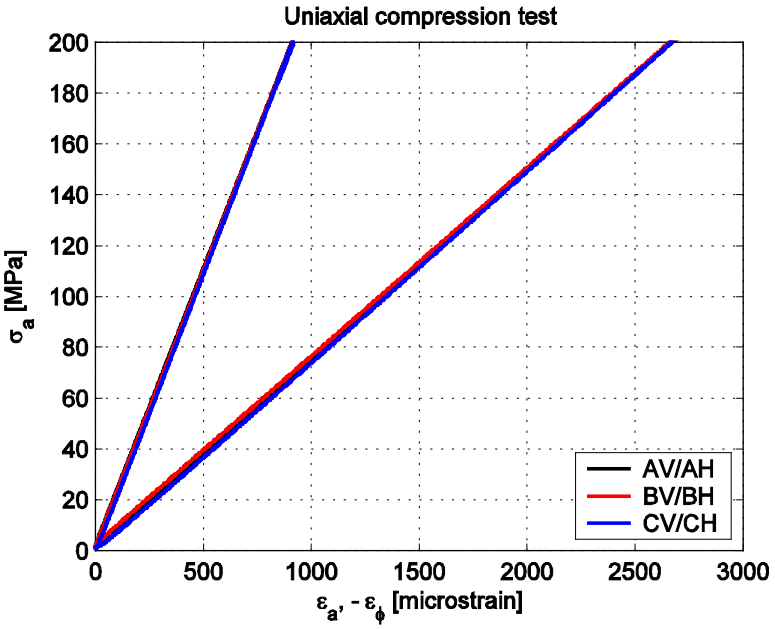

Figure A-3. *Results from uniaxial compression tests.*

The lateral pressure effect on strain gauge measurements were investigated by carrying out hydrostatic compression tests on steel specimens which had plane surfaces. The results showed that the strain values were underestimated by about 23–33 microstrains at a pressure of 50 MPa.

A.5 Conclusions

The effect of lateral pressure acting on foil strain gauges have successfully been quantified by means of hydrostatic compression tests. It is seen that lateral pressure acting on strain gauges yields an underestimation of the measured strain values of approximately 22–34 microstrains (0.0022–0.0034%) at a lateral pressure of 50 MPa after compensating for the surface curvature for the strain gauged mounted in the circumferential direction. The values correlate well with earlier experimental investigations found in the literature cf /14, 22/.

The mounting process is of great importance for successful results. In order to succeed with achieving a thin adhesive layer with equal thickness it is important to apply the adhesive, place the strain gauge and put controlled pressure on the strain gauge within working time of the adhesive including a margin. A defect bonding can not be guaranteed to be observed by visual inspection. The people that carry out the mounting have to be observant on if any small mistakes occur during the mounting process and, if so, make a note about that. Moreover, a defect bonding will likely yield an initial non-linearity or a large deviation in the strain measurements as compared to other strain gauge readings.

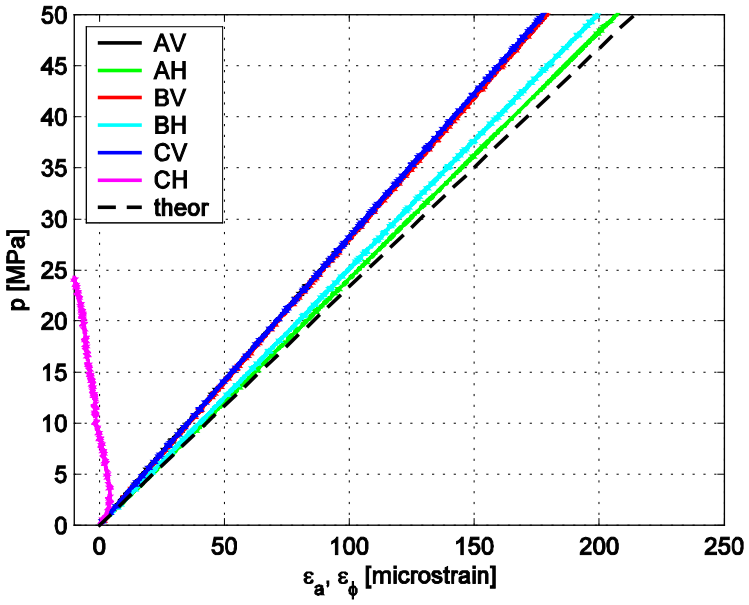

Figure A-4. *Results from hydrostatic compression tests. Values of all six strain gauges(solid lines) and theoretical response (dashed line).*

Table A-2. Strain values for respective strain gauge at full loading (p = 50 MPa). The values of strain gauge CH should be omitted due to erroneous mounting.

Strain values at p = 50 MPa	AV (microstr)	BV (microstr)	CV (microstr)	AH (microstr)	BH (microstr)	CH (microstr)
ε_{expr}	178.1	179.2	177.4	207.0	199.3	(–12.1)
$\varepsilon_{curvature}$ (cf /21/)	0.0	0.0	0.0	17.5	17.5	17.5
$\varepsilon_{expr,corr} = \varepsilon_{expr} - \varepsilon_{curvature}$	178.1	179.2	177.4	189.4	181.8	(–29.6)
$\varepsilon_{theor} = p/K$ (cf (A2))	211.8	211.8	211.8	211.8	211.8	211.8
$\varepsilon_{theor} - \varepsilon_{expr,corr}$ = pressure effect	33.7	32.6	34.4	22.4	30.0	(–241.4)
Pressure effect determined by /14, 22/	23–33	23–33	23–33	23–33	23–33	23–33

Appendix B

Results from mechanical tests without lateral pressure correction

Results from both KFM01A and KFM02B based on strain measurements in which no adjustment for the effect of lateral pressure are shown below in Tables B-1 to B-4.

Table B-1. Summary of results – KFM01A based on original strain data.

Identification	Hydrostatic compr tests			Triaxial compression tests				
	β_{max} (GPa^{-1})	ε_{MC} (%)	$\varepsilon_{vol,20}$ (%)	Conf press (MPa)	Density (kg/m^3)	Compressive strength (MPa)	Young's modulus (GPa)	Poisson ratio (–)
KFM01A-115-21	0.0195	0.037	0.071	10	2,660	319.5	75.3	0.34
KFM01A-115-22	0.0192	0.035	0.068	50	2,660	598.7	78.2	0.32
KFM01A-115-23	0.0200	0.046	0.082	10	2,660	327.5	74.4	0.31
KFM01A-115-24	0.0200	0.078	0.110	50	2,660	515.4	77.8	0.31
KFM01A-115-25	0.0184	0.054	0.091	10	2,660	356.8	74.6	0.32
KFM01A-115-26	0.0197	0.057	0.091	50	2,660	682.8	77.9	0.29

Table B-2. Calculated mean values and standard deviation – KFM01A based on original strain data.

	Density (kg/m^3)	Young's modulus (GPa)	Poisson ratio (–)
Mean value	2,660	76.4	0.31
Std dev	0	1.8	0.02

Table B-3. Summary of results – KFM02B based on original strain data.

Identification	Hydrostatic compr tests			Triaxial compression tests				
	β_{max} (GPa^{-1})	ε_{MC} (%)	$\varepsilon_{vol,20}$ (%)	Conf press (MPa)	Density (kg/m^3)	Compressive strength (MPa)	Young's modulus (GPa)	Poisson ratio (–)
KFM02B-115-1	0.0191	0.021	0.055	10	(*)	355.5	69.5	0.32
KFM02B-115-2	0.0197	0.030	0.065	50	(*)	603.4	71.1	0.29
KFM02B-115-4	0.0199	0.024	0.061	50	(*)	628.9	78.2	0.34
KFM02B-115-5	0.0193	0.038	0.071	10	(*)	356.5	70.4	0.31
KFM02B-115-6	0.0195	0.041	0.074	10	(*)	335.0	68.6	0.30
KFM02B-115-012606	0.0194	0.024	0.060	50	(*)	623.7	72.6	0.29

(*) Not measured for these specimens. See results in Section 5.1 for density results on neighbouring specimens.

Table B-4. Calculated mean values and standard deviation – KFM02B based on original strain data.

	Density (kg/m^3)	Young's modulus (GPa)	Poisson ratio (–)
Mean value	–	71.7	0.31
Std dev	–	3.5	0.02